UNIVERSIDAD AUTÓNOMA DE MADRID

DEPARTMENT OF MOLECULAR BIOLOGY

FACULTY OF SCIENCES

Role of microtubule-dependent transport in synaptic plasticity in hippocampal neurons

Argentina Lario Lago

Madrid, 2014

UNIVERSIDAD AUTÓNOMA DE MADRID

DEPARTMENT OF MOLECULAR BIOLOGY

FACULTY OF SCIENCES

Role of microtubule-dependent transport in synaptic plasticity in hippocampal neurons

Doctoral thesis submitted to the Universidad Autónoma de Madrid for the degree of Doctor of Philosophy by M.Sci. in Molecular Biosciences,

Argentina Lario Lago

Thesis Director:

Dr. José A. Esteban

Thesis Tutor:

Dr. Francisco Zafra

Centro de Biología Molecular “Severo Ochoa” (CBMSO – UAM/CSIC)

La realización de esta tesis doctoral ha sido posible gracias a la concesión de una ayuda Predoctoral de Formación de Personal Investigador (Ayudas FPI) del extinto Ministerio de Ciencia e Innovación (Ayuda BES-2009-015414, Proyecto SAF2008-04616). Su desarrollo ha tenido lugar en laboratorio del Doctor José A. Esteban García, bajo su dirección, en el Centro de Biología Molecular "Severo Ochoa", centro mixto de la Universidad Autónoma de Madrid y del Consejo Superior de Investigaciones Científicas (CBMSO – UAM/CSIC).

A vosotros

Acknowledgments

En primer lugar, gracias al Dr. José A. Esteban por haber sido mi director científico todos estos años. Gracias por la confianza depositada en mí cuando no era más que una estudiante de 4º de carrera, por la extraordinaria paciencia, por las muchas oportunidades profesionales, y por dejarme crecer como persona y como científica en el Esteban Lab.

Gracias a los miembros del tribunal de tesis por dedicar tiempo a la discusión de este trabajo. Gracias también a mi tutor, el Dr. Francisco Zafra, por hacerme la vida fácil.

Gracias a todos los miembros del Esteban Lab: los que se fueron, los que llevan un *ratete* y los que acaban de llegar. Gracias, porque de todos vosotros he aprendido. Gracias también a los distintos Servicios del CBMSO. Mi trabajo no habría sido posible sin la ayuda de Microscopía, Instrumentación, Mantenimiento, Informática, Fermentación, Cocinas, Cultivos y Limpieza. Gracias por vuestra buena disposición, por hacer un trabajo generalmente poco reconocido pero vital.

Gracias al artista Daniel Orson Ybarra, y a su fotógrafo Sergio Primavera, por facilitarme la imagen que sirve de portada de esta tesis. La obra pertenece a la serie “Epiphany” y se titula “Fiesta I” (espray acrílico y tinta sobre lino, 2014). Gracias a mi madre por dar con la imagen adecuada. Gracias, también, a Alfonso por dedicar el tiempo que no tiene a diseñar el conjunto final.

Y se supone que ahora viene la parte melodramática... Espero no decepcionar a nadie.

Gracias, evidentemente, a mis padres. Gracias Salvador y Argentina, por el apoyo incondicional, las riñas (casi siempre telefónicas, que así duelen menos), los chistes (que casi nunca me hacen gracia), los recursos, los medios y las oportunidades. Gracias por no rendiros, aunque yo no lo haya puesto siempre fácil. Gracias a mi otra madre, la madre estival, la madre científica y electrónica. Amparo, mi tía la del pueblo, la de la ciudad del Ave Fénix. Cómo te quiero. Gracias por darme una familia española maravillosa en suelo yankee, por compartir tu preciado café matutino y por sacar siempre siempre siempre el tiempo para hablar conmigo. Y gracias por descubrirme el albariño, mi vida ahora es un lugar mejor.

Thank you to my CNIO family. You guys are just… AWESOME. I really have no words to explain how grateful and lucky I am for having you all in my life. You are people incredibly good hearted. Thank you for accepting me how I am, for including me in all the games, for not giving up on me, for helping me discover myself and for making my life a better and a more balanced place. Javi, you are of course in this crowd! Özge, thank you for comforting me during a very particular time of my life. Iva, thanks for evolving with me, for taking me with you when I needed it (and also when I didn’t!). And Ljilja… Thank you for everything, you’ve helped me in countless ways… I simply can’t put it into words. Thank you, especially, for being compassionate, honest, cynical and pragmatical. Thank you for being part of the process. Thank you for deciding that I like changes – period. Hvala. And, oh well... We all should go to India!

Gracias, por supuesto, a la familia del CBM. Esta es muy diversa, así que la cosa se complica... Como es lógico, empiezo por la madre del trabajo: gracias Ilu, sencillamente porque sí. ¡Y a Mari José también! Gracias, indiscutiblemente, a María R, cofundadora de esta odisea, míranos... ¡Quién nos lo iba a decir! Parece que al final hemos visto florecer *el árbol rojo*, y yo no lo habría visto sin tu ayuda… También gracias a Cris, Carla (no me mires así que me pongo *trihte*, y tú ya sabes que yo te llevaría conmigo al fin del mundo), Yolanda y Mónica... Gracias chicas por todo el drama, pero sobre todo por las risas que hemos conseguido hacer a costa del drama, y porque hemos salido queriéndonos (un poco) a pesar de ello. *Conqueasiejeque* podemos decir que bien está lo que bien acaba, ¿no? Anna, gracias por el apoyo personal y científico, por los vicios compartidos a escondidas y por enseñarme las maravillas del *spinning*. Sin ti, de verdad que no lo habría conseguido, pero prometo no abrazarte (mucho). Gracias también a los compañeros que hacen que ir a la impresora sea mucho más entretenido; a las compañeras de tupper que no fallan truene o haga un sol de justicia; a los vecinos a los que siempre les puedes pedir un poco de saponina aunque sea de los años 80, y que te siguen hablando aunque les hayas echado de su labo; a las chicas del SMOC, que me separan los caramelos de limón, y a su jefe, que me deja entrar a robarlos alegremente; a los compañeros de cultivos que te observan detenidamente mientras haces primarios… Gracias, en resumen, a la vida "de pasillo".

De manera muy especial, gracias a los participantes en *la metamorfosis*: Joana (mi medio tándem, el terror del CBM, mi *nueva mejor amiga*), Pascu, Nata, Lara, Álex, y Alfonso (es que a mí lo de Fons no me sale muy natural, y mira que yo lo intento…). Gracias por ayudarme en un año muy especial de mi vida. ¡Cómo cambian las cosas! Alfonso, gracias por los muchos momentos sorpresivos de felicidad genuina… ¡Y por recordarme que existe! Gracias por ser capaz, incluso, de capturarla en una fotografía... Gracias también por todas esas conversaciones más o menos profundas en la pérgola, en terrazas varias, y en otros muchos lares (y a muy diversas horas); por los gintonics y los vinos a medias. Gracias por leerme, y por ayudarme a encontrar respuestas (al hacer las preguntas adecuadas). Pascu, gracias por calarme tan rápido como lo hiciste y no hacer (mucha) leña a pesar de ello; gracias por incluirme; gracias por el asesoramiento a través del *gmail chat*, y por los bailes en la fiesta de verano. Joana, gracias por las risas, las confesiones, las preguntas absurdas (y embarazosas), y los gritos en formato *whatsapp*. Gracias por tirar de mí. Gracias Nata por las charlas de apoyo en las escaleras y a la salida del SMOC; por escucharme aunque no tengas tiempo y te aborde por el pasillo; gracias por preocuparte por mí. Lara, gracias por intentar convencerme de que puedo conseguir aquello que me proponga, y por arrastrarme y meterme la cabeza debajo de la pila (con la ayuda de Joana y ante el asombro de alguna que otra señora que pasaba por allá). En definitiva, gracias por los ánimos y los abrazos que tan ricos saben cuando son de verdad; y gracias, sobre todo, por enseñarme cosas nuevas, más o menos sanas, cada día. ¡Y gracias Nuri por invitarme (y acogerme a pesar de tu asombro) a aquellas cañas que fueron un poco el principio del fin!

Gracias también a los cabos sueltos. Danae, mi hermanita pequeña y postiza, gracias por ser como eres, aunque sea un topicazo es cierto. ¡Por una cena de Navidad a base de mortadela! Marisol, gracias por todos estos años de apoyo, por estar siempre disponible, y por buscar la mejor manera de ayudarme. Dolors, me salvaste en Burdeos al grito de "tú, la que sales por la puerta, eres española, ¿no?". ¡Qué buenos los paseos, los viajes en tren, los helados y las conversaciones! Gracias por ayudarme a ser mejor persona, gracias por no olvidarte de mí. Inma… Gracias por sacarme de mi escondrijo (por no decir agujero negro), por ser dura y cariñosa conmigo a partes iguales, por estar siempre siempre siempre al otro lado del *gmail*. Tú dices que esto es recíproco, y yo estoy convencida de que recibo mucho más de lo que doy. Gracias por ser mi amiga, mi familia, y mi mentora. Ana Franco, Vero, gracias por la compañía en el CBM a horas intempestivas, por hablar conmigo de calcetines y terapias alternativas. Aroallb, gracias por los correos veloces, porque sé que no te es fácil, y consigues sacar el tiempo para hablar conmigo. Marta Magariños, gracias por las comidas, también veloces, y por ayudarme a sacar los pies del tiesto (pero también a volver a meterlos). JJ, parece que te he hecho caso y no me voy a Nebraska... Gracias por quererme como soy y acogerme siempre con los brazos abiertos. Tania... ¡Tramos de mi vida! Gracias se me queda tan pequeño... Gracias por recordarme lo que es estar viva, por hacerme ver que siempre se puede elegir, y por estar pendiente de mí. Gracias porque me hiciste llegar a Suecia cuando llegar al CBM me parecía todo un mundo.

Y un gracias genérico, pero no por ello menos importante. Gracias a toda esa gente que ha estado conmigo a lo largo del camino, aunque solamente fuera por un tiempo, a toda esa gente que ha ido entrando y saliendo de mi vida: mentores, profesores, monitores, compañeros de carrera, compañeros de trabajo, compañeros de cafés, amigos, familia… También a esa gente que, de momento, solamente ha entrado. En cualquier caso, gente de la que siempre he aprendido, de la que siempre me he quedado un pedacito más o menos grande, y sin la que hoy no sería como soy.

Por último, gracias a mi *esposo académico*, Curro. Porque si hace 10 años nos dicen que ahora íbamos a estar en estas, no nos lo hubiéramos creído. Gracias porque no me has fallado nunca, gracias por tener siempre un ojo encima de mí (y por hacer la vista gorda de vez en cuando confiando en que se me pase la tontería). Espero que me des trabajo algún día, cariño.

Gracias a todos por acompañarme en esta etapa del viaje. Vosotros sabéis quienes sois, estéis o no entre los nombres de arriba. Sois mi familia, la genética y la epigenética.

Y yo creo que ya, ¿no?

“Es lo que es” Erich Fried

Abstract

Abstract

The majority of excitatory synapses in the central nervous system are located at dendritic spines. These structures are considered key compartments for synaptic plasticity. During synaptic plasticity expression, spines alter their morphology and structure, and neurotransmitter receptor trafficking events take place. These phenomena have been related to actin cytoskeleton changes, but recently, microtubules (MT) have also been shown to modulate their own dynamics in an activity-dependent manner. Considering the close relationship between MT-dependent transport and endomembrane trafficking, and that between endomembrane trafficking and synaptic plasticity, we analyzed whether MT-dependent transport would play a role in modulating synaptic plasticity.

Using a multidisciplinary approach that includes biochemistry, live confocal imaging, electrophysiology techniques and molecular biology for the development of new molecular tools, we have investigated the interaction of AMPA Receptors (AMPARs) with members of the kinesin family (KIF5, KIF17) and dynein during synaptic function. In particular, we have mapped-down the domains of these molecular motors that are required for the maintenance of basal transmission and for the allowance of synaptic plasticity expression in CA1 excitatory synapses from hippocampal slices.

The data obtained suggested that the motor domain of KIF5 is not needed either for the maintenance of basal transmission or for the transport of GluA2 subunits along dendrites. However, its motor activity, as well as the motor activity of KIF17, seems to be crucial for long-term depression (LTD) to occur normally. Complementarily to these results, we have found that maintenance of basal transmission most likely depends on either regulatory domains of the neck-stalk region, or on interactions depending on the cargo binding domain of KIF5 and KIF17. Finally, we have also addressed whether minus-end transport, based on dynein, could modulate synaptic function. Our preliminary results indicate that dynein transport is not required for proper synaptic function.

Our results suggest that MT-dependent transport is one of the many intracellular mechanisms finely tuning NMDAR-dependent LTD. Altogehter, this thesis shed some light into the interplay between cytoskeletal elements and the regulation of synaptic strength.

Resumen

Resumen

La mayoría de las sinapsis excitatorias en el sistema nervioso central se encuentran en espinas dendríticas. Por tanto, se consideran estructuras clave en las que la maquinaria necesaria para el desarrollo de la plasticidad sináptica debe funcionar correctamente. Cuando los fenómenos de plasticidad sináptica tienen lugar, las espinas modifican su morfología y estructura, y eventos de transporte de neurorreceptores tienen lugar. Estos procesos se han relacionado, clásicamente, con cambios en el citoesqueleto de actina, pero de un tiempo a esta parte se ha visto como los microtúbulos (MT) pueden alterar su dinámica en función de la actividad sináptica. Considerando, por una parte, la relación entre el transporte dependiente de MT y el tráfico endosomal; y, por otra, la relación entre el tráfico endosomal y los fenómenos de plasticidad sináptica; nos preguntamos explorar la posible relación entre el transporte mediado por MT y la plasticidad sináptica. Sirviéndonos de un enfoque multidisciplinar, en el que hemos utilizado técnicas de bioquímica, videomicroscopía confocal y electrofisiología, así como el desarrollo de nuevas herramientas moleculares; hemos investigado la interacción entre los receptores AMPA (AMPARs) y miembros de la familia de las kinesinas (KIF5, KIF17) y la dineina durante la expresión de la función sináptica. En concreto, hemos tratado de identificar los dominios de estos motores necesarios tanto para el mantenimiento de la transmisión basal, como para que tenga lugar una correcta plasticidad sináptica en sinapsis excitatorias de CA1 en rodajas de hipocampo.

Así, hemos descubierto que, sorprendentemente, el dominio motor de KIF5 no es necesario ni para el mantenimiento de la transmisión basal, ni para el transporte de las subunidades GluA2 a lo largo de las dendritas. Sin embargo, su actividad motora, así como la de KIF17, sí parece crucial para una correcta expresión de la depresión a largo plazo (“long-term-depression” o LTD). De manera complementaria, hemos descubierto que el mantenimiento de la transmisión basal parece depender de dominios reguladores presentes en la región del cuello-tallo, o de interacciones mediadas por el dominio de unión a cargo de KIF5 o de KIF17. Por último, también hemos estudiado el posible papel del transporte en dirección menos, basado fundamentalmente en la actividad de la dineina. De manera preliminar, podemos concluir que el transporte en dirección menos no es necesario para el mantenimiento de la función sináptica.

Nuestros resultados sugieren que la LTD dependiente de NMDA es un proceso altamente regulado por una gran variedad de mecanismos intracelulares, incluyendo el transporte mediado por MT.

Table of contents

Abbreviations

ACSF artificial cerebrospinal fluid

AMPA α-amino-3-hydroxy-5-methyl-4-isoxazolepropionic acid

AMPAR receptor activated by α-amino-3-hydroxy-5-methyl-4-isoxazolepropionic acid

APP amyloid precursor protein

ATP adenosine triphosphate

BDNF brain-derived neurotrophic factor

BHK baby hamster kidney

CA *cornu ammonis*

CaMKII Ca^{2+}/calmodulin-dependent protein kinase II

cAMP cyclic adenosine monophosphate

cDNA complementary deoxyribonucleic acid

C-KIF proteins of the kinesin superfamily with the motor domain at their C-terminus

cLTD chemical LTD

CNS central nervous system

DG dentate gyrus, *fascia dentate*

DHC dynein heavy chain

DIV days *in vitro*

DNA deoxyribonucleic acid

dpi days post-infection

EDTA ethylenediaminetetraacetic acid

EE early endosome

EEA1	early endosome antigen 1
EGTA	ethylene glycol tetraacetic acid
EPSC	excitatory postsynaptic current
EPSP	excitatory postsynaptic potential
ER	endoplasmic reticulum
ERGIC	ER-Golgi intermediate compartment
FRAP	fluorescence recovery after photobleaching
GFP	green fluorescent protein
GRIP1	glutamate receptor interacting protein 1
GTP	guanosine triphosphate
GTPase	guanosine triphosphatase
HBSS	Hank's buffered salt solution
HEK	human embryonic kidney
HEPES	N-2-hydroxyethylpiperazine-N-2-ethanesulfonic acid.
HRP	horseradish peroxidase
iGluR	ionotropic glutamate receptor
KAP	kinesin associate protein
KBD	kinesin binding domain
KHC	kinesin heavy chain
KIF	kinesin superfamily protein
KLC	kinesin light chain
KO	knock-out
LAMP2	lysosome associate membrane protein 2

LB	lysogeny broth medium
LE	late endosome
-LT	long tail
LTD	long term depression
LTP	long term potentiation
MAPK	mitogen-activated protein kinase
MEM	minimum essential medium
mGluR	metabotropic glutamate receptor
M-KIF	proteins of the kinesin superfamily with the motor domain in the middle
mRNA	messenger ribonucleic acid
MT	microtubule
N-KIF	proteins of the kinesin superfamily with the motor domain at their N-terminus
NLS	nuclear localization sequence
NMDA	*N*-methyl-D-aspartate
NMDAR	receptor activated by *N*-methyl-D-aspartate
PBD	PDZ binding domain
PBS	phosphate buffered saline
PCR	polymerase chain reaction
PDZ	post synaptic density protein (PSD95), drosophila disc large tumor suppressor (Dlg1), and zonula occludens-1 protein (zo-1)
PKA	cAMP-dependent protein kinase A
PKC	protein kinase C

PKMξ	protein kinase M zeta
PLC-PI	phospholipase C-phospoinositide
pSR5	Sindbis replicon, pSinRep5
PVDF	polyvinylidene fluoride
RE	recycling endosome
RFP	red fluorescence protein
RNA	messenger ribonucleic acid
RT-PCR	reverse transcription polymerase chain reaction
SDS	sodium dodecyl sulfate
SDS-PAGE	sodium dodecyl sulfate polyacrylamide gel electrophoresis
shRNA	small hairpin RNA
SNAP25	synaptosomal associated protein 25
-ST	short tail
TBS	tris-buffered saline
TGN	trans-Golgi network

Introduction

The brain can be considered as a circuit, in which neurons would be the wiring. One of its most appealing characteristics is that it is a highly dynamic one, meaning that the connections between the different components can be modulated, created and even destroyed in an experience-dependent manner. This ability is thought to be the underlying mechanism for extraordinary processes such as memory formation and learning.

But, what does this exactly mean? What does memory formation mean on the molecular level? How are memories formed and retrieved when needed? Why do we forget some memories while others seem to be written in stone?

Even if many of these questions can be addressed from a philosophical point of view, Neurobiology has been trying to shed some light into this field for decades.

1. THE NEURON AS THE KEY COMPONENT OF THE CIRCUIT

The Central Nervous System (CNS) is mainly composed of two cell types: neurons and glia. Neurons are highly polarized cells that present three major morphologically and functionally different compartments: the soma from which one axon and dendrites, that might or not be spiny, emerge. In general, the somatodendritic compartment is the input-receiving part, and the axon is the output-emitting one. Besides their high level of polarization and functional regionalization, neurons present two other major characteristics: they are both excitable and secretory cells.

These three characteristics can be reflected in what Cajal established to be the tight contacts that neurons use to communicate with each other and what Sherrington named “synapses”. Synapses can be classified, depending on their transmission mechanism, into electrical or chemical synapses.

Electrical synapses are formed between two cells that are in close apposition, having the pre- and post-synaptic terminal physically connected through gap junctions. In this configuration, current flows passively through the channels from one cell to the next, without needing a chemical transmitter and without delay. These types of synapses are common, for example, between glial cells.

Chemical synapses are formed without physical connection between the two cells involved, and communication occurs using secreted molecules. In neurons, when an action potential reaches the pre-synaptic terminal, voltage-gated calcium channels open

and Ca^{2+} ions diffuse into the terminal. The increase in the concentration of Ca^{2+} in the pre-synaptic terminal results in synaptic vesicles fusing with the plasma membrane, liberating their content (neurotransmitters) to the synaptic cleft (the physical space that, in these synapses separates the pre- from the post-synaptic terminal). Next, neurotransmitter molecules will bind to their specific receptors on the post-synaptic terminal, and specific signaling cascades will be initiated. Chemical synapses can be excitatory or inhibitory, and they are the preferred means of communication between neurons.

2. THE HIPPOCAMPAL CIRCUIT AS A MODEL TO STUDY MEMORY FORMATION AND LEARNING

One of the first and most convincing pieces of evidence suggesting that the hippocampus is a key structure in memory formation comes from the study of one single patient: H.M. He developed severe amnesia after bilateral removal of the medial structures of the temporal lobe for the treatment of epileptic seizures (Penfield and Milner, 1958; Scoville and Milner, 1957).

The hippocampus is a structure that belongs to the limbic system, and that is located in the temporal lobe in primates, whereas in rats it is more of a rostro-caudal structure. It is composed of two interconnected regions: the dentate gyrus (*fascia dentata*, DG) and the Ammon's horn (*cornu Ammonis*, CA), which can be subdivided in several regions; CA1 and CA3 being the most studied ones.

For the questions addressed in this thesis, the so-called tri-neural circuit formed between principal neurons (granular cells of DG, pyramidal cells of CA3 and CA1) is our primary model. Granular cells project their axons, mossy fibers, to CA3 pyramidal cells, to the spines on their apical dendrites. In turn, CA3 send axon collaterals, Schaffer collaterals, to CA1 pyramidal neurons, on the proximal part of their apical dendrites. Obviously, this is not a closed circuit, and there are local connections that superimpose on the main circuit modulating it (Figure 1).

In this thesis, we are interested in the synapses formed between CA3 and CA1, which are excitatory glutamatergic synapses that occur at specialized structures called dendritic spines. Dendritic spines are small protrusions on the dendritic surface that contain organelles, neurotransmitter receptors and all the subcellular machinery, including

cytoskeletal components, needed to transduce the signals that are being received from the excitatory pre-synaptic input (Nimchinsky et al., 2002).

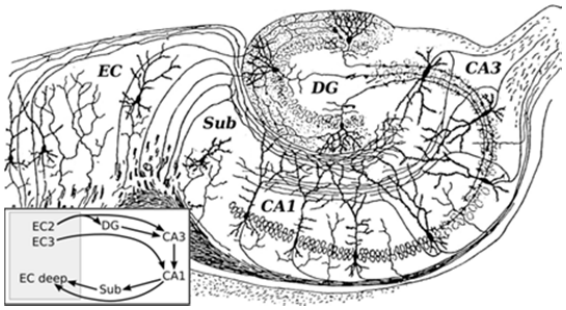

Figure 1. Hippocampal circuit. Drawing of the hippocampus by Santiago Ramón y Cajal (adapted from *Histologie du Systeme Nerveux de l'Homme et des Vertebretes, Vols. 1 and 2.* A. Maloine. Paris. 1911). The arrows indicate the proposed direction of impulse propagation throughout the hippocampus. DG: dentate gyrus. Sub: subiculum. EC: entorhinal cortex.

3. GLUTAMATERGIC EXCITATORY TRANSMISSION

Similarly to the case of other neurotransmitter-mediated signaling, glutamate-mediated transmission in the hippocampus is highly regulated. Once glutamate is released from the pre-synaptic terminal in response to an action potential and it reaches the post-synaptic terminal via synaptic cleft, it can activate several types of receptors, and still lead to very specific signaling.

These receptors are ionotropic α-amino-3-hydroxy-5-methyl-4-isoxazolepropionic acid receptors (AMPARs), *N*-methyl-D-aspartate receptors (NMDARs) (named after their sensitivity to the glutamate analogues) and kainate receptors (Collingridge et al., 2009; Lodge, 2009), as well as G protein-coupled metabotropic receptors (Niswender and Conn, 2010).

3.1. Ionotropic receptors (iGluRs)

To date, 18 cDNAs have been identified by molecular cloning (Dingledine et al., 1999) to be responsible to form glutamate receptor subunits. GluA1- GluA4 form AMPA receptors (AMPARs); GluN1, GluN2A to GluN2D, GluN3A to 3B are involved in the formation of NMDA receptors (NMDARs); and kainate receptors are assembled by the combination of GluK1-3 with GluK4 or 5. All iGluRs are tetramers, dimers of dimers actually, in which each monomer carries a ligand binding site and is composed of an extracellular amino-terminal domain, three transmembrane domains interrupted by a re-entrant loop into the plasma membrane, and the cytoplasmic carboxyl terminus, which can interact with proteins of the post-synaptic density (Madden, 2002) (Figure 2).

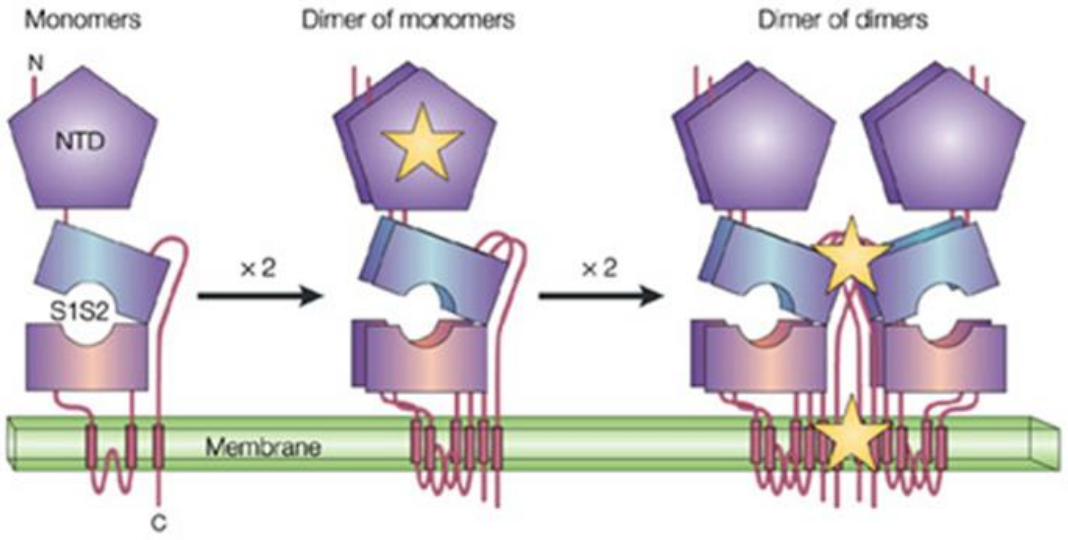

Figure 2. General structure of iGluRs. The amino-terminal domain (NTD), always extracellular, is followed by the S1 half domain, two transmembrane domains separated by a re-entrant P loop where the Q/R editing site is, the S2 half domain and the third transmembrane domain, prior to which the *flip/flop* splicing site is located. The S1 and S2 half-domains form the iGluR ligand-binding domain. Finally, the carboxyl-terminus is located at the cytoplasm, where it can interact with other proteins. Monomers tend to associate by interactions bewteen their NTDs, and dimers do so by interactions between their S2 and/or transmembrane domains. Sites of interaction are indicated with stars (adapted from Madden, 2002).

AMPARs. The speed and duration of AMPAR-mediated synaptic currents varies significantly depending on AMPAR subunit composition and on the splice variant (*flip* or *flop* (Coleman et al., 2006; Pei et al., 2009)) involved. Also, depending on whether they are GluA2 lacking or containing receptors, and to which extent its mRNA is edited, their Ca^{2+} permeability can be affected. In general, AMPARs are also considered highly mobile (Sommer et al., 1991; Tardin et al., 2003).

In our system of study, the adult hippocampus, the combinations GluA1-GluA2 and GluA2-GluA3 are the most abundant ones (Wenthold et al., 1996). AMPARs formed by GluA1-GluA2 dimers participate in regulated trafficking, meaning their delivery to synapses occurs upon induction of activity; whereas the AMPARs composed of GluA2-GluA3 subunit combination are continuously cycling in and out of synapses in what is referred to as “constitutive pathway” maintaining synaptic strength (Passafaro et al., 2001; S. Shi et al., 2001).

NMDARs. In general, they show slower kinetics and much higher permeability to Ca^{2+} than AMPARs, although these properties are also dependent on their subunit composition (Paoletti et al., 2013) They are blocked by Mg^{2+} at resting membrane potential (Mayer et al., 1984; Nowak et al., 1984). As a consequence, they only allow ions influx when the membrane depolarizes (thus relieving Mg^{2+} block) and when their ligand is present.

Kainate receptors. They are both pre- and post-synaptic and they have smaller currents and slower deactivation kinetics than AMPARs (Lerma, 2003). Far less characterized than AMPA and NMDA receptors, they have been shown to play a role in regulating both excitatory and inhibitory transmission (González-González et al., 2012).

3.2. Metabotropic receptors

They can be classified in three groups: I (mGluR1,5), II (mGluR2,3) and III (mGluR4,6,7,8) depending on their localization and mechanism of action. Group I receptors are post-synaptic, and act by coupling to the G protein G_q, activating the phospholipase C-phosphoinositide pathway (PLC-PI). Group II receptors are also post-synaptically represented, but they have a strong presence in the pre-synaptic element, where they are coupled to G protein G_o, inhibiting Ca^{2+} channels and, therefore, inhibiting neurontransmitter release in a negative feedback manner. Lastly, Group III receptors are also predominantly pre-synaptic (except in the ON-bipolar retinal cells), and they also work by inhibiting adenylyl cyclase and Ca^{2+} channels, and activating K^+ ones (Niswender and Conn, 2010).

4. AMPAR-MEDIATED SYNAPTIC TRANSMISION IN THE HIPPOCAMPUS

Synaptic strength can be modified as the consequence of patterns of ongoing activity, and this susceptibility to modification is referred to as synaptic plasticity, which is commonly accepted to be the molecular basis for memory and learning. Speaking from a molecular point of view, modification of synaptic strength relies up to a great extent on the regulated trafficking of receptors (Esteban, 2003) to and from the synapse.

The two most studied forms of synaptic plasticity in the CA1 pyramidal cells of hippocampus are Long-Term Potentiation (LTP) and Long-Term Depression (LTD).

LTP was first described by Bliss and Lømo in 1973 using rabbit hippocampus as a model. They demonstrated that high frequency stimulation of inputs to cells in the dentate gyrus

leads to the increase in the amplitude of excitatory synaptic potentials that lasted for hours, up to 10 hours in some cases (Bliss and Lomo, 1973) (Figure 3).

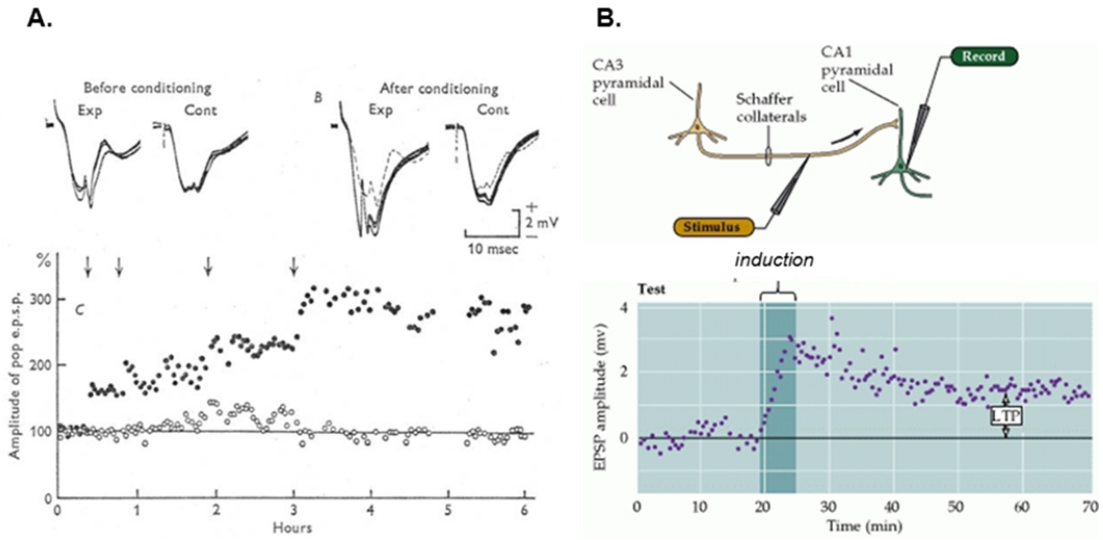

Figure 3. Long Term Potentiation (LTP). A. Recordings from Bliss and Lomo's experiments where LTP was first shown in 1973. **B.** In hippocampus, high frequency stimulation of the Schaffer collaterals can induce a persistent increase in the excitatory postsynaptic currents (EPSCs) or potentials (EPSPs), when coupled to depolarization of the postsynaptic CA1 neuron (adapted from Purves et al., 2001).

Decades after, it is still not clear whether LTP expression is due to pre-synaptic mechanisms (enhancement of neurotransmitter release); post-synaptic ones (increase of the number of receptors); or both (Lisman et al., 2003; Lisman, 2009). However, it is accepted that a key step in the expression of LTP is the entry of Ca^{2+} in the post-synaptic cell through NMDARs. This increase in Ca^{2+} concentration would lead to activation of different intracellular cascades that are required to trigger LTP. In this sense, kinase activation happens after NMDA-dependent LTP induction, i.e., with activation of Ca^{2+}/calmodulin-dependent protein kinase II (CaMKII), cAMP-dependent protein kinase (PKA), protein kinase C (PKC), protein kinase M zeta (PKMξ) or mitogen-activated protein kinase (MAPK) (Malenka and Bear, 2004). As the result of these signaling cascades, additional AMPARs would be inserted into the post-synaptic membrane, increasing sensitivity of the post-synaptic cell to glutamate (Figure 4). It remains to be determined if these newly inserted AMPARs have to contain the GluA1 subunit, as reported (Hayashi,

2000; Lu et al., 2001; S.-H. Shi et al., 2001), or any AMPARs subunit can be called to "step in" and contribute to normal LTP expression (Granger et al., 2013).

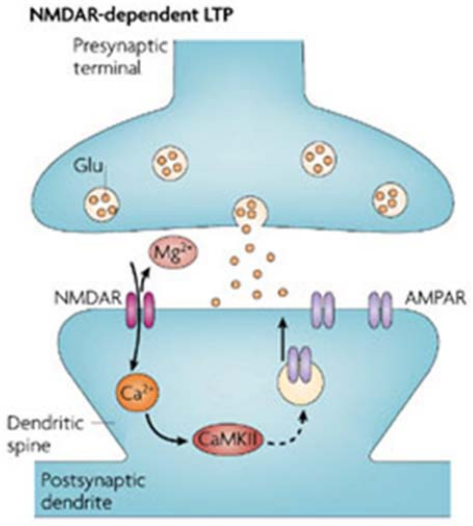

Figure 4. Simplified representation of the molecular consequences of NMDA-dependent LTP. The voltage-dependent relief of the Mg^{2+} block of the NMDAR channel allows the synapse to detect coincident presynaptic release of glutamate (Glu) and postsynaptic depolarization. Different signaling molecules are activated, such as CaMKII, and AMPARs are inserted into the postsynaptic membrane increasing the sensitivity of the post-synaptic cell to glutamate and augmenting synaptic strength (adapted from Kauer and Malenka, 2007).

LTD. The very first evidence for LTD comes from habituation and dishabituation performed in *Aplysia* by Kandel in the 70's (Castellucci et al., 1970). Few years later it was found in rat hippocampus that, opposite to the LTP exhibited by CA1 synapses in response to brief and high frequency stimulation of the Schaffer collaterals, long and low frequency stimulation of the same fibers would lead to a decrease in the excitatory post-synaptic potentials (EPSP) or LTD (Dunwiddie and Lynch, 1978) (Figure 5).

Same as for LTP, there are many induction protocols and still much controversy regarding LTD. However, there are also some common grounds to explain this phenomenon. As for LTP, LTD is dependent on NMDAR activity and changes in intracellular Ca^{2+}. Ca^{2+} changes occurs through extracellular Ca^{2+} permeation via NMDARs and release of Ca^{2+} from intracellular storages (Malenka and Bear, 2004). In the early studies, LTD was also shown to depend mainly on phosphatases such as protein phosphatase 1 (PP1) or 2A (PP2A) (Mulkey et al., 1994), but new evidence is arising proposing roles for kinases in LTD, such as glycogen synthase kinase (GSK)-3 (Peineau et al., 2009) or CaMKII (Coultrap et al., 2014). Subunit specificity has been also proposed: same as GluA1 was thought to be the key player for LTP, GluA2 was thought to be necessary for LTD to occur (Mulkey et al., 1994). However, novel work from Nicoll and colleagues show that LTD can be induced independently of the AMPAR subunits present (Granger and Nicoll, 2014). In

any case, the molecular outcome of NMDAR-dependent LTD consists on the internalization of AMPARs from the post-synaptic density (PSD), leading to a net downregulation of surface receptors and a decrease in the synaptic strength (Figure 6).

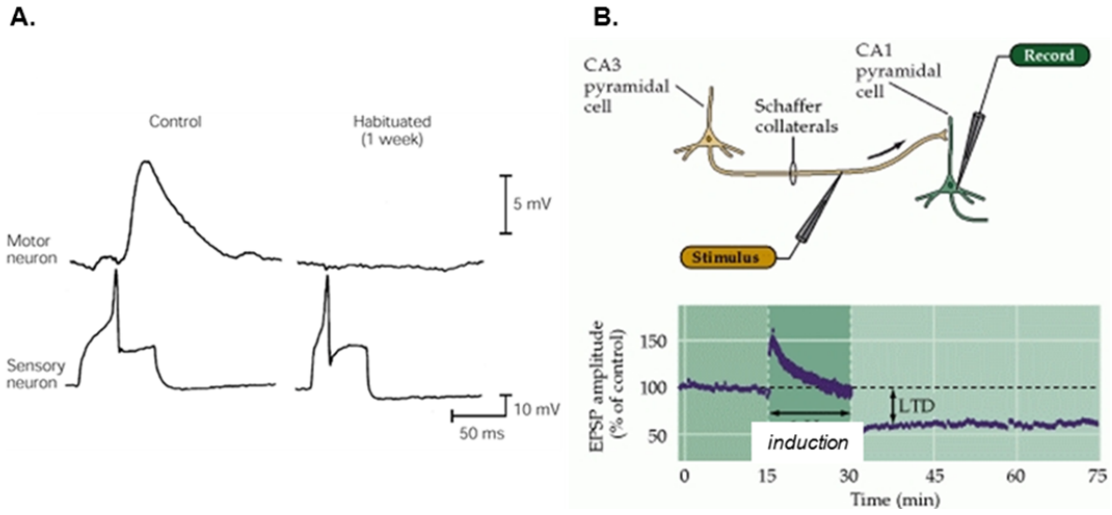

Figure 5. Long Term Depression (LTD). A. Recordings from Kandel and colleagues showing inactivation of synaptic connections by long term habituation in *Aplysia* in 1978, in what is considered to be the first evidence pointing to LTD. **B.** In hippocampus, low frequency stimulation of the Schaffer collaterals coupled to a slight depolarization of the postsynaptic CA1 neuron, causes long-lasting depression of synaptic transmission (adapted from Purves et al., 2001).

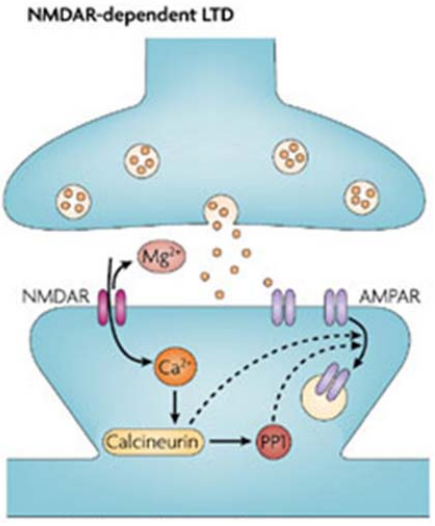

Figure 6. Simplified representation of the molecular consequences of NMDA-dependent LTD. NMDAR-dependent long-term depression is triggered by Ca^{2+} entry through postsynaptic NMDAR channels (once the Mg^{2+} block is release), leading to increases in the activity of the protein phosphatases calcineurin and protein phosphatase 1 (PP1). The major molecular outcome of this type of LTD consists of the internalization of AMPARs (adapted from Kauer and Malenka, 2007).

5. ENDOSOMAL TRAFFICKING

Both for LTD and LTP, trafficking of receptors is critical, and such transport depends highly on the endocytic machinery. The endosomal network consists of a large number of endomembrane compartments devoted to the biosynthetic transport of molecules to and from the surface. These compartments are dynamically interconnected, either by vesicular carriers or by maturation of earlier into later compartments.

Briefly, the route of endomembrane compartments can be described as follows. Compartments coming from the internalization of the plasma membrane are early endosomes (EE), which can traffic to four different destinations: (1) back to the membrane; (2) to late endosomes (LE) that would lead them to lysosomes for degradation; (3) to recycling endosomes (RE) that would be the previous stop before either the plasma membrane or the trans-Golgi network (TGN); or (4) directly to the TGN (Yap and Winckler, 2012) (Figure 7A).

Many of the consecutive stages of endosomal trafficking are controlled by Rab proteins and their effectors. Rab proteins are GTPases that alternate between an active-GTP bound state and an inactive-GDP bound state (Barr and Lambright, 2010; Grosshans et al., 2006). In their GTP-bound state, Rabs recruit their effectors and activate different signaling cascades. Some of these effectors might actually act as adaptor molecules for molecular motors that move along MTs, and that will transport the endomembrane compartment from one station to the next (anterograde transport, usually kinesin dependent) or to the previous one (retrograde transport, usually dynein dependent) (Horgan and McCaffrey, 2011) (Figure 7B).

5.1. Peculiarities of endosomal trafficking in neurons

In polarized cells, such as epithelial cells or neurons, the endosomal pathways get more complicated, as different plasma membrane proteins have to be delivered to functionally different membrane domains. It has been known for long time that MT-dependent transport is essential for proper endosomal trafficking in neurons (Parton et al., 1992).

However, there are still open questions regarding the intrinsic dynamics, localization and architecture of the endoplasmic reticulum (ER), ER-Golgi intermediate compartment (ERGIC), Golgi apparatus and post-Golgi compartment in neurons . The ER is an irregular network, with a variety of microdomains, which extends along the axon and the dendrites.

It is a very dynamic structure that can be found in close proximity to the plasma membrane and also inside dendritic spines. The Golgi apparatus in hippocampal neurons is a perinuclear organelle, but it presents additional satellite structures, the Golgi outposts, distributed throughout the whole dendritic arbor (Ramírez and Couve, 2011).

Regarding endosomes *per se* in neurons, they are known to present differences in their sorting abilities and in their recruitment of Rabs and other adaptors. For instance, the fusion of EE is thought to require the early endosomal regulator (EEA1), a Rab5 effector, but EEA1 is only present in the somatodendritic endosomes and not in the axonal ones. Suggesting that endosomes are also polarized when they are in polarized cells (Yap and Winckler, 2012).

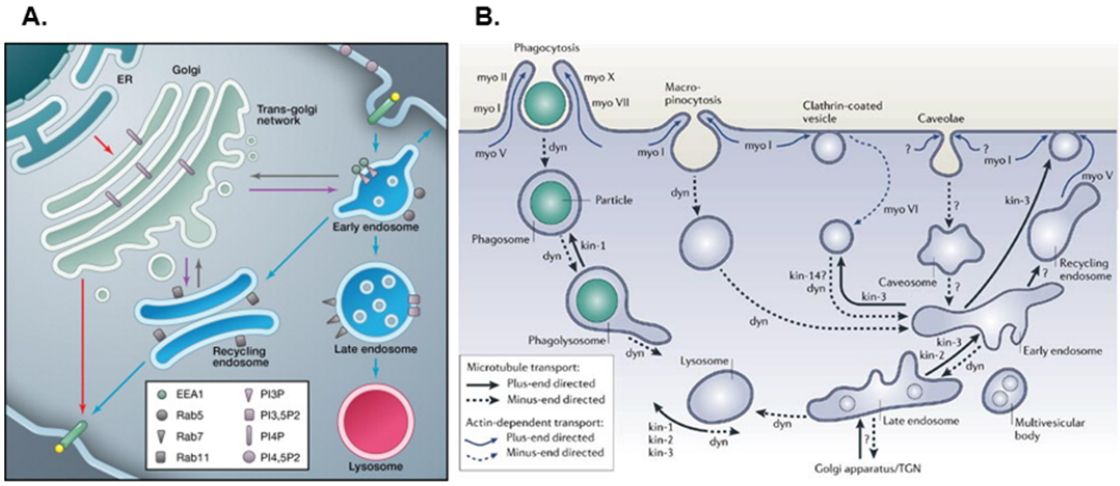

Figure 7. Traffic of endomembrane compartments in non-polarized cells. A. Schematic representation of the endocytic pathway in a non-polarized cell where the different Rabs and phosphoinositides (PIs) are shown as markers of the main different compartments. **B.** Involvement of motor proteins myosin (myo), kinesin (kin) or dynein (dyn) in the transport of endomembrane compartments. Dotted arrows correspond to minus-end directed transport, (black arrows, actin cytoskeleton; blue arrows, MT cytoskeleton); and solid arrows correspond to plus-end directed transport (Soldati and Schliwa, 2006; Yap and Winckler, 2012).

5.2. Interactions between the endosomal network and molecular motors in neurons

For instance, KIF5 has been shown to interact with Rab4, Rab6, Rab11 and Rab27 (Granger et al., 2014; Horgan and McCaffrey, 2011; Matsuzaki et al., 2011). Dynein/dynactin has also been proven to bind to different endosomal compartments, such

as Rab4 (Granger et al., 2014) or Rab11 positive (Horgan and McCaffrey, 2011) ones. In this case, a particularly interesting association is between dynactin and Rab7 via the adaptor RILP, which recruits dynein to the LE/lysosomal compartment (Johansson et al., 2007; Jordens et al., 2001; Tan et al., 2011).

The Rab proteins have been involved in synaptic plasticity (Baskys et al., 2007). Rab5 participates in endocytic processes during NMDAR-dependent LTD (Brown et al., 2005). Rab8 is implicated in the exocytosis that occurs during AMPA basal transmission and during LTP (Brown et al., 2007; Gerges et al., 2004). Rab7 has been shown to regulate the lysosomal degradation of AMPARs upon LTD expression (Fernández-Monreal et al., 2012). Finally, Rab11 directs recycling and comeback to the plasma membrane of AMPARs after LTD induction (Fernández-Monreal et al., 2012), as well as the insertion of endosomes into the spines upon NMDAR-activation (Brown et al., 2007).

6. MICRTOTUBULE-DEPENDENDT TRANSPORT DURING SYNAPTIC ACTIVITY: KIF5, KIF17 AND DYNEIN

Neurons are highly polarized cells that need to have differential and highly regulated delivery of organelles, proteins, etc, to different subcellular locations that could be very distant from each other. Therefore, the maintenance of a proper transport system is crucial, and for that the cytoskeleton plays a central role.

There are three main types of cytoskeletal tracks: actin filaments, microtubules (MTs) and a group of polymers known collectively as intermediate filaments. All three are responsible for the control of the shape and the mechanics of eukaryotic cells, as they are organized in highly resistant, but at the same time very dynamic networks (Fletcher and Mullins, 2010). As little is known about the relationship between MT-dependent transport and synaptic plasticity, we wanted to expand the knowledge on this topic.

AMPAR trafficking occurs at two levels: along dendrites and within the dendritic spine. AMPARs, as many other proteins, are mainly synthesized in the vicinity of the soma, and then they are transported in a regulated manner to their final destination, contributing to the maintenance of the neuronal polarity and functional regionalization (Kennedy and Ehlers, 2006; Shepherd and Huganir, 2007). This dendritic transport occurs in a MT-dependent manner, as MTs have been shown to be the major cytoskeletal components of the dendrites. Molecular motors, kinesins and dyneins, transport cargo vesicles along MTs

in a regulated, energy-consuming and oriented manner (Goldstein and Yang, 2000). However, transport within the spine, is consider to rely mainly on the actin cytoskeleton and myosin motors (Kneussel and Wagner, 2013).

This association of dendrites with MTs vs. association of actin with spines comes from years of imaging and biochemical studies, where an almost perfect segregation was systematically observed (Hotulainen and Hoogenraad, 2010; Korobova and Svitkina, 2010; Matus, 2000; Schubert and Dotti, 2007). However, circa 2009 several groups showed independently, that such segregation is not absolute, and that MT-associated proteins such as EB3 or even MTs themselves can enter spines in an activity dependent manner and during dendritic spine development (Dent et al., 2011; Gu et al., 2008; Hoogenraad and Bradke, 2009; Hu et al., 2008; Jaworski et al., 2009; Merriam et al., 2011; Penzes et al., 2009). Therefore, the possible role of MTs and MT-associated transport remains an open and appealing question.

6.1. Microtubules in neurons

MTs are polarized structures composed of α- and β-tubulin heterodimer subunits assembled into linear protofilaments that associate laterally to form a hollow cylinder. The αβ dimers are oriented within the MT, leaving the α subunit oriented to the slower-growing (minus) end and the β facing the fast-growing (plus) end. They are also highly dynamic structures that can undergo cycles of rapid depolymerization (catastrophe) or polymerization (rescue), in a characteristic that is referred to as “dynamic instability” (Conde and Cáceres, 2009).

MTs present different properties depending on the tubulin isoforms they are made of and on post-translational modifications that they might have suffered (tyrosination, detyrosination, acetylation, polyglutamylation, polyglycylation, phosphorylation and

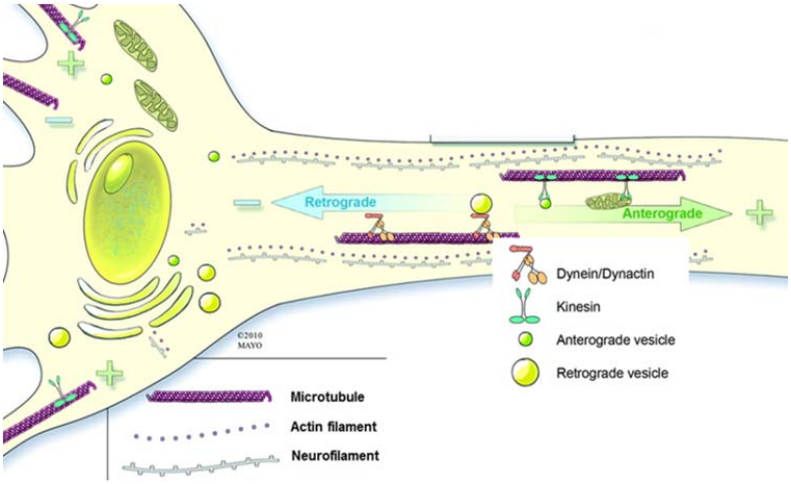

Figure 8. Cytoskeletal tracks in neurons and MT-dependent motors. (Adapted from Staff et al., 2011).

palmitoylation), which affect their binding affinity to different proteins. For instance, KIF5 presents preferential affinity for detyrosinated MTs (Konishi and Setou, 2009; Prota et al., 2013).

Regarding their distribution in the neuron, MTs present the same orientation in the axon, with the minus-end towards the soma, which makes distinction between anterograde (plus-end directed) and retrograde (minus-end directed) transport fairly simple (Figure 8). However, MTs in dendrites (at least in the proximal part) present mixed polarities (Kapitein and Hoogenraad, 2011).

6.2. Kinesins

Kinesin superfamily proteins (KIFs) conform an abundant family classified into 14 classes. They contain a motor domain, a neck and stalk domain (composed of a different number of coil-coiled regions), and a tail or cargo binding domain. They are classified into three major groups depending on whether the motor domain is at the N-terminus (N-KIFs), in the middle of the protein (M-KIFs), or at the C-terminus (C-KIFs). The position of the motor domain determines their speed and their directionality: N-KIFs move towards the plus end of MTs, M-KIFs do not undergo directed motility but instead destabilize MTs, and C-KIFs move towards the minus end of MTs (Hirokawa et al., 2010; Verhey and Hammond, 2009) (Figure 9).

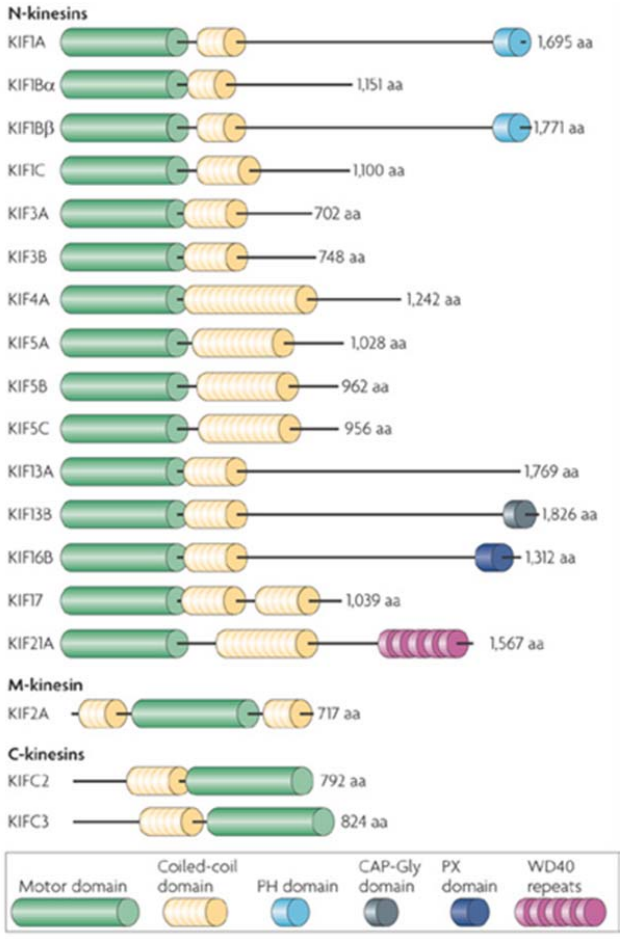

Figure 9. Domain structure of the major kinesins. (Adapted from Hirokawa et al., 2009).

Normally, the motor domain binds to MTs and moves on them by hydrolyzing ATP, while the tail region recognizes and binds the cargo (Hirokawa and Noda, 2008).In some rare cases, the cargo binding can also happen through the stalk region, as in the case of KIF1-

DENN/MAD-Rab3 binding (Niwa et al., 2008). Most of them exist in the cell as homodimers, as KIF17. They can also exist as heterotetramers composed of two different subunits, as the case of Kinesin-1, that is formed by two heavy and two light chains (KHC, actually KIF5, and KLC), heterotrimers, as KIF3A-KIF3B-kinesin-associated protein (KAP), homotetramers, as Kinesin-5 family members, or even monomers, as the case of Kinesin-3 family members (Verhey and Hammond, 2009).

For the reasons explained below, we initially focused our attention on the study of KIF5 and KIF17.

KIF5 (also called KHC, conventional kinesin, or Kinesin-1). KIF5 was the first kinesin to be identified, and the 3 subtypes, KIF5a, KIF5b and KIF5c, have been identified so far. They present very high homology at the amino acid sequence level, except for two regions: one after the motor domain, and one at the very end of the tail domain (Kanai et al., 2000). KIF5b is ubiquitously expressed, while KIF5a and KIF5c are neuron specific. KIF5c is indeed the most abundant one in neuons. Structurally speaking, they can exist in several combinations: homodimers, heterodimers, and tetramers, as they can bind two kinesin light chains (KLCs) through light chain-binding domains present in stalk and tail domains (Hirokawa and Noda, 2008).

It is well known that KIF5 is a promiscuous protein, in the sense that it can bind many cargoes through several adaptors, playing a major role in fast anterograde axonal transport. Among any other cargoes, it has been shown to bind to mitochondrial proteins, lysosome associated membrane protein 2 (LAMP2), synaptotagmin, syntaxin 1, synaptosomal associated protein 25 (SNAP25), amyloid precursor protein (APP), mRNAs, TrkB receptor, and retrograde motors among many other cargoes (Hirokawa et al., 2009). However, our main focus of interest is the role of KIF5 in dendritic transport,

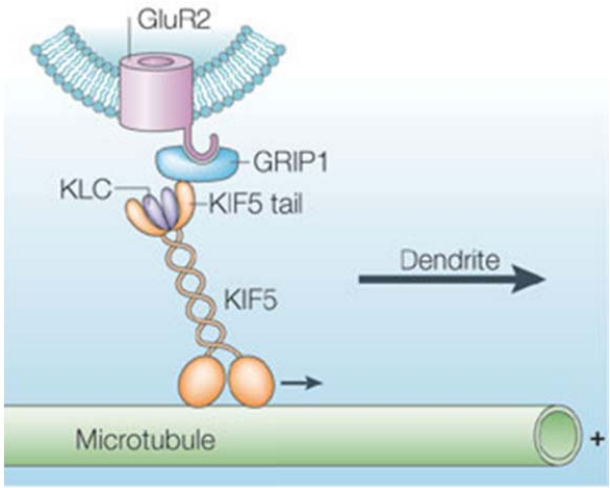

Figure 10. Structure of the KIF5-GRIP1-GluA2 complex. Proposed assembly of this complex based on moleculaarl, biochemical and imaging data (adapted from Hirokawa et al., 2010).

which has been extensively studied (Figure 10). Biochemical experiments, mainly coming from Hirokawa and collaborators, have shown that KIF5 binds glutamate receptor interacting protein 1 (GRIP1) in two-yeast hybrid assays, as well as that it coprecipitates in the same complex as GRIP1 and GluA2 (Setou et al., 2002). By using different *dominant* negative constructs, imaging experiments have shown that, at least in primary hippocampal cultures, the interaction between KIF5 and GRIP1 is needed for normal targeting of GluA2 to the dendritic surface (Hoogenraad et al., 2005). Finally, electrophysiological data suggests that the KIF5-GRIP1-GluA2 complex is required for the maintenance of glutamatergic transmission, since when it is disrupted by the overexprerssion of mutant hungtintin, an impairment in AMPA-mediated currents is observed (Mandal et al., 2011).

These evidences made KIF5 a very appealing candidate to study its possible role in synaptic plasticity in the hippocampus. Specifically, we were interested in KIF5c (the predominant isoform in neurons) as knocking out its gene in mice did not present a lethal effect, in contrast with KIF5a and KIF5b knockouts (Kanai et al., 2000; Tanaka et al., 1998; Xia et al., 2003). These data suggest that KIF5c would not be as crucial as KIF5a or KIF5b, but relevant in a modulatory fashion.

KIF17. It is the homomeric molecular motor of the Kinesin-2 family, and unlike KIF5, it is dendrite-specific. Hirokawa's group used again the yeast-two hybrid method to isolate KIF17 and its binding partners, along with imaging experiments to verify those findings. KIF17 directly interacts with a PDZ domain of m-Lin10 (Mint1/X11), that belongs to a bigger complex formed by m-Lin2 (CASK) and m-Lin7 (MALS/Velis), and with GluN2B (Setou et al., 2000) (Figure 11). Moreover, cellular knockdown or functional blockade of KIF17 causes a decrease on both net and

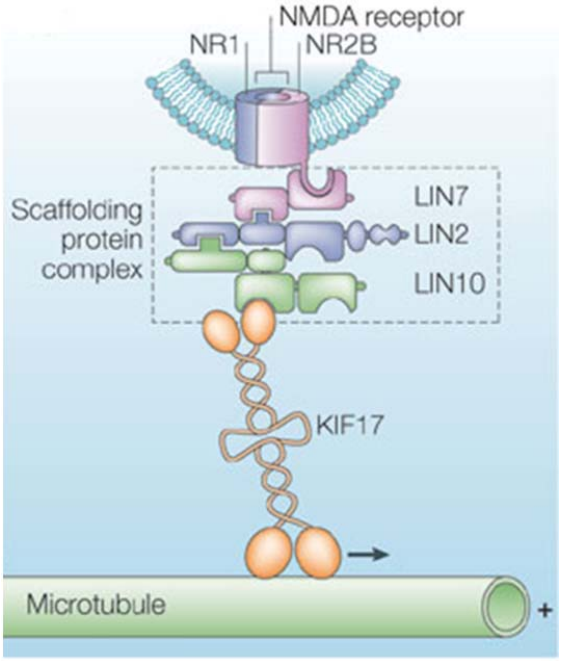

Figure 11. Structure of the KIF17-mLin10-GluN2 complex. Proposed assembly of this complex based on molecularl, biochemical and imaging data. KIF17 binds to mLin10 directly via a PDZ interaction (adapted from Hirokawa et al., 2010).

synaptic levels of GluN2B (Guillaud et al., 2003).

But the most convincing data to support that KIF17 is responsible for the transport of NMDARs comes from the functional experiments done by the same group using two different mouse models: one that overexpresses KIF17 (Wong et al., 2002) and another one where KIF17 is knocked-out (KO) (Yin et al., 2011). Their data point to a positive feedback-loop in which the more KIF17 is present, the more GluN2B is synthesized in a CREB-dependent manner. And concomitantly, the more GluN2B is synthesized, the more KIF17 is needed and, therefore, synthesized too. Furthermore, the results of behavioral experiments show that transgenic animals that present more KIF17 actually conduct better than their wild-type littermates when it comes to perform spatial learning and working memory related tasks. The KO model confirmed these results, and showed decreased NMDAR-mediated synaptic currents and decreased NMDAR-dependent plasticity.

Besides NMDAR-containing vesicles, KIF17 has been shown to transport other cargoes, although not as many as KIF5. Some examples are: the potassium channel Kv4.2, several mRNAs, ciliary components and even the kainate receptor subunits GluK5 and GluK6 (Wong-Riley and Besharse, 2012).

Based on these properties, KIF17 presented itself as a good control to compare it with KIF5.

6.3. Dynein

Dynein superfamily proteins include cytoplasmic dyneins and axonemal/ciliary/flagellar dyneins. They form megastructures with two heavy chains, four intermediate light chains, and several light chains (Karki and Holzbaur, 1999; Pfister et al., 2006). There are only two family members: DYNC1H1, the one involved in the minus-end directed transport both in axons and dendrites, and DYNC2H1, mainly

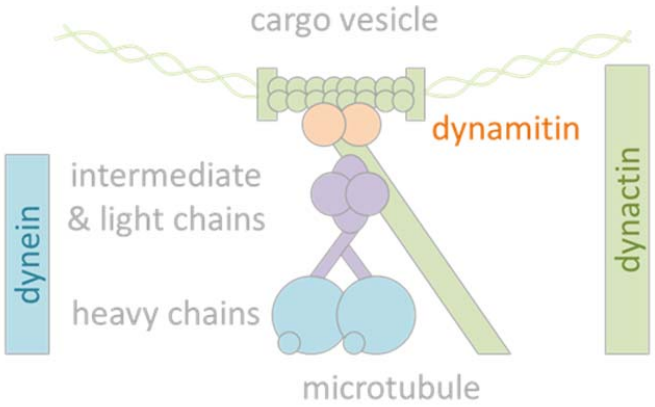

Figure 12. Structure of the dynein-dynactin complex.

associated with intraflagellar transport (Hirokawa et al., 2010). Cytoplasmic dynein also has an associated complex, dynactin, formed by several proteins including dynamitin or p50 (its relevance will be explained in the Results section) that regulates dynein activity and binding capacity (Schroer, 2004) and that has been described to disrupt the assembly of the dynein-dynactin complex when overexpressed (Burkhardt et al., 1997) (Figure 12).

Dynein has been shown to transport several cargoes, also through several adaptor proteins, such as brain-derived neurotrophic factor (BDNF) vesicles, glycine receptor, Rab5-endosomes, TrkA and TrkB receptors, neurotrophin receptors or active-zone-protein vesicles, among many others (Hirokawa et al., 2010).

Dynein was also an interesting candidate of study, not only because of its role as a minus-end directed motor, but because it is the molecular motor responsible for most of the inward endosomal trafficking (Figure 7B).

In the context described above, we can see that MT-dependent transport is intimately related to endosomal trafficking, which is a key player in maintenance and modulation of synaptic function. We can also see that synaptic activity has been shown to regulate MT-dynamics. Therefore, our hypothesis is that MT-dependent transport, via kinesins and/or dynein, can play a modulatory and novel role in regulating synaptic function.

Objectives

The main goal of the present work was to address whether microtubule (MT)-dependent transport is relevant in the maintenance or modulation of synaptic plasticity processes in the hippocampus. To this end, two objectives were proposed:

1. Design and validation of molecular tools that interfere with MT–dependent transport.

2. Evaluation of the effects of these tools on basal synaptic transmission and synaptic plasticity paradigms.

Materials and Methods

1. MATERIALS

For simplicity, solutions and antibodies are listed in tables below. Origin of other reagents such as commercial kits, restriction enzymes or drugs are specified there where their use is explained.

1.1. Solutions and media

Solutions and Media	Composition
ACSF	119 mM NaCl, 2.5 mM KCl, 1 mM NaH_2PO_4, 11 mM glucose, 26 mM $NaHCO_3$, 4 mM $MgCl_2$ and 4 mM $CaCl_2$ (osmolarity 290 mOsm)
Internal solution for electrophysiological recordings	115 mM cesium methanesulfonate, 20 mM CsCl, 10 mM HEPES, 2.5 mM $MgCl_2$, 4 mM Na_2ATP, 0.4 mM Na_3GTP, 10 mM sodium phosphocreatine, and 0.6 mM EGTA (pH 7.25)
Dissection solution for organotypic hippocampal slices	10 mM glucose, 4 mM KCl, 26 mM $NaHCO_3$, 233 mM sucrose, 5 mM $MgCl_2$ and 1 mM $CaCl_2$, (pH 7.4 adjusted with carbogen: 95% O_2 and 5% CO_2)
Dissection solution for primary hippocampal dissociated cultures	1X HBSS (Hank's Balanced Salt Solution, GIBCO #14065-056), 11 mM HEPES pH 7.3, 1X Antibiotics
Culture medium for organotypic hippocampal slices	MEM powder (SIGMA #4642), 20% horse serum (Invitrogen #26050-088), 1 mM L-glutamine, 1 mM $CaCl_2$, 2 mM $MgSO_4$, 1 mg/L insulin, 0.0012% ascorbic acid, 30 mM HEPES, 13 mM D-glucose, and 5.2 mM $NaHCO_3$ (pH 7.25 – 7.26, osmolarity 320 mOsm)
Plating medium for primary hippocampal dissociated cultures	MEM (prepared at a facility at the CBMSO), 20% D-Glucose, 10% Horse serum (Invitrogen)

Culture medium for primary hippocampal dissociated cultures	Neurobasal (GIBCO #12348-017), B27 supplement (GIBCO #17504-044), 0.2 mM L-glutamine
Culture medium for Human Embryonic Kidney (HEK) and Baby Hamster Kidney (BHK) cells	MEM, 2mM glutamine, 5% FBS
Borate Buffer	0.05 M Boric Acid, 0.01 M Na-Borate (pH 8.5)
Poly-L-Lysine	0.1 mg/ml (prepared in borate buffer)
PBS 1X	137 mM NaCl, 2.7 KCl, 10 mM Na_2HPO_4, 1.75 mM KH_2PO_4 (pH 7.4)
Fixative solution	4% paraformaldehyde, 4% sucrose (prepared in PBS 1X)
Homogenization buffer for protein extracts	150 mM NaCl, 10 mM HEPES, 1% Triton X-100, 10 mM EDTA, and a cocktail of proteases (Roche #04 693 159 001) and phosphatases (Roche #04 906 837 001) inhibitors
Running buffer for SDS-PAGE	Tris-glycine, 0.1% SDS
Transfer buffer for SDS-PAGE	Tris-glycine, 10% to 20% Ethanol (v/v), 0.1% SDS (optionally, just in cases where the proteins to transfer are very large)
Loading sample buffer for SDS-PAGE (5X)	125 mM Tris-HCl, 20% Glycerol, 4% SDS, 0.02% DTT
Loading sample buffer for DNA electrophoresis	1.5 M Sucrose, 1 mM EDTA, 38% Glycerol
TBS (10X)	0.1 M Tris, 1.5 M NaCl (adjust pH 7.4 with HCl)
TBS-Tween (10X)	0.1 M Tris, 1.5 M NaCl, 0.5% Tween-20 (adjust pH 8.0 with HCl)
Red Ponceau	1% Red Ponceau, 1% Acetic Acid
LB	1% Triptone, 0.5% Yeast extract, 171 mM NaCl

1.2. Antibodies

Primary Antibodies	Species	Provider	Use (WB)
Anti-Actin, clone C4	Mouse	Millipore	1:2000
Anti-mCherry	Rabbit	GeneTex	1:5000
Anti-GFP	Mouse	Roche	1:1000
Anti-KIF5c	Rabbit	Abcam	1:1000
Anti-KIF17 (M-20)	Goat	Santa Cruz	1:200
Anti-Dynein HC (R-325)	Rabbit	Santa Cruz	1:200
Anti-KIF1A	Rabbit	Abcam	1:1000
Anti-KIF3A	Rabbit	Abcam	1:1000
Anti-KIF13A (C-20)	Goat	Santa Cruz	1:200

Secondary Antibodies	Species	Provider	Use (WB)
Anti-Mouse HRP	Donkey	Jackson	1:6000 (50% Glycerol)
Anti-Rabbit HRP	Donkey	Jackson	1:6000 (50% Glycerol)
Anti-Goat HRP	Rabbit	SIGMA	1:6000 (50% Glycerol)

2. METHODS

2.1. Cloning of DNA constructs

To generate most of the DNA constructs used in this project, the same general protocol was used. Cloning strategies were designed using pDraw32 DNA Analysis Software (Acaclone Software). Both *insert* and *vector* were digested with the restriction enzymes of interest (from NewEnglandBiolabs, and with their corresponding buffers) at either 25°C or 37°C for 3 hours – overnight, always following manufacturer's instructions. Once digestion was done, DNA fragments of interest were normally gel-purified using commercial kits from either Quiagen or Machery-Nagel. Ligation of the fragments was done using the

TaKaRa DNA Ligation Kit (Clontech) and incubating the fragments for 1 hour – overnight at 16°C prior to transformation of the competent bacteria.

All the clonings and DNA amplifications were done using DH5α bacteria prepared at the Microbiology facility in the Centro de Biología Molecular "Severo Ochoa" CBMSO, UAM-CSIC. Bacteria were transformed following a general heat shock protocol (Froger and Hall, 2007), and plated on LB + agar plates with the corresponding antibiotic (either ampicillin or kanamycin) to allow selection of positive clones. Prospective positive colonies were picked from the plates, and verified either by doing "minipreps" (small-scale DNA preparation kit from either Quiagen or Machery-Nagel) followed by restriction pattern analysis or by doing colony-PCR (using bacterial colonies as a template for an specific PCR). Once positives were confirmed, DNA of interest was amplified by doing "maxipreps" (large-scale DNA preparation, using a commercial kit from either Quiagen or Machery-Nagel) and ultimately verified by sequencing with the adequate primers (SIGMA) using Macrogen sequencing services.

Specifics of cloning strategies and origins of the plasmids used are described below:

- **eGFP-GluA2 (RQ)**

This plasmid was a kind gift from Dr. Roberto Malinow (University of California, San Diego) (S. Shi et al., 2001).

- **mCherry-KIF5c-LT, pSR5-mCherry-KIF5c-LT**

mCherry-KIF5c-LT, where LT stands for Long Tail corresponds to the plasmid mCherry-KIF5c (566-955) that was a gift from Dr. Kristen J. Verhey (University of Michigan). Then, it was subcloned by ligation into the corresponding pSR5 vector (Invitrogen).

- **eGFP-KIF17-LT, pSR5-eGFP-KIF17-LT**

eGFP-KIF17-LT, where LT stands for Long Tail corresponds to the plasmid eGFP-KIF17b (343-1029) that was a gift from Dr. Kristen J. Verhey (University of Michigan). Then, it was subcloned by ligation into the corresponding pSR5 vector (Invitrogen).

- **mCherry-KIF5c-ST, pSR5-mCherry-KIF5c-ST**

mCherry-KIF5c-ST, where ST stands for Short Tail corresponds to the plasmid mCherry-KIF5c (908-955) that was generated by PCR amplification using mCherry-KIF5c-LT as a

template. The fragment of interest was amplified (primers in table below), and subsequently digested with *Sac*II and *BsR*GI to generate the *insert*. The *insert* was cloned in the same restriction sites of mCherry-KIF5c-LT (substituting KIFc-LT with KIF5c-ST). Then, it was subcloned by ligation into the corresponding pSR5 vector (Invitrogen).

Sense Oligo	5'-CGATGATGTACAGCGCCAAGAACATGGCCAGGAGGG-3'
Antisense Oligo	5'-CGATGTCCGCGGTTCATGCTACGTGGGGTCATATTCTGC-3'

- **mCherry-KIF17-ST, pSR5-mCherry-KIF17-ST**

mCherry-KIF17-ST, where ST stands for Short Tail corresponds to the plasmid mCherry-KIF17 (801-1021) that was generated by PCR amplification using pCitrine-KIF17b (801-1029), also a gift from Dr. Kristen J. Verhey (University of Michigan), as a template. The fragment of interest was amplified (primers in table below), and subsequently digested with *Sac*II and *BsR*GI to generate the *insert*. The *insert* was cloned in the same restriction sites of mCherry-KIF5c-LT (substituting KIFc-LT with KIF5c-ST). Then, it was subcloned by ligation into the corresponding pSR5 vector (Invitrogen).

Sense Oligo	5'-CCGGGATCACTCTCGGCATGGACGAGC-3'
Antisense Oligo	5'-GGATGTCCGCGGTCAGGTGAAAGGGATGTCGAGGGACTC-3'

- **eGFP-GRIP1-KBD, pSR5-eGFP-GRIP1-KBD**

eGFP-GRIP1-KBD where KBD stands for Kinesin Binding Domain was generated by María Muñoz in the Esteban Lab by PCR using the adequate primers (see table below) and using a longer GRIP1 version as template, which was a gift from Dr. Daniel Choquet (Interdisciplinary Institute for NeuroSciences, Bordeaux). Then, it was subcloned by ligation into the corresponding pSR5 vector (Invitrogen).

Sense Oligo	5'-GACAGCCTCGAGCAGACAGATGCTCAACCTGCCTC-3
Antisense Oligo	5'- GACAGCCCGCGGCTAGTGAAGCTCCACGGGAGTTGGGGAC-3'

- **eGFP-Dynamitin, pSR5-eGFP-Dynamitin**

Coding sequence of Dynamitin was a gift from Dr. Fernando Martín-Belmonte (Centro de Biología Molecular "Severo Ochoa" CBMSO, UAM-CSIC, Madrid). It was then subcloned by in-frame ligation into eGFP-C1 (Clontech) and pSR5 (Invitrogen) vectors.

- **mRFP**

This plasmid was generated by Dr. Mónica Fernández-Monreal in the Esteban Lab (Centro de Biología Molecular "Severo Ochoa" CBMSO, UAM-CSIC, Madrid).

- **KH1-LV-mCherry**

This plasmid was generated by Dr. Rocío Palenzuela in the Esteban Lab (Centro de Biología Molecular "Severo Ochoa" CBMSO, UAM-CSIC, Madrid).

- **KH1-LV-mCherry-shKIF5a**

Short pairs of oligonucleotides from SIGMA, specifically targeting KIF5a sequence to downregulate its expression (Konishi and Setou, 2009), were subcloned into the corresponding KH1-LV vector, gift from Dr. María S. Soengas (Centro Nacional de Investigaciones Oncolológicas, CNIO-ISCIII, Madrid).

Sense Oligo	5'- AGA TCC GTT CGC TCA CGG ATT CAA GAG ATC CGT GAG CGA ACG GAT CTT TTT TTG T -3'
Antisense Oligo	5'- CTA GAC AAA AAA AGA TCC GTT CGC TCA CGG ATC TCT TGA ATC CGT GAG CGA ACG GAT CT -3'

- **KH1-LV-mCherry-shKIF5c**

Short pairs oligonucleotides from SIGMA, specifically targeting KIF5c sequence to downregulate (Konishi and Setou, 2009), were subcloned into the corresponding KH1-LV vector, gift from Dr. Maria S. Soengas (Centro Nacional de Investigaciones Oncolológicas, CNIO-ISCIII, Madrid).

Sense Oligo (I)	5'- GGA TCT TCA AAC TCC ACT CTT CAA GAG AGA GTG GAG TTT GAA GAT CCT TTT TTG T -3'
Antisense Oligo (I)	5'- CTA GAC AAA AAA GGA TCT TCA AAC TCC ACT CTC TCT TGA AGA GTG GAG TTT GAA GAT CC -3'

Sense Oligo (II)	5'-CGG ACT CCA ACA GGA AGA TTT CAA GAG AAT CTT CCT GTT GGA GTC CGT TTT TTG T-3'
Antisense Oligo (II)	5'-CTA GAC AAA AAA CGG ACT CCA ACA GGA AGA TTC TCT TGA AAT CTT CCT GTT GGA GTC CG-3'

- **KH1-LV-mCherry-shKIF17**

Short pairs oligonucleotides from SIGMA, specifically targeting KIF17 sequence (GeneBank accession number XM_003754135.1) to downregulate its expression were designed using the online tool http://www.genelink.com/ (January, 2013). They were subcloned into the corresponding KH1-LV vector, gift from Dr. María S. Soengas (Centro Nacional de Investigaciones Oncolológicas, CNIO-ISCIII, Madrid).

As none of the sequences assayed so far seem to cause a downregulation in the levels of expression of KIF17, the oligos are not detailed here.

- **KH1-LV-mCherry-shDHC**

Short pairs of oligonucleotides from SIGMA, specifically targeting DHC sequence (GeneBank accession number NM_019226) to downregulate its expression were designed using the online tool http://www.genelink.com/ (January, 2013). They were subcloned into the corresponding KH1-LV vector, gift from Dr. María S. Soengas (Centro Nacional de Investigaciones Oncolológicas, CNIO-ISCIII, Madrid).

Sense Oligo (I)	5'-GAT GTG GAT GAG AAG CGT TTT CAA GAG AAA CGC TTC TCA TCC ACA TCT TTT TTG T-3'
Antisense Oligo (I)	5'-CTA GAC AAA AAA GAT GTG GAT GAG AAG CGT TTC TCT TGA AAA CGC TTC TCA TCC ACA TC-3'
Sense Oligo (II)	5'- ATG TGG ATG AGA AGC GTT CTT CAA GAG AGA ACG CTT CTC ATC CAC ATT TTT TTG T-3'
Antisense Oligo (II)	5'- CTA GAC AAA AAA ATG TGG ATG AGA AGC GTT CTC TCT TGA AGA ACG CTT CTC ATC CAC AT -3'

- **KH1-LV-mCherry-shKIF1A**

Short pairs of oligonucleotides from SIGMA, specifically targeting KIF1A sequence (GeneBank accession number XM_34360) to downregulate its expression were designed

using the online tool http://www.genelink.com/ (May, 2014). They were subcloned into the corresponding KH1-LV vector, gift from Dr. María S. Soengas (Centro Nacional de Investigaciones Oncolológicas, CNIO-ISCIII, Madrid).

As none of the sequences assayed so far seem to cause a downregulation in the levels of expression of KIF1A, the oligos are not detailed here.

- **KH1-LV-mCherry-shKIF13A**

Short pairs of oligonucleotides from SIGMA, specifically targeting KIF13A sequence (GeneBank accession number NM_001107462) to downregulate its expression were designed using the online tool http://www.genelink.com/ (May, 2014). They were subcloned into the corresponding KH1-LV vector, gift from Dr. María S. Soengas (Centro Nacional de Investigaciones Oncolológicas, CNIO-ISCIII, Madrid).

As none of the sequences assayed so far seem to cause a downregulation in the levels of expression of KIF13, the oligos are not detailed here.

- **KH1-LV-mCherry-shKIF3A**

Short pairs of oligonucleotides from SIGMA, specifically targeting KIF3A sequence (GeneBank accession number NM_053377) to downregulate its expression were dedigned using the online tool http://www.genelink.com/ (May, 2014). They were subcloned into the corresponding KH1-LV vector, gift from Dr. María S. Soengas (Centro Nacional de Investigaciones Oncolológicas, CNIO-ISCIII, Madrid).

Sense Oligo (I)	5'-AAA TCA GAG AAG CCA GAA AGC TTC AAG AGA GCT TTC TGG CTT CTC TGA TTT TTT TTT GT-3'
Antisense Oligo (I)	5'-CTA GAC AAA AAA AAA TCA GAG AAG CCA GAA AGC TCT CTT GAA GCT TTC TGG CTT CTC TGA TTT-3'
Sense Oligo (II)	5'-TGC GAC AAC GTG AAG GTA GTT TTC AAG AGA AAC TAC CTT CAC GTT GTC GCA TTT TTT GT-3'
Antisense Oligo (II)	5'-CTA GAC AAA AAA TGC GAC AAC GTG AAG GTA GTT TCT CTT GAA AAC TAC CTT CAC GTT GTC GCA-3'

2.2. Cell and tissue cultures

2.2.1. Hippocampal organotypic slice cultures

Organotypic cultures were used because they preserve spatial and functional relationships between nerve cells, and therefore are the closest approximation to an acute preparation (Gähwiler, 1997).

To prepare the slices, Wistar rats were decapitated 5 to 7 days after birth (P5 to P7). Brain was immediately extracted and immersed in almost frozen dissection buffer that was being gassed with carbogen (95% O_2 and 5% CO_2) to reach pH 7.4. Afterwards, and with the brain still immersed in cold buffer, both hippocampi were extracted and placed on the tissue slicer, where 400 µm slices were made. Slices were then transferred to culture medium to be separated from each other (Fuller and Dailey, 2010) and placed on 30 mm diameter semiporous membrane filters (Millipore #PICM03050) serving as support to culture the explants, either in 6-well or 35-mm-diameter plates. The fact that the slices were in intimate contact with the medium but not immersed, prevents them from suffering anoxia and allows them to be properly nourished. Once prepared, slices were maintained in a 5% CO_2 incubator at 35.5°C, and can be cultured for few weeks, exchanging the culture medium 3 times per week.

2.2.2. Hippocampal primary cultures

As previously described (Kaech and Banker, 2006), a Wistar pregnant rat (embryonic age 19, E19) was sacrificed by asphyxiation with CO_2 or by neck dislocation and embryos were collected and placed into cold dissection solution. In this solution, embryos were dissected to extract both hippocampi from every one of them. Hippocampi were incubated at 37°C in dissection solution with 0.22% trypsin for 15 minutes to facilitate mechanical disgregation. Once disgregated, cells were counted using a Neubauer chamber and plated at a convenient density on either glass coverslips (for imaging experiments, 300.000 cells/35-mm-diameter plate) or plastic plates (for biochemistry experiments, 100.000 cells/well in a 12-well plate) previously coated with 0.1 mg/ml poly-L-Lysine prepared on borate buffer using plating medium. Cells were plated in plating medium and kept in a 5% CO_2 incubator at 37°C for 3 to 6 hours post-dissection. The medium was then replaced by culture medium, where they were maintained for 1 to 3 weeks, depending on the requirements of the experiments.

2.3. Expression systems for recombinant proteins

Different methods were used to deliver the DNA of interest into the cells, depending on whether a protein, or a protein fragment, was expressed or knocked-down in cultures.

2.3.1. Infection

- **Sindbis virus**

This system was used to transiently overexpress recombinant proteins in our culture systems, either hippocampal dissociated neurons or organotypic slices (Schlesinger, 1999).

The system is based in the use of a Sindbis replicon (pSinRep5, pSR5) (Frolov et al., 1999) to express the protein of interest, together with the DH-DNA, encoding the Sindbis virus capsid proteins. These DNAs are in vitro transcribed prior to cell transfection. First, both DNAs were linearized by digesting them with *Xho*I in the case of the DH-DNA, and with *Xho*I, *Not*I or *Pac*I in the case of the pSinRep5 containing the protein of interest. To start the purification process of these linear DNA fragments, Proteinase K (NewEnglandBiolabs) was added until it constitutes one tenth of the volume of the sample, along with SDS to a final concentration of 0.5%, and this was incubated at 55°C for 30 minutes. DNAs were then extracted by using phenol/chloroform and precipitated with ethanol and ammonium acetate. These clean fragments of DNA were the templates for the transcription reaction that was carried out using the mMessage mMachine SP6 transcription kit (Ambion).

The two mRNA molecules obtained, one coding for the protein of interest and the other one coding for the viral capsid proteins, were introduced in BHK cells by electroporation in 1X PBS containing RNAse inhibitor (Promega). After the electroporation, the cells were plated in cell culture medium and grown for 48 hours. Since the two mRNA molecules have the corresponding CAP in the 5' position and the poly-A tail in the 3' position, they will be recognized by the cells as endogenous mRNA and they will be processed normally, and viral particles containing the RNA coding for the protein of interest will be produced and liberated to the medium. At 48 hours post-transfection (hpt), cell culture medium was collected, filtered using 0.45 µm pore-size filters to remove cellular debris, and ultracentrifuged at 30.000 rpm using a SW40 rotor (Beckman) for 2 hours to concentrate

the viruses present in it. This solution, which can be aliquoted and stored at -80°C, was used to deliver the recombinant proteins to the hippocampal CA1 pyramidal neurons from organotypic slice cultures by microinjection, or simply by adding 1 to 10 µl of it to the medium of cell cultures medium. Recombinant protein expression time varied from 15 to 48 hours post-infection (hpi), depending on the experiments.

- **Lentiviruses**

This system was used to produce a stable down-expression of the proteins of interest by using shRNA technology.

First, and in a similar way to the Sindbis system, the shRNA designed against the protein of interest was subcloned into the KH1-LV vector (Lois et al., 2002). Secondly, two more plasmids, pCMV-dR8.74 and pMD2.G, kindly provided by Dr. Jesús Ávila (Centro de Biología Molecular "Severo Ochoa" CBMSO, UAM-CSIC, Madrid), were needed, as they code for several components of the viral particles (structural proteins, enzymes, etc) (Dull et al., 1998).

The DNAs mentioned above, were introduced into HEK-293T cells by classical calcium phosphate transfection method (Kingston et al., 2001), which will cause DNA to precipitate and adhere to the cell surface before it is internalized. Briefly, cell culture medium was replaced with cell culture medium containing 25 µM chloroquine, which would prevent lysosomal degradation of the DNA, right before transfection. At 8 – 12 hpt, cell culture medium was exchanged to remove the chloroquine. At 48 hpt, medium from the HEK cells was collected, filtered using 0.45 µm pore-size filters to remove cellular debris, and ultracentrifuged at 30.000 rpm using a SW40 rotor (Beckman) for 2 hours to concentrate the viruses present in it. This solution, than can be aliquoted and stored at -80°C, was used to deliver the recombinant proteins to the hippocampal CA1 pyramidal neurons from organotypic slice cultures by microinjection on day in vitro (DIV) 0 or DIV 1, or simply by 1 to 10 µl of it to the medium of primary hippocampal cultures on DIV 7. Down-expression was evaluated biochemically in primary hippocampal cultures at 7 days post-infection (dpi), and the effects were tested electrophysiologically in organotypic hippocampal slices 6 to 9 dpi.

2.3.2. Transfection

To overexpress two recombinant proteins at the same time, in the same cell, in organotypic hippocampal slices, biolistic transfection was used instead of viral infection.

Briefly, the BioRad hand-held Helios gene gun along with the accessories commercialized by the manufacturer was used. Gold particles of subcelullar size (1.6 μm diameter in our case) were coated with the DNAs of interest, introduced into cartridges, and finally fired as bullets using helium as the source of pressure (Woods and Zito, 2008).

2.4. Biochemical techniques

2.4.1. Generation of protein extracts

Protein extracts were prepared from organotypic hippocampal slices, whole hippocampi, or cell cultures (primary neuronal hippocampal cultures or cell lines), always following the same procedure. Tissue or cells were collected and placed in cold Eppendorf tubes with the adequate volume of cold homogenization buffer and mechanical disgregation of the samples was done. Once samples were properly homogenized, they were centrifuged at *11.000xg* for 3 min and at 4ºC, and supernatant was used for protein quantification using Bradford reagent assay (BioRad).

2.4.2. Protein electrophoresis and immunodetection

For Western blot (WB) analysis, 10 – 100 μg of protein extracts were boiled in 1X loading sample buffer and separated by SDS-PAGE using 4%, 8% or 12% acrylamide/bisacrilamide gels. Gels were run, using the Mini-Protean Cell system (BioRad) in running buffer at constant voltage (70 – 100 V) for approximately 2 hours at room temperature. Afterwards, proteins were transferred to Immobilon-P PVDF membranes (Millipore), previously activated by immersion in ethanol, distilled water and transfer buffer. Transference was done in transfer buffer at 4°C, maintaining constant amperage. Depending on the requirements of the experiment, the transference was carried out in 90 minutes at 0.33 Amps or overnight at either 0.04 Amps or 0.1 Amps (this last amperage was used for the transfer of large proteins in 4% gels). Transfer was always verified by Red Ponceau staining.

To avoid the non-specific binding of the antibodies used for the immunodetection, the PVDF membrane was blocked with an irrelevant protein (5% fat-free milk, prepared in TBS with 0.1% Tween-20) for 1 hour at room temperature. Afterwards, incubation with the desired primary antibody diluted in blocking solution was done for 1 – 2 hours at room temperature or overnight at 4°C. To maintain stringent conditions while removing the excess of primary antibody, PVDF membranes were thoroughly washed at room temperature with blocking solution. Incubation with the secondary antibody, also diluted in blocking solution, lasted 1 hour at room temperature. To remove the excess of secondary antibody, PVDF membranes were thoroughly washed at room temperature with TBS-Tween.

Protein detection was performed using Western chemiluminiscent substrate (Millipore), following manufacturer's recommendations. Protein amounts were estimated by densitometric analysis using Quantity-One densitometer (BioRad). At least three different experiments and appropriate gel exposures were used in all cases. In addition, different exposures of the same experiment were analyzed to ensure that data were obtained from films within linear range. Further analysis of the data is done using ImageJ software (Schneider et al., 2012).

2.5. Pharmacological induction of NMDA-dependent LTD in organotypic hippocampal slices

Bath application of 20 μM NMDA (SIGMA) for 5 minutes has been described to induce NMDA-dependent LTD (Lee et al., 1998). Effects of this so-called chemical LTD (cLTD) can be addressed biochemically (looking for a dephosphorylation on the Ser^{845} of $GluA_1$), and electrophysiologically (looking for a decrease in the AMPAR-mediated currents). In this thesis, the electrophysiological approach has been the one used (see below).

2.6. Electrophysiology

Voltage-clamp whole-cell recordings were obtained from CA1 pyramidal neurons, patched under visual guidance using transmitted light illumination. When studying the effects of mutant proteins on synaptic transmission, one infected and one not-infected nearby cell were recorded (sometimes in parallel).

For the vast majority of the experiments, the recording chamber was perfused with ACSF at 29°C containing 0.1 mM picrotoxin (SIGMA) (a $GABA_A$ receptor antagonist, to block

inhibitory transmission) and 2 μM 2-chloroadenosine (SIGMA) (an adenosine receptor agonist, to reduce neurotransmitter release and therefore decrease neuronal bursting activity), at pH 7.4 and permanently gassed with carbogen. Patch recording pipettes (3 – 6 MΩ) were filled with internal solution. Synaptic responses were evoked with bipolar electrodes using single-voltage pulse (200 μs, up to 20 V). The stimulating electrodes were placed over Schaffer collateral fibres between 200 and 400 μm from the recorded cells. It is important to mention that the CA3 – CA1 intersection was cut to prevent any propagation of recurrent activity from CA3.

2.6.1. Basal transmission

Synaptic AMPAR-mediated responses were measured when the membrane potential is set at -60 mV, and NMDAR-mediated responses were measured when the membrane potential is set at +40 mV. In all cases, 60 – 120 trials were averaged.

2.6.2. Synaptic plasticity

LTD was induced using a pairing protocol by stimulating Schaffer collaterals fibres at 1 Hz (300 or 500 pulses) while the postsynaptic cells were held at depolarized potential of -40 mV. LTP is induced using a different pairing protocol by stimulating Schaffer collaterals fibres at 3 Hz (300 pulses), while the postsynaptic cells were held at depolarized potential of 0 mV.

cLTD can also be electrophysiologically evaluated. In order to do so, synaptic responses were evoked at -60 mV for 5 minutes in the above described perfusion configuration. After this *baseline*, the recording chamber was perfused for 5 minutes with 20 μM NMDA in ACSF maintaining the cell in the voltage-clamped configuration (stimulation was also maintained constant). After the bath application of the NMDA, the recording chamber was perfused again with NMDA-free ACSF for up to 40 minutes while registering AMPAR-mediated responses.

All electrophysiological data were collected with pCLAMP software (Axon Instruments) and analyzed with Microsoft Excel (Microsoft).

2.7. Fluorescence microscopy

2.7.1. Sample preparation for fluorescence imaging

Most of the imaging presented in this thesis consists of images taken to show the basal distribution of a recombinant protein in organotypic hippocampal slices. For this type of image acquisition, slices were simply fixed by immersing them overnight in fixative solution at 4ºC, and then washed abundantly with PBS1x prior to mounting with Prolong Gold (Invitrogen).

Images were acquired with a LSM510 scanning confocal microscope coupled to an inverted Axiovert 200 microscope (Zeiss) at the imaging facility of the Centro de Biología Molecular "Severo Ochoa" (CBMSO, CSIC-IUAM). Posterior analysis was done using ImageJ software.

2.7.2. Videomicroscopy

Independently of the experiments to be carried out, the set-up was always configured as described next. The imaging chamber (Live Cell Instruments #AC-B25 Chamlide AC for 25 mm round coverslips) was perfused with ACSF constantly gassed with carbogen. All the microscopes used have a temperature control system that maintains the temperature constant (29°) in the surroundings of the sample, including the objectives of the microscope.

Images were acquired either with a LSM710 scanning confocal and multiphoton microscope coupled to an inverted AxioObserver (Zeiss), or with a LSM510 META scanning confocal microscope coupled to an inverted Axiovert 200 microscope (Zeiss) at the Imaging facility of the Centro de Biología Molecular "Severo Ochoa" CBMSO, UAM-CSIC. Posterior analysis was done using ImageJ software.

- **Fluorescence Recovery After Photobleaching (FRAP) experiments: acquisition and quantification**

In the configuration described above, healthy-looking CA1 neurons overexpressing the proteins of interest (mCherry-KIF5c-LT ore GFP-KIF17-LT) were selected to perform FRAP experiments and asses the motility of these proteins under basal conditions. The rationale behind a FRAP experiment is that, once the fluorescence coming from the

fluorescent-tagged recombinant protein is bleached in a specific region, this region would fluoresce again only if fluorescent-tagged recombinant proteins can move, either by diffusion or by directed transport, and fill in this region again. However, if the fluorescent-tagged recombinant protein is immobile, the bleached region will not show a recovery in the fluorescence intensity.

In this particular case, 2-5 single plane images of the whole field of view were acquired before bleaching a small region in the apical dendrite. The photobleaching was performed by using the same laser as the one used for imaging, but with a higher potency and in a faster and iterative manner. After bleaching, imaging of the whole field of view (and not only of the bleached region) was done using the same parameters as used in the pre-photobleaching images. As in these particular experiments fluorescence was very intense, images were acquired with the shortest posible time interval in between frames (stream acquisition).

To quantify and normalize these experiments, background and fluorescence decay due to the imaging itself have to be taken into consideration. In order to do so, the following formula was used (Fernández-Monreal et al., 2009):

$$Percent\ fluo = \frac{(Fi - Fbckg)(Fnb0 - Fbckg)}{(Fi0 - Fbckg)(Fnb\ - Fbckg)}\ 100$$

where: Fi = fluorescence of the bleached region at a given time; Fi0 = fluorescence of the bleached region before the bleaching; Fbckg = fluorescence of the corresponding background; Fnb = fluorescence of the not bleached (control) region at a given time; Fnb0 = fluorescence of the not bleached (control) region before the bleaching.

2.8. Statistical analysis

All graphs represent averaged values along with the standard error of the mean (± s.e.m.). When comparing mean values, statistical significance was determined by the Mann – Whitney test if only two distributions were being compared. When comparing paired data, Wilcoxon test was used.

Results

A. ASSESMENT OF THE ROLE OF THE PLUS-END DIRECTED MICROTUBULE-DEPENDENT TRANSPORT IN MODULATION OF SYNAPTIC FUNCTION

To address whether KIF5c or KIF17 play a role in synaptic plasticity modulation in our system, we used two different approaches: the use of *dominant negative* versions of these proteins, and knockdown of their endogenous expression levels. Both approaches are based on the removal of endogenous protein function. The rationale behind a *dominant negative* is to introduce in the system a modified version of the protein of interest without removing the endogenous one, so that it will compete with it. Moreover, the use of *dominant negatives* lacking different domains would allow mapping the specific roles of those domains. In contrast, the knockdown approach substantially decreases the total amount of expressed protein, allowing to determine whether the presence of the whole protein is required or not for normal, in this case, synaptic function.

1. VALIDATION OF THE MUTANT KINESINS KIF5C-LT AND KIF17-LT: LACK OF THE MOTOR DOMAIN

As their own name shows, motor proteins have a motor domain that qualifies them as such. To study if the motor capacity of KIF5c and KIF17 is needed for synaptic function, we decided to use *dominant negative* forms that lack just the motor domain (Figure 13).

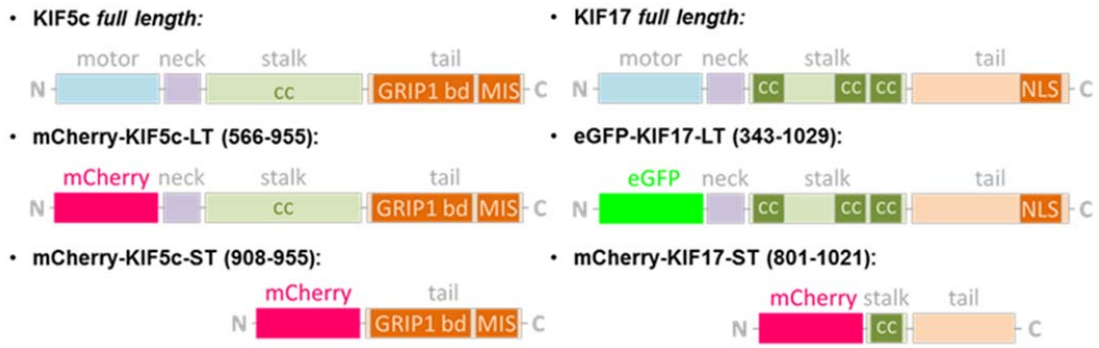

Figure 13. Schematic representation of the different KIF5 and KIF17 dominant negatives used. Structure of the full length protein is shown to illustrate the missing domains on the two dominant negatives designed. cc, coiled coil; GRIP1bd, GRIP1 binding domain; MIS, motor inhibiting site; NLS, nuclear localization sequence.

It has been shown that when KIF5c-LT is introduced in eukaryotic cells, transport of its cargo is impaired, suggesting that it can still dimerize and bind the cargo because it has the neck and cargo biding domains, but it cannot transport it as it lacks the motor domain

(Cai et al., 2009). KIF17-LT has been also characterized, in other systems, leading to a similar conclusion. When the motor domain is not present, it can still bind the cargo, but its transport is affected (Cai et al., 2009; Dishinger et al., 2010). In addition, KIF17 is autoinhibited by regulation of its motor domain (Hammond et al., 2010), suggesting that KIF17-LT would, in principle, bind its cargo with a higher affinity resulting in a stronger *dominant negative*.

Organotypic hippocampal slices were infected with Sindbis virus expressing either KIF5c-LT or KIF17-LT, and proteins were detected by Western blot 2 days post infection (dpi) (Figure 14A and B, upper panels). Both endogenous KIF5c and recombinant KIF5c-LT were detected. Unfortunately, antibodies specific for KIF17 were not available in our laboratory at this time. Therefore, only KIF17-LT expression was detected in organotypic hippocampal slices. Both recombinant KIF5c-LT and KIF17-LT are identified as two bands on the Western blot, where the smaller band is most probably the result of some protein degradation.

To address the subcellular location of KIF5c-LT and KIF17-LT mutant proteins in oranotypic hippocampal slices, confocal imaging experiments were performed (Figure 14A and B, lower panels). Same as for the biochemical approach, organotypic hippocampal slices were infected with Sindbis viruses expressing either KIF5c-LT or KIF17-LT, and cells were imaged 2 dpi. In both cases, the recombinant proteins were distributed all over the cell but excluded from the nucleus. It is somewhat striking that these proteins, lacking the motor domain, presented a more distal distribution than expected. This result might indicate that KIF5c-LT and KIF17-LT could be transported as cargoes.

Interestingly, KIF5c-LT distribution pattern was very filamentous, coherent with a microtubule-bound situation. Co-localizations with acetylated, detyrosinated and tyrosinated tubulin were then attempted, but unfortunately, we faced technical problems to perform immunhistochemistries that prevented us from drawing any conclusion. However, the pattern of distribution that we observed suggested that KIF5c-LT might still bind to MT even lacking the motor domain. This data was in agreement with previous observation that KIF5c-LT could bind to MT through the tail domain where it contains an additional MT binding site (Konishi and Setou, 2009; Navone et al., 1992; Seeger and Rice, 2010).

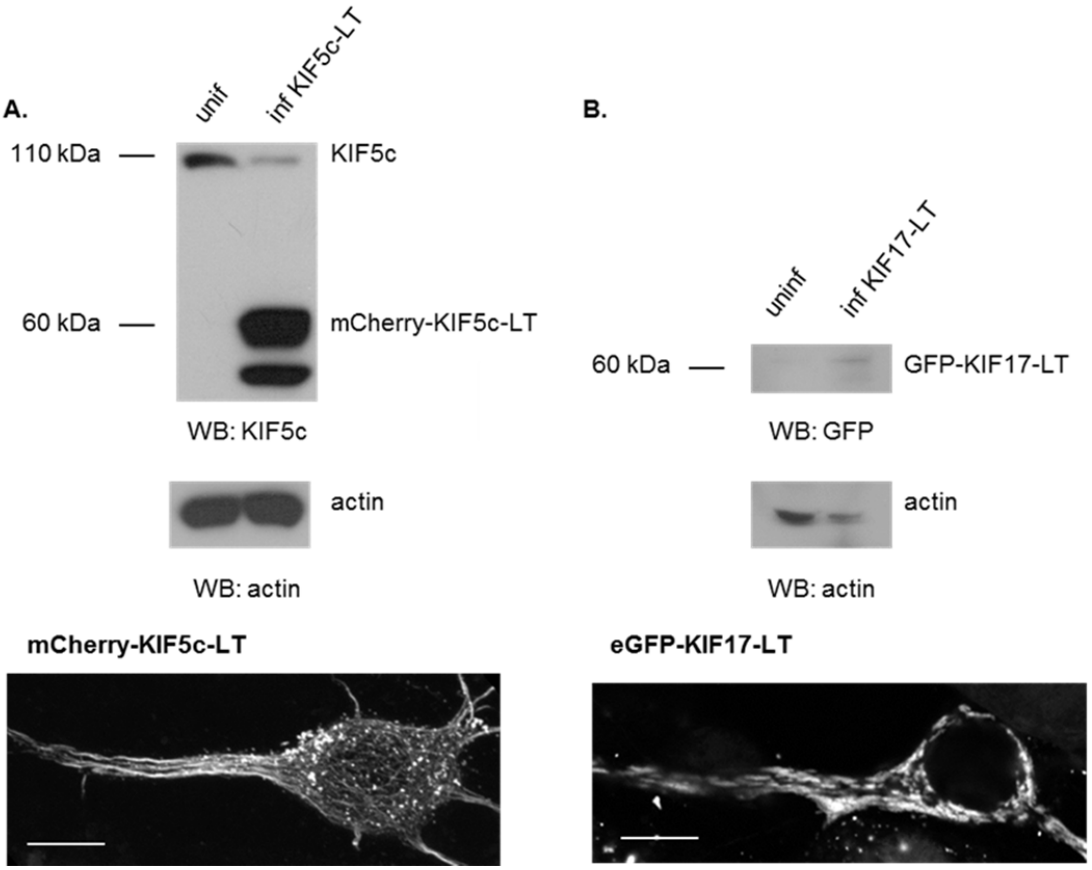

Figure 14. Detection of KIF5c-LT and KIF17-LT. A. Western blot (upper panel) showing detection of both endogenous KIF5c and the recombinant mCherry-KIF5c-LT using an anti-KIF5c antibody. Actin was used as a loading control. uninf, uninfected; inf KIF5c-LT, sample from Sindbis mCherry-KIF5c-LT infected cells 2 days post-infection (dpi). Representative confocal image (lower panel) of a CA1 neuron overexpressing mCherry-KIF5c-LT 2 dpi. Scale bar: 10 μm. **B.** Western blot (upper panel) showing detection of the recombinant eGFP-KIF17-LT using an anti-GFP antibody. Actin was used as a loading control. uninf, uninfected; inf KIF17-LT, sample from Sindbis eGFP-KIF17-LT infected cells 2 dpi. Representative confocal image (lower panel) of a CA1 neuron overexpressing eGFP-KIF17-LT 2 dpi. Scale bar: 10 μm.

In the case of KIF17-LT, the pattern of distribution was quite different. The protein localized in a series of cisternae-like structures, which could indicate an association to mitochondrial or reticular structures. Further analyses, using specific tools suitable for imaging techniques with our system, or using subcellular fractionation techniques, would be needed to answer this question.

To confirm that KIF5c-LT and KIF17-LT could not move along MTs, as expected due to their lack of the motor domain, fluorescence recovery after photobleaching (FRAP) experiments were performed in live organotypic hippocampal slices overexpressing KIF5c-LT and KIF17-LT (Figure 15).

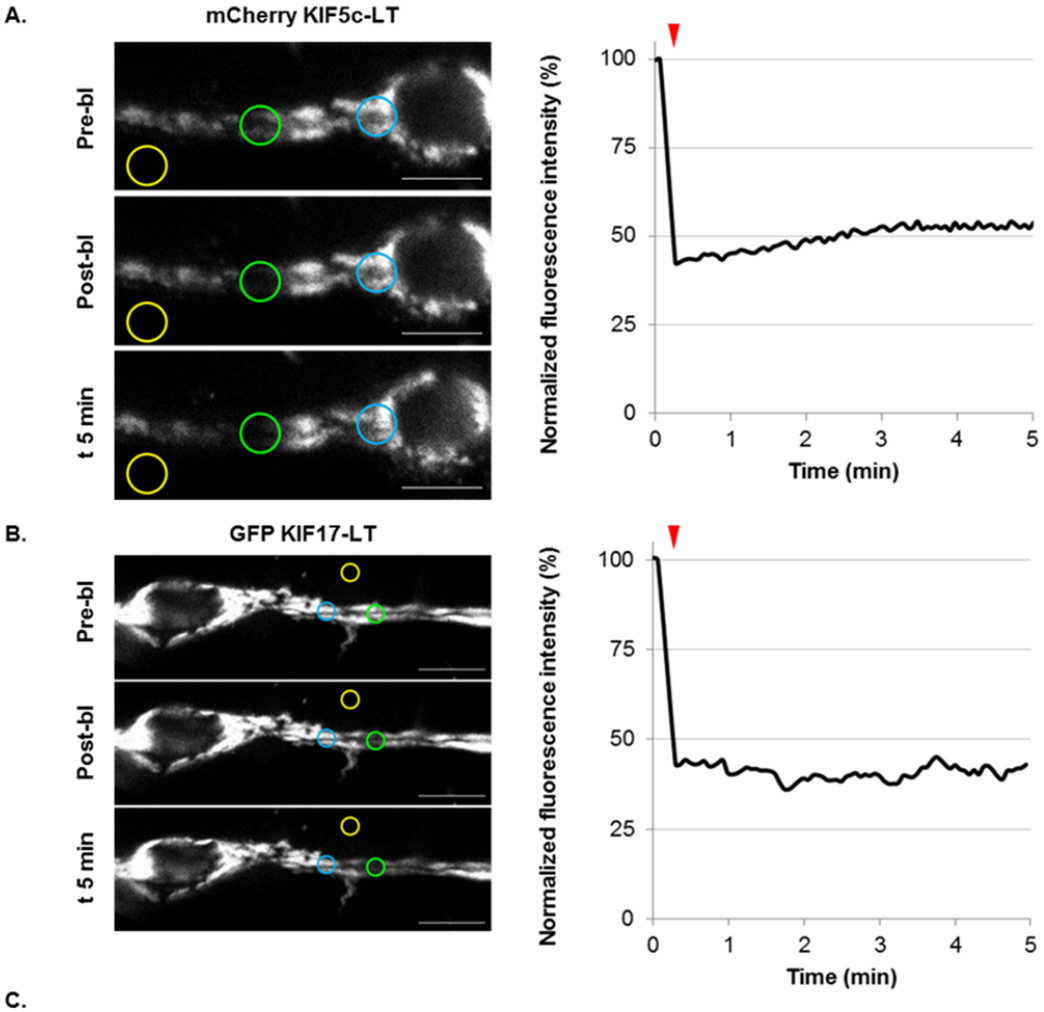

Figure 15. Representative FRAP experiments to analyze the mobility of KIF5c-LT and KIF17-LT. Left panels, representative time points for one experiment looking at mCherry-KIF5c-LT in **A.** and at eGFP-KIF17-LT in **B**. The quantifications are shown on the right panels. The "Pre-bl" image was acquired before photobleacing the area inside the green region, the "Post-bl" was acquired immediately after photobleaching the area in the green region (this time point is also indicated with a red arrowhead in the graphs), and the "t 5 min" image corresponds to the last time point of the experiment. **C.** Formula used for the quantification, where the photobleached region (green circle, Fi), a control not bleached region (cyan circle, Fnb) and a background region (yellow circle, Fbckg) were taken into consideration (see Materials & Methods). Scale bar: 10 µm.

Based on the representative experiment showed in Figure 15, we can state that both KIF5c-LT and KIF-17-LT proteins were mostly immobile. For KIF5c-LT, a slight recovery of the fluorescence was observed in the photobleached area suggesting a "residual mobility". As KIF5c-LT can be transported as a cargo (see above), the recovery of fluorescence could be due to KIF5c-LT being transported passively as part of a cargo vesicle moved by a different molecular motor. In contrast, no fluorescence recovery was observed for KIF17-LT. Similarly, we could infer that KIF17-LT was also being transported, in agreement with its distribution all over the neurons. This data could allow us to speculate that the kinetics of the molecular motor transporting KIF17-LT as cargo was just slower than the one of the molecular motor transporting KIF5c-LT.

Altogether, our data indicate that, KIF5c-LT and KIF17-LT were successfully expressed in organotypic hippocampal slices, and were almost completely immobile, as expected due to the lack of their motor domain.

2. VALIDATION OF THE MUTANT KINESINS KIF5C-ST AND KIF17-ST: LACK OF EVERY DOMAIN BUT THE CARGO BINDING DOMAIN

To map down the regions that might be critical for the possible function of KIF5 and KIF17 in modulating synaptic function, we decided to design new tools. In this line, short tail versions of KIF5c and KIF17 were generated (KIF5c-ST and KIF17-ST), just containing the cargo binding domain of the kinesin fused to a fluorescent tag (Figure 13).

To design the KIF5c-ST construct, KIF5c-LT was used as a template, maintaining just the core of the globular cargo binding domain, basing our decision on what is known about the structure and sequence of KIF5c (Kanai et al., 2000) in order to generate a *minimal dominant negative*, almost like an interfering peptide (47 amino acids long). In a similar approach, to design the KIF17-ST construct, we also took advantage of previous work that had characterized some of the different domains of KIF17 (Hammond et al., 2010; Setou, 2000). We used as template a version of KIF17 (see Materials and Methods) from which we had to remove the nuclear localization signal (NLS) to prevent it from accumulating in the nucleus, since when we first tried to use this construct it proved to be highly toxic for the cell (data not shown).

Organotypic hippocampal slices were infected with Sindbis virus expressing either KIF5c-ST or KIF17-ST, and proteins were detected by Western blot and imaging at 1 dpi. The

expression of both KIF5c-ST and KIF17-ST was detected by Western blot, using antibodies that would recognize endogenous and –ST KIFs (Figure 16A and B, upper panels).

The distribution of KIF5c-ST and KIF17-ST in organotypic hippocampal slices was also addressed (Figure 16A and B, lower panels). Both short tail mutants showed a rather diffuse cytoplasmic distribution. Interestingly, KIF5c-ST was also present inside the nucleus of the neurons. This atypical localization of KIF5c-ST seemed not to interfere with the viability of the neurons, as functional experiments could be carried out (see below). In contrast, KIF17-ST was excluded from the nucleus, as expected because it lacks the NLS.

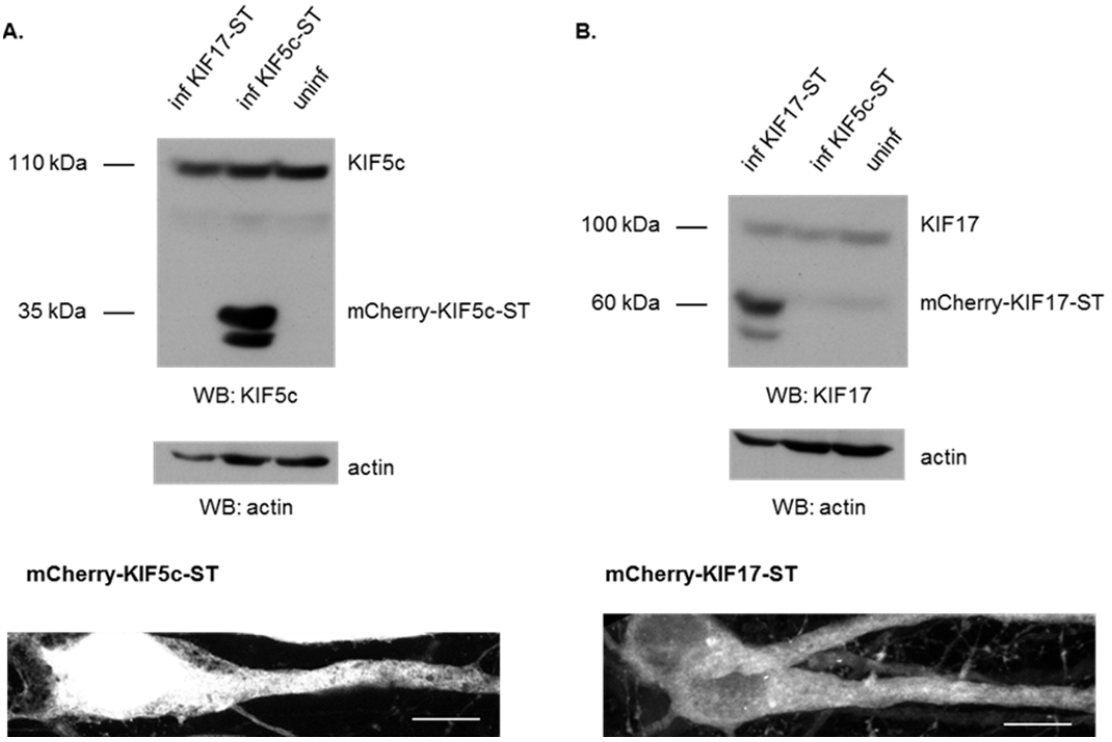

Figure 16. Detection of KIF5c-ST and KIF17-ST. A. Western blot (upper panel) showing detection of both endogenous KIF5c and the recombinant mCherry-KIF5c-ST using an anti-KIF5c antibody. Actin was used as a loading control. uninf, uninfected; inf KIF5c-LT, sample from Sindbis mCherry-KIF5c-ST infected cells 1 day post-infection (dpi). Representative confocal image (lower panel) of a CA1 neuron overexpressing mCherry-KIF5c-sT 1 dpi. Scale bar: 10 µm. **B.** Western blot (upper panel) showing detection of the recombinant mCherry-KIF17-ST using an anti-KIF17 antibody. Actin was used as a loading control. uninf, uninfected; inf KIF17-ST, sample from Sindbis mCherry-KIF17-ST infected cells 1 dpi. Representative confocal image (lower panel) of a CA1 neuron overexpressing mCherry-KIF17-ST 1 dpi. Scale bar: 10 µm.

3. FUNCTIONAL CHARACTERIZATION OF THE DIFFERENT DOMAINS OF KINESINS KIF5C AND KIF17

The tools previously generated and validated were subsequently used to analyze the possible modulatory roles of KIF5c or KIF17 in synaptic function.

3.1. Functional characterization of the motor domain of kinesins KIF5c and KIF17

As a first step to evaluate the role of the motor function of KIF5c or KIF17 in excitatory synaptic function, organotypic hippocampal slices were infected with Sindbis virus expressing either KIF5c-LT or KIF17-LT. At 2 dpi, simultaneous double-whole cell electrophysiological recordings were performed from nearby pairs of CA1 neurons. Excitatory post-synaptic currents (EPSCs) were evoked by stimulation of the afferent Schaffer collateral fibers (see Materials and Methods).

Neurons overexpressing KIF5c-LT show unaltered AMPA and NMDA transmission (Figure 17A). Similar results were obtained for neurons overexpressing KIF17-LT (Figure 17B). These data suggested that the motor function of KIF5c or of KIF17 was not needed for maintenance of basal synaptic transmission.

KIF5 and KIF17 have been previously proposed to transport AMPA (Setou et al., 2002) and NMDA (Setou, 2000) receptors, respectively, along dendrites. In contrast, our results suggested that KIF5c was not needed for the maintenance of basal AMPA mediated transmission. This allowed us to speculate that KIF5c is not required to transport AMPARs along the dendrites, from the synthesis area to the synaptic targets. To answer this question, imaging experiments were performed, co-expressing a fluorescently tagged GluA2 along with either KIF5c-LT or with soluble mRFP as a control, using the biolistic method (see Materials and Methods). Organotypic hippocampal slices were transfected at DIV0/1 and left expressing both proteins for 2-3 days before fixation and image acquisition. It was expected that both the *dominant negative* molecular motor KIF5c-LT and the AMPAR subunit GluA2 would be present in the neuron for the same amount of time. Then, if KIF5c is indeed responsible for the transport of AMPARs, both recombinant proteins would be present and the chances of all AMPARs interacting with endogenous KIF5c (or the other way around) would be minimal.

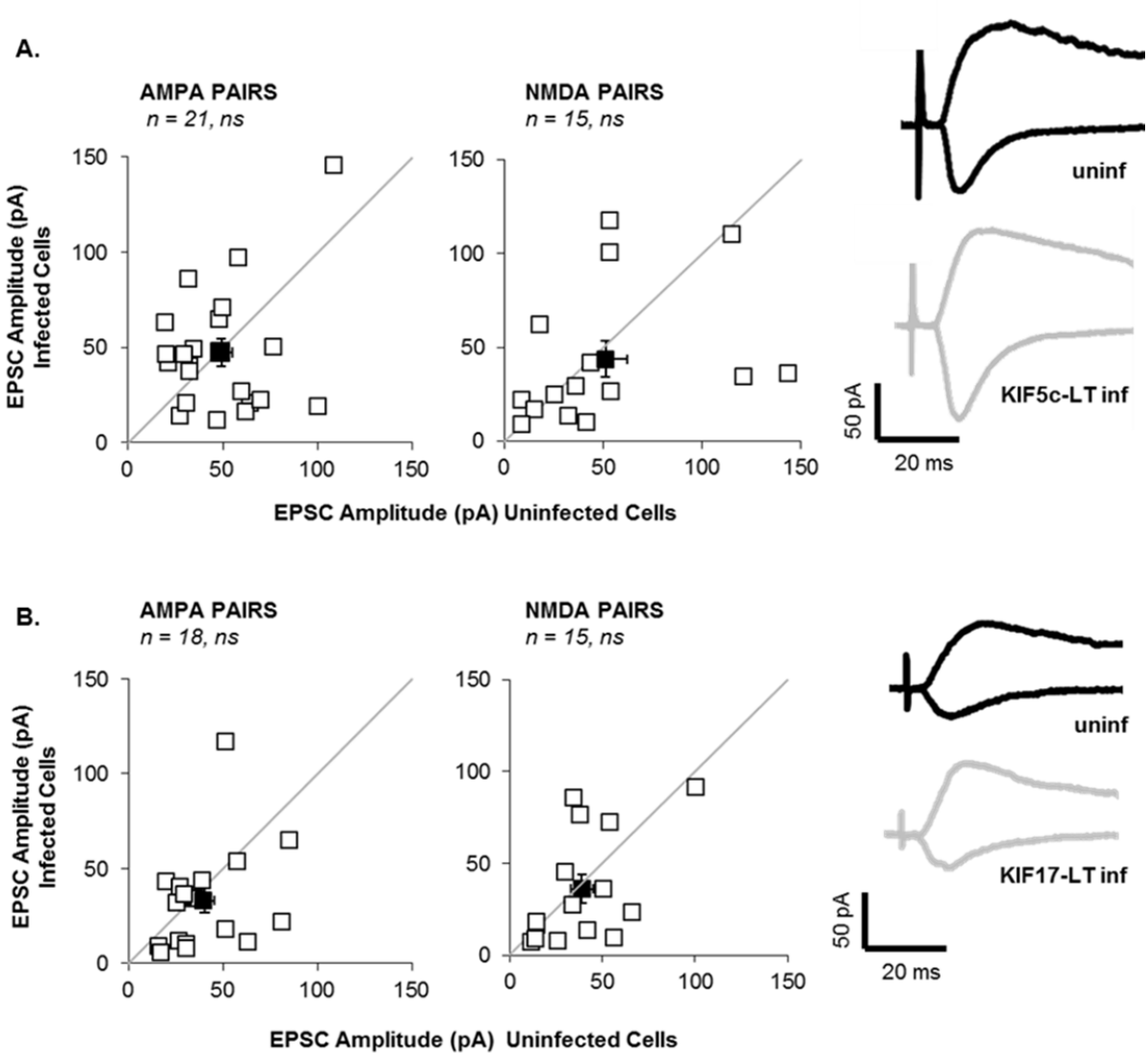

Figure 17. Analysis of the overexpression of KIF5c-LT or KIF17-LT on basal synaptic transmission. A. Synaptic AMPAR- and NMDA R-mediated responses were recorded at -60 mV and +40 mV, respectively, from pairs of neighboring CA1 neurons in organotypic hippocampal slices. uninf, uninfected, representative traces in black; inf KIF5c-LT, Sindbis mCherry-KIF5c-LT infected cells 2 days post-infection (dpi), representative traces in grey. Absolute values of the responses (amplitude, pA) of the two cells that were simultaneously recorded under the same stimulation paradigm are shown. AMPAR-mediated responses (pA): uninf 49.15 ± 5.51, inf KIF5c-LT 47.36 ± 7.14. NMDA R-mediated responses (pA): uninf 51.35 ± 10.88, inf KIF5c-LT 43.88 ± 9.44. **B.** Same experiment as in **A.**, but corresponding to the overexpression of eGFP-KIF17-LT. uninf, uninfected, representative traces in black; inf KIF17-LT, Sindbis eGFP-KIF17-LT infected cells 2 dpi, representative traces in grey. AMPA R-mediated responses (pA): uninf 40.15 ± 4.88, inf KIF17-LT 33.15 ± 6.41. NMDA R-mediated responses (pA): uninf 39.04 ± 6.19, inf KIF17-LT 36.04 ± 7.89. *ns*, not significant; n number of cells; Wilcoxon test.

We found that when KIF5c-LT is overexpressed, recombinant GluA2 transport along dendrites is completely normal (Figure 18). These results were in agreement with our electrophysiological results, strongly suggesting that KIF5c motor function was not required for proper AMPAR transport along the dendrites in CA1 neurons.

Although our results indicated that neither KIF5c nor KIF17 motor activity was required for basal synaptic transmission, this function could be needed for the modulation of long term synaptic plasticity processes.

KIF5c seemed as the most appealing candidate due to its relationship with AMPARs (Setou et al., 2002). Therefore, different synaptic plasticity paradigms were analyzed (see Materials and Methods) in organotypic hippocampal slices in which some cells were overexpressing KIF5c-LT.

When LTP was induced in neurons overexpressing KIF5c-LT, an approximate 3-fold potentiation of the AMPA response was observed. This level of potentiation was virtually the same as the one observed in not infected neurons (Figure 19). Therefore, the motor domain of KIF5c was not needed either for the long distance transport along the dendrites of the AMPARs, or for the short distance transport from the surroundings of the spine to the synaptic membrane once LTP is induced.

After discarding a role in LTP, the possible effect of overexpressing KIF5c-LT on LTD was analyzed. First, the effects of KIF5c-LT overexpression were studied when cLTD was induced. This type of plasticity was impaired/reduced in those cells where KIF5c-LT (35% of depression) was present, compared with the uninfected ones (60% of depression) (Figure 20). In addition, the effect of the presence of KIF5c-LT during synaptically induced LTD was also analyzed. These two complementary techniques were utilized as the latter cannot be used in combination with imaging (in our equipment) and biochemical techniques, potentially required to dissect the molecular mechanisms underlying KIF5c functions. In this case, cells infected with KIF5c-LT show less than 20% depression, whereas not infected ones show up to 40% depression (Figure 21). These data indicate a significant impairment in LTD in the presence of the mutant KIF5c lacking the motor domain.

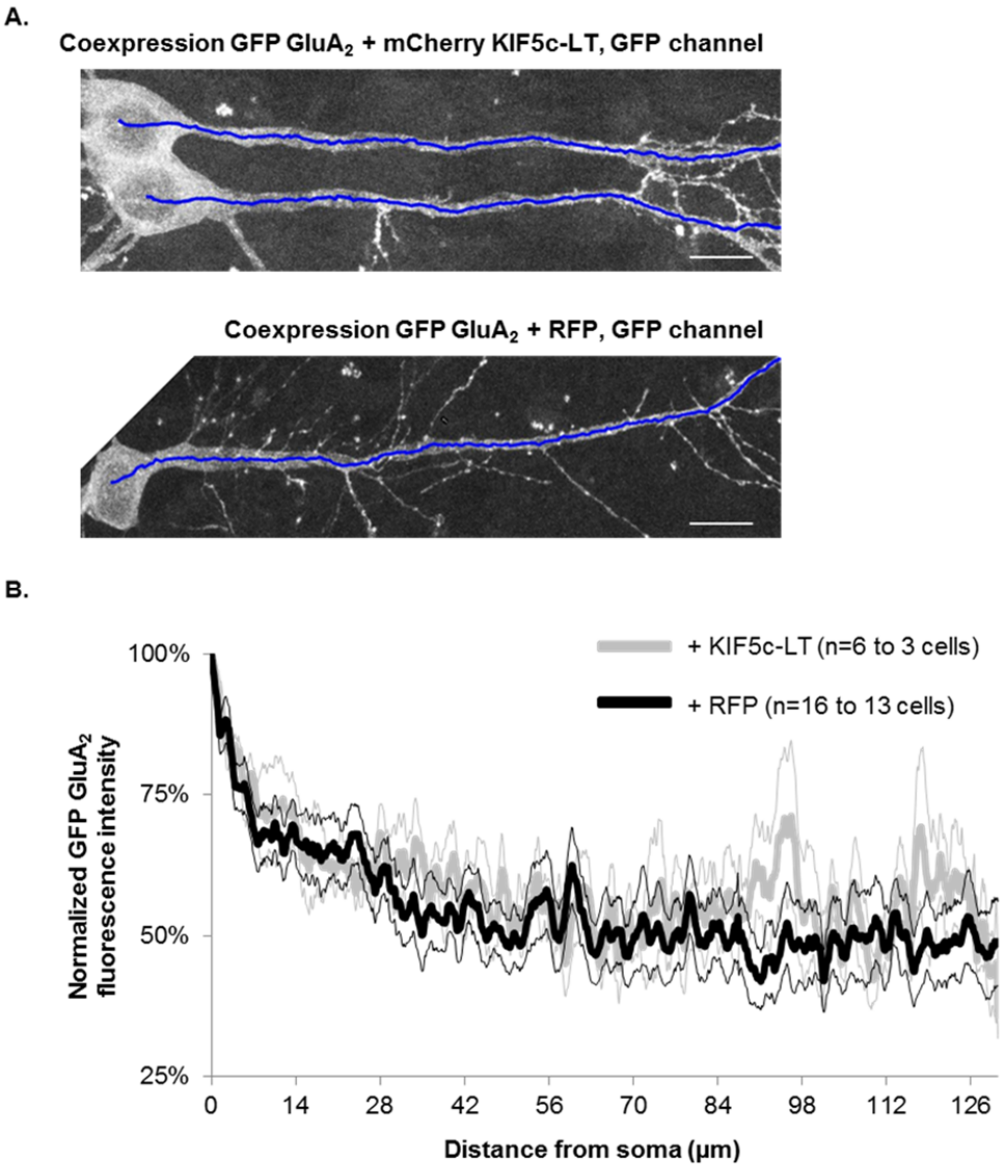

Figure 18. Analysis of the overexpression of KIF5c-LT on basal trasnport of GluA2 along the dendrites. Using the biolistic method (see Materials & Methods), GFP-GluA2 was coexpressed in organotypic hippocampal slices with either mCherry-KIF5c-LT (**A.** upper image) or mRFP (**A.** lower image). **A.** Representative images of the samples and of the method used for quantification. Briefly, a line of 1-pixel width (blue line) was drawn from the the soma to the end of the apical dendrite using ImageJ software on the GFP-GluA2 channel. The values of fluorescence intensity, once they are normalized to the maximum value of fluorescence at the soma, along this line are interpreted as the quantity of GFP GluA2. Only green channel is shown due to technical difficulties to image the red one (very dim fluorescence, difficult to avoid photobleaching). **B.** Quantification of the GFP-GluA2 fluorescence intensity along the dendrites. +KIF5c-LT, cells overexpressing GFP-GluA2 and mCherry-KIF5c-LT, grey lines; +mRFP, cells overexpressing GFP-GluA2 and mRFP, black lines. Thick line represents the average, and thin lines represent ±s.e.m. n, number of cells (the number of cells varies along the curve as not all dendrites were the same length). Scale bar: 10 µm.

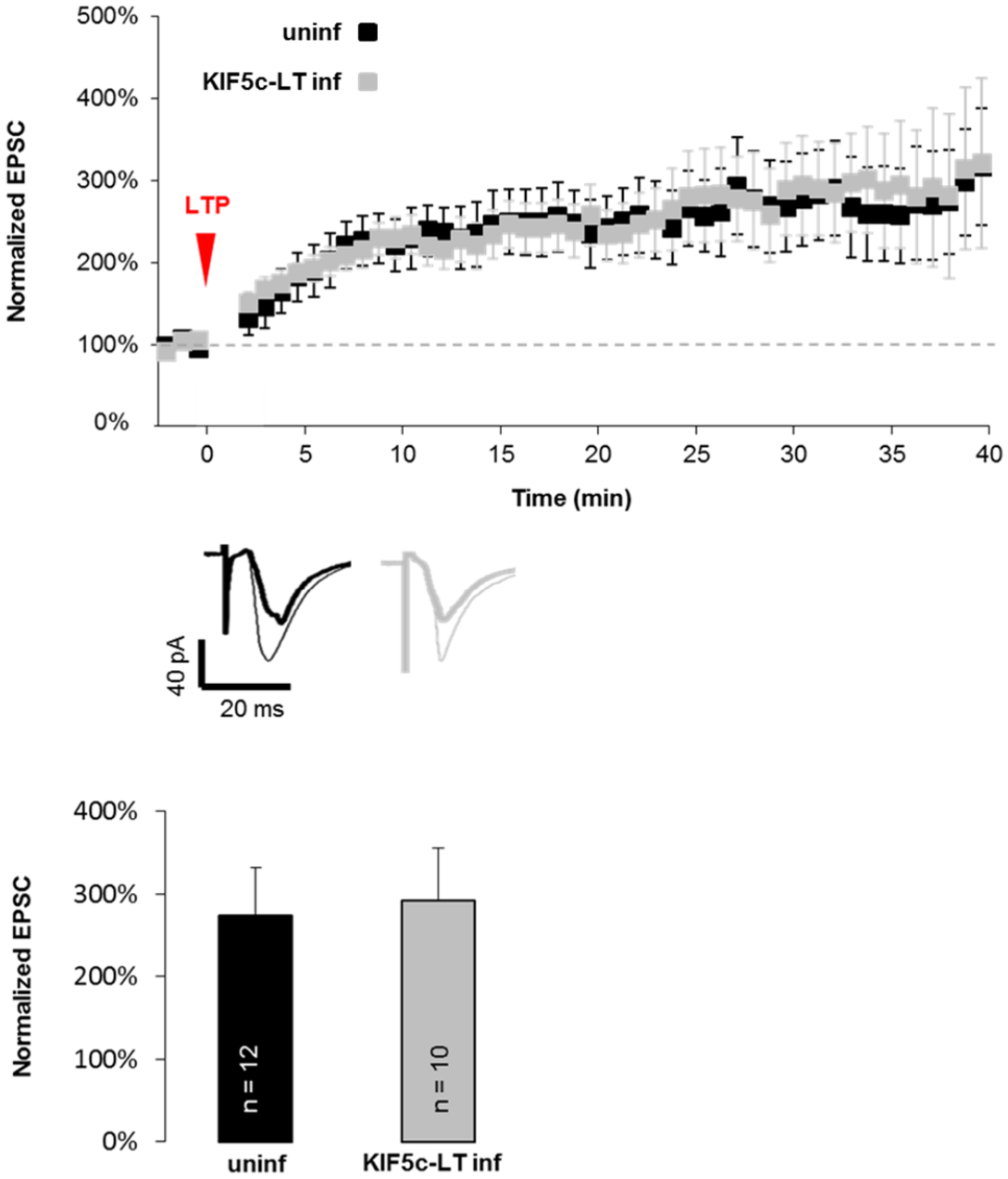

Figure 19. Analysis of the overexpression of KIF5c-LT on LTP. AMPAR-mediated responses were recorded at -60 mV from CA1 neurons prior to LTP induction (indicated with a red arrow head) using a pairing protocol (300 pulses, 3 Hz) coupled to depolarization of the postsynaptic neuron to 0 mV. uninf, uninfected, black symbols, representative traces in black; inf KIF5c-LT, Sindbis mCherry-KIF5c-LT infected cells 2 days post-infection (dpi), grey symbols, representative traces in grey. Time course reflects that uninfected (n=12 cells, 273 ± 58%, p value 0.003 Wilcoxon test) and KIF5c-LT infected cells (n=10 cells, 292 ± 63%, p value 0.023 Wilcoxon test) show similar LTP. Histogram represents averaged values ± s.e.m. of the amplitude of AMPAR-mediated responses (pA) during the 35 to 40 min time window. In the representative traces the thick line corresponds to the averaged responses of the baseline, and the thin line corresponds to the averaged responses of the last 10 min of the time course.

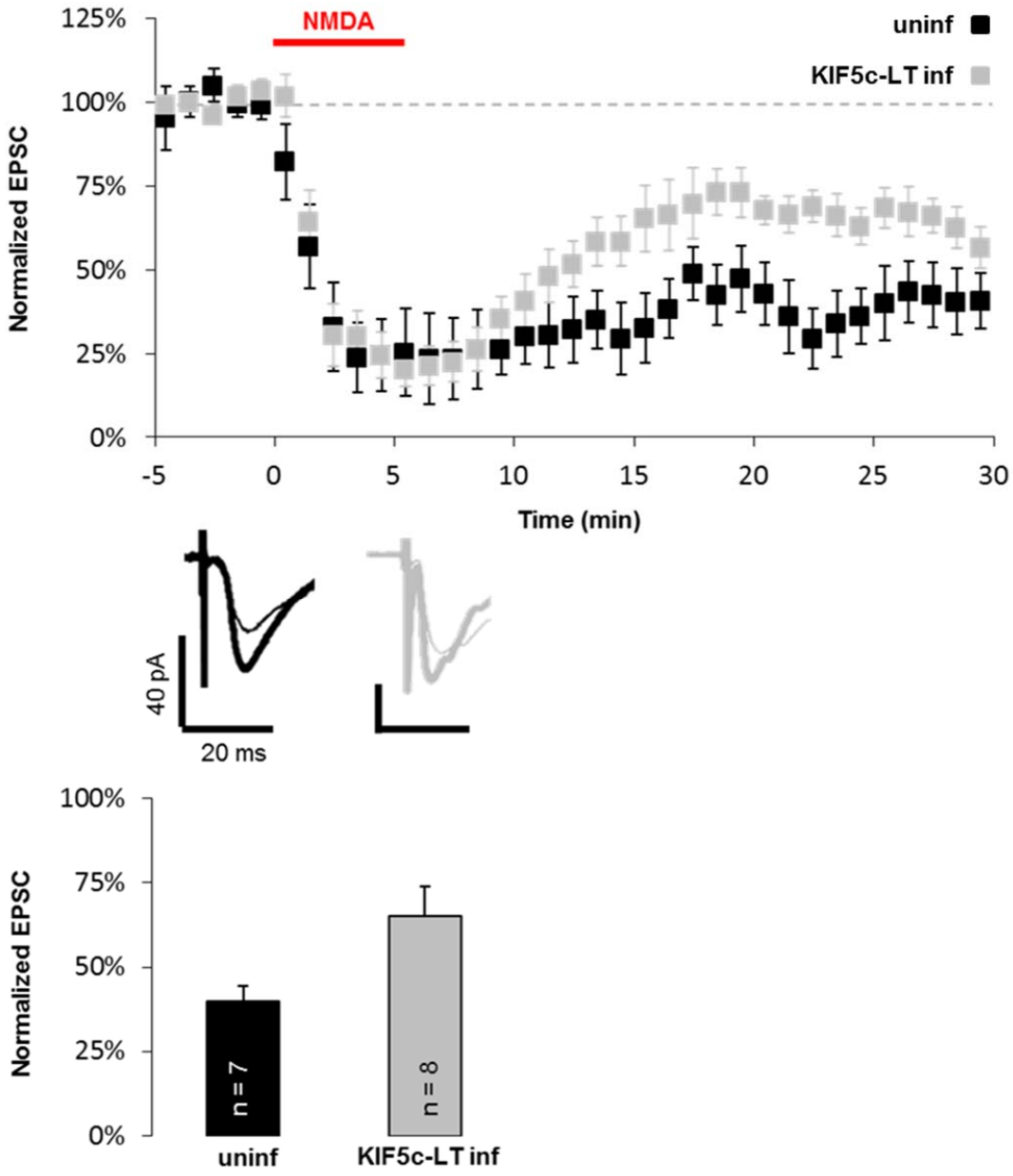

Figure 20. Analysis of the overexpression of KIF5c-LT on cLTD. AMPAR-mediated responses were recorded at -60 mV from CA1 neurons prior to cLTD induction by bath application of 20 μM NMDA for 5 minutes (see Materials & Methods, indicated with a red line). uninf, uninfected, black symbols, representative traces in black; inf KIF5c-LT, Sindbis mCherry-KIF5c-LT infected cells 2 days post-infection (dpi), grey symbols, representative traces in grey. Time course reflects that uninfected (n=7 cells, 40 ± 8%, p value 0.02 Wilcoxon test) and KIF5c-LT infected cells (n=8 cells, 65 ± 5%, p value 0.01 Wilcoxon test) show LTD, but KIFc-LT infected cells show slightly smaller depression when compared to unifected cells (p value 0.056 Mann-Whitney). Histogram represents averaged values ± s.e.m . of the amplitude of AMPAR-mediated responses (pA) during the 25 to 30 min time window. In the representative traces the thick line corresponds to the averaged responses of the baseline, and the thin line corresponds to the averaged responses of the last 5 min of the time course.

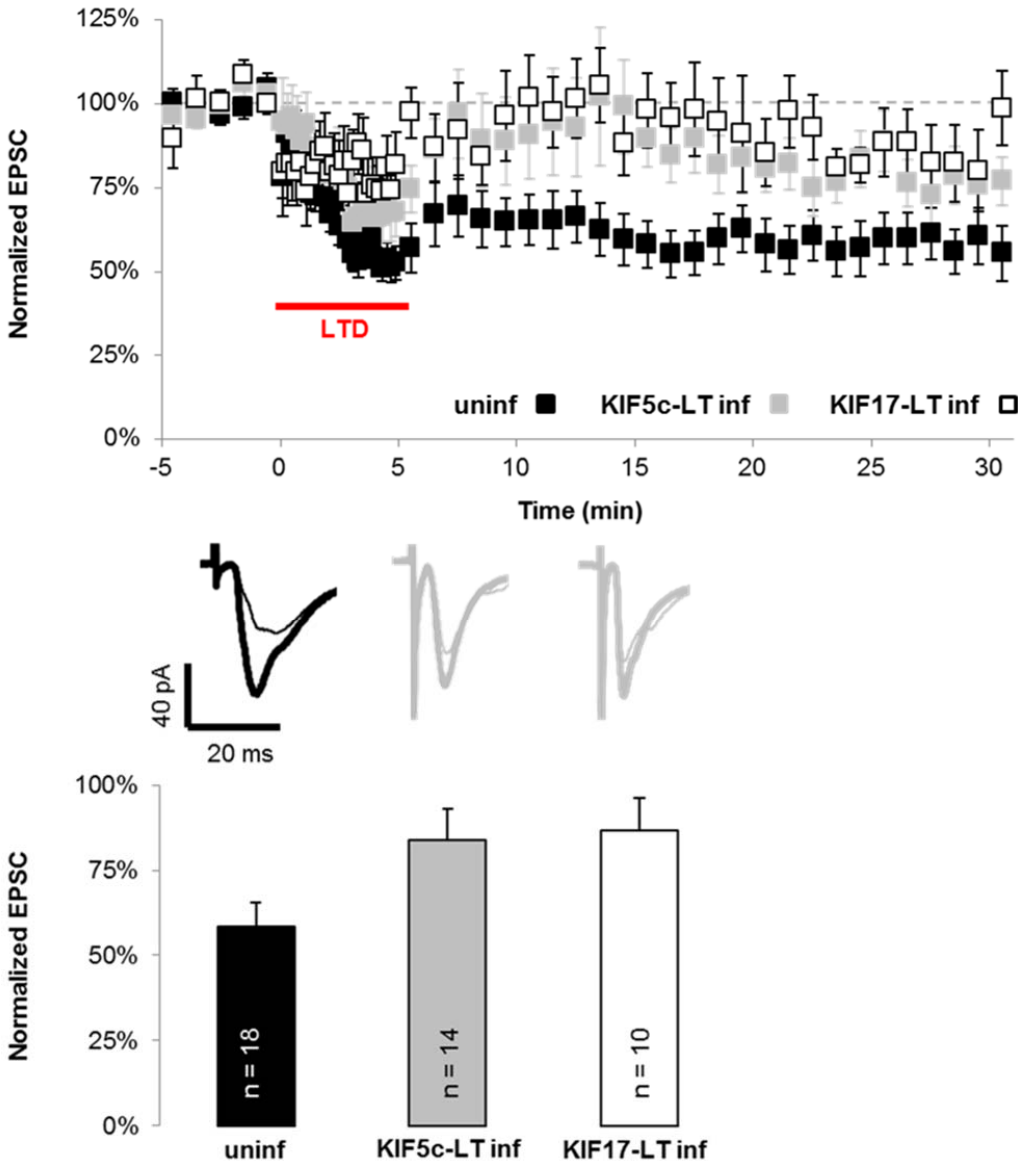

Figure 21. Analysis of the overexpression of KIF5c-LT and KIF17-LT on LTD. AMPAR-mediated responses were recorded at -60 mV from CA1 neurons prior to LTD induction (indicated with a red line) using a pairing protocol (300 pulses, 1 Hz) coupled to depolarization of the postsynaptic neuron to -40 mV. uninf, uninfected, black symbols, representative traces in black; inf KIF5c-LT, Sindbis mCherry-KIF5c-LT infected cells 2 days post-infection (dpi), grey symbols, representative traces in grey, inf KIF17-LT, Sindbis eGFP-KIF17-LT infected cells 2 dpi, white symbols, representative traces in grey. Time course reflects that uninfected cells (n=18 cells, 58 ± 7%, p value < 0.001 Wilcoxon test) show significant LTD whereas inf KIF5c-LT (n=14 cells, 84 ± 9%, p value 0.07 Wilcoxon test) or inf KIF17-LT (n=10 cells, 87 ± 9%, p value 0.12 Wilcoxon test) don't. Histogram represents averaged values ± s.e.m . of the amplitude of AMPAR-mediated responses (pA) during the 25 to 30 min time window. When uninfected cells are compared to inf KIF5c-LT (p value 0.05 Mann-Whitney test) or to inf KIF17-LT (p value 0.03 Mann-Whitney), the impairment in LTD becomes obvious. In the representative traces the thick line corresponds to the averaged responses of the baseline, and the thin line corresponds to the averaged responses of the last 5 min of the time course.

This impairment in LTD could be interpreted as a failure in the transport of AMPARs away from the spine once LTD was induced. After LTD, AMPARs are internalized and they leave the spine to go to other subcellular locations, such as lysosomes (Fernández-Monreal et al., 2012).

It could be hypothesized that MT-dependent transport via KIF5c was needed for this removal. That being the case, when such traffic was impaired by the presence of KIF5c-LT, there was an increase of the recycling of AMPARs within the spine.

After seeing these promising results pointing to a defect in NMDAR-dependent LTD maintenance and expression when KIF5c motor function is impaired, we immediately wondered if proper functioning of the KIF17 motor domain would be needed for this process too. To answer this question, the synaptically induced LTD was analyzed in the presence of KIF17-LT. Similar results were obtained: cells in which KIF17-LT was overexpressed showed significantly less LTD, less than 20%, than the non-infected ones, which show more than 40% depression (Figure 21). This was a surprising result as KIF17 is mainly responsible for NMDARs transport, which could reflect a specificity problem.

3.2. Functional characterization of the cargo binding domain of kinesins KIF5c and KIF17

Due to the exciting but controversial results with the *dominant negatives* of both KIF5 and KIF17 that lack just the motor domain, the possible functional role of the cargo binding domain of the same kinesins was explored, using the KIF5c-ST and KIF17-ST constructs.

Following the same rationale as before, basal transmission was analyzed in the presence of KIF5c-ST or KIF17-ST. Basal AMPAR- and NMDAR-dependent transmission was recorded in parallel from cells overexpressing KIF5c-ST and from not infected cells, finding that both forms of basal transmission are significantly depressed (Figure 22A). In contrast, when basal transmission was recorded comparing cells overexpressing KIF17-ST and control cells only NMDA transmission was significantly depressed (Figure 22B). The fact that KIF17-ST overexpression depressed NMDA basal transmission was in clear agreement with previous studies where KIF17 and NMDARs transport have been related (Setou, 2000; Yin et al., 2011). Similarly, it has been previously described that KIF5c-ST affects AMPA basal transmission (Setou et al., 2002). Nevertheless, our data indicated that overexpression of just the cargo binding domain of KIF5c depressed NMDA

transmission. This novel observation, KIF5c cargo binding domain regulates NMDA-mediated transmission, may reflect a specificity problem.

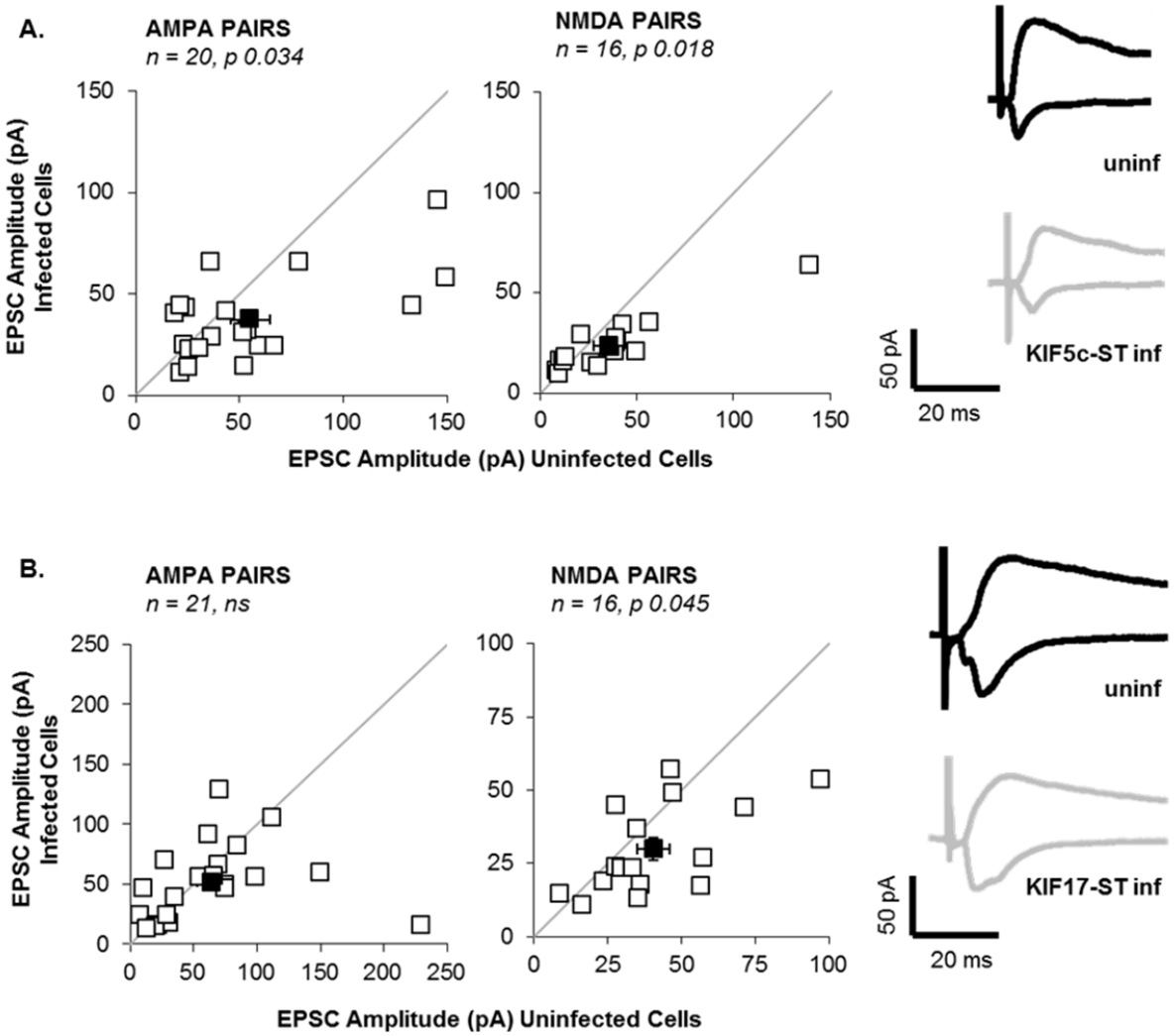

Figure 22. Analysis of the overexpression of KIF5c-ST or KIF17-ST on basal synaptic transmission. A. Synaptic AMPAR- and NMDAR-mediated responses were recorded at -60 mV and +40 mV, respectively, from pairs of neighboring CA1 neurons in organotypic hippocampal slices. uninf, uninfected, representative traces in black; inf KIF5c-ST, Sindbis mCherry-KIF5c-ST infected cells 1 day post-infection (dpi), representative traces in grey. Absolute values of the responses of the two cells that were simultaneously recorded under the same stimulation paradigm are shown. AMPAR-mediated responses (pA): uninf 55.09 ± 9.23, inf KIF5c-ST 37.46 ± 4.73. NMDAR-mediated responses (pA): uninf 35.47 ± 7.89, inf KIF5c-ST 23.67 ± 3.3. **B.** Same experiment as in **A.**, but corresponding to the overexpression of mCherry-KIF17-ST. uninf, uninfected, representative traces in black; inf KIF17-LT, Sindbis mCherry-KIF17-ST infected cells 1 dpi, representative traces in grey. AMPAR-mediated responses (pA): uninf 64.35 ± 11.54, inf KIF17-ST 51.89 ± 6.94. NMDAR-mediated responses (pA): uninf 40.41 ± 5.94, inf KIF17-ST 29.93 ± 3.86. *ns*, not significant; n number of cells; Wilcoxon test.

With these results and concerns in mind, the effects of overexpressing KIF5c-ST or KIF17-ST for 1 day were evaluated in the electrically induced LTD paradigm. In this case, even when basal transmission was impaired, LTD was statistically equal in uninfected cells when compared with those overexpressing either KIF5c-ST or KIF17-ST (Figure 23).

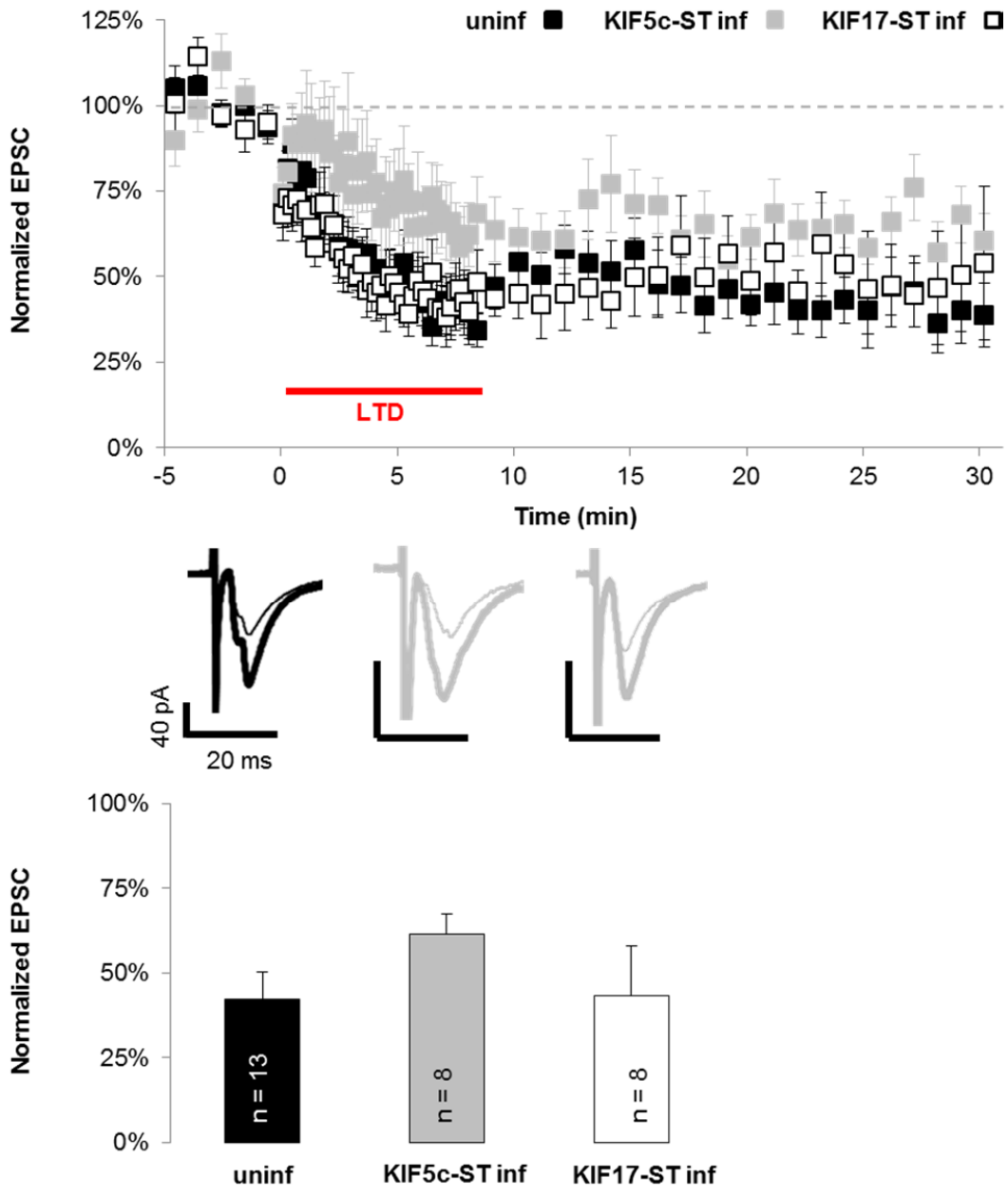

Figure 23. Analysis of the overexpression of KIF5c-ST and KIF17-ST on LTD.

Figure 23. Analysis of the overexpression of KIF5c-ST and KIF17-ST on LTD. AMPAR-mediated responses were recorded at -60 mV from CA1 neurons prior to LTD induction (indicated with a red arrow head) using a pairing protocol (500 pulses, 1 Hz) coupled to depolarization of the postsynaptic neuron to -40 mV. uninf, uninfected, black symbols, representative traces in black; inf KIF5c-ST, Sindbis mCherry-KIF5c-ST infected cells 1 day post-infection (dpi), grey symbols, representative traces in grey, inf KIF17-ST, Sindbis mCherry-KIF17-ST infected cells 1 dpi, white symbols, representative traces in grey. Time course reflects that uninfected cells (n=13 cells, 42 ± 8%, p value 0.002 Wilcoxon test) show significant LTD, exactly the same as inf KIF5c-ST (n=8 cells, 61 ± 6%, p value 0.01 Wilcoxon test) or inf KIF17-ST (n=8, 0.43 ± 0.15, p value 0.02 Wilcoxon test). Histogram represents averaged values ± s.e.m . of the amplitude of AMPAR-mediated responses (pA) during the 25 to 30 min time window. In the representative traces the thick line corresponds to the averaged responses of the baseline, and the thin line corresponds to the averaged responses of the last 5 min of the time course.

4. POSSIBLE FUNCTION OF GRIP1 IN THE MODULATION OF SYNAPTIC RESPONSE VIA ITS KINESIN BINDING DOMAIN

Our results indicated that KIF5c motor domain does not seem to be needed for basal transmission but for LTD, and the neck-stalk region seems to be needed for basal transmission but not for LTD. To study the underlying molecular mechanism, we decided to disrupt the KIF5-AMPAR containing vesicle interaction by interfering with GRIP1, the proposed adaptor molecule (Setou et al., 2002).

To do so, GRIP1-KBD was used, representing a minimal version of GRIP that consists of the region between the 6th and 7th PDZ domains of the protein fused to GFP (see Materials and Methods) (Figure 24). It is expected that GRIP1-KBD would act as a *dominant negative* by competing with endogenous GRIP1 and preventing the assembly of the KIF5-GRIP1-AMPA containing vesicle superstructure.

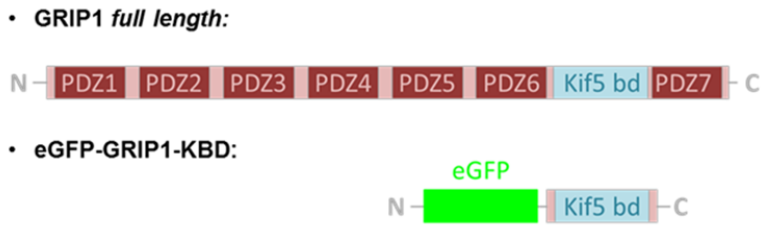

Figure 24. Schematic representation of the GRIP1 dominant negative used. Structure of the full length protein is shown to illustrate the missing domains on the dominant negative designed. KIF5 bd, KIF5 binding domain.

4.1. Validation of the mutant GRIP1-KBD

By the use of confocal imaging techniques, the distribution of GRIP1-KBD was analyzed when overexpressed in organotypic hippocampal slices. The recombinant protein was excluded from the nucleus, and presented a diffuse but not completely smooth or homogeneous pattern of expression in the whole cell (Figure 25).

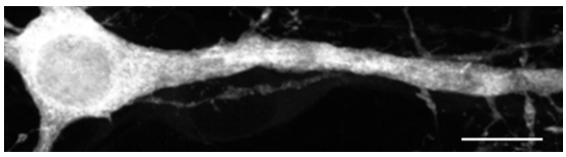

Figure 25. Detection of GRIP1 KBD.. Representative confocal image (right panel) of a CA1 neuron overexpressing eGFP-GRIP1-KBD 1 day post-infection (dpi). Scale bar: 10 µm.

4.2. Functional characterization of the mutant GRIP1-KBD

The effects of the overexpression of GRIP1-KBD in organotypic hippocampal slices in basal transmission and in synaptically induced LTD were evaluated as previously described (see above). Those cells in which GRIP1-KBD was overexpressed presented normal AMPA and NMDA basal transmission (Figure 26).

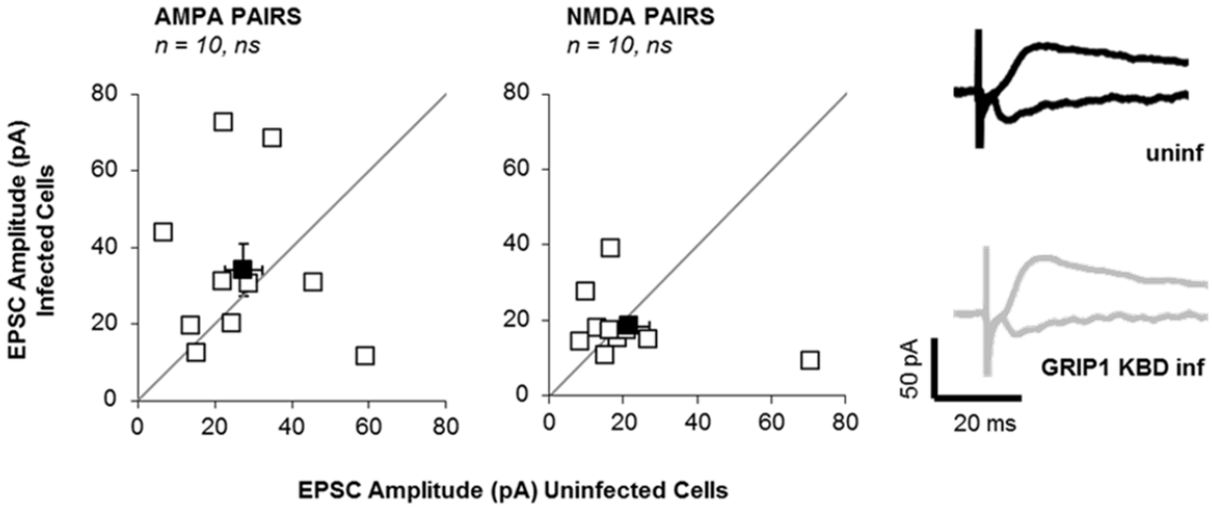

Figure 26. Analysis of the overexpression of GRIP1-KBD on basal synaptic transmission. Synaptic AMPA and NMDA responses were recorded at -60 mV and +40 mV, respectively, from pairs of neighboring CA1 neurons in organotypic hippocampal slices. uninf, uninfected, representative traces in black; inf GRIP1-KBD, Sindbis eGFP-GRIP1-KBD infected cells 1 day post-infection (dpi), representative traces in grey. Absolute values of the responses of the two cells that were simultaneously recorded under the same stimulation paradigm are plotted. AMPA responses (pA): uninf 27.39 ± 4.96, inf GRIP1-KBD 34.04 ± 6.81. NMDA responses (pA): uninf 21.49 ± 5.68, inf GRIP1-KBD 18.35 ± 2.78. *ns*, not significant; n number of cells; Wilcoxon test.

Similarly, GRIP1-KBD infected cells presented a degree of NMDAR-dependent LTD comparable to not infected cells that were recorded as controls (Figure 27).

These results suggested that those mechanisms by which KIF5c different domains modulate synaptic transmission, either basal AMPA and NMDA responses or NMDA-dependent LTD, were independent from its ability to bind GRIP1.

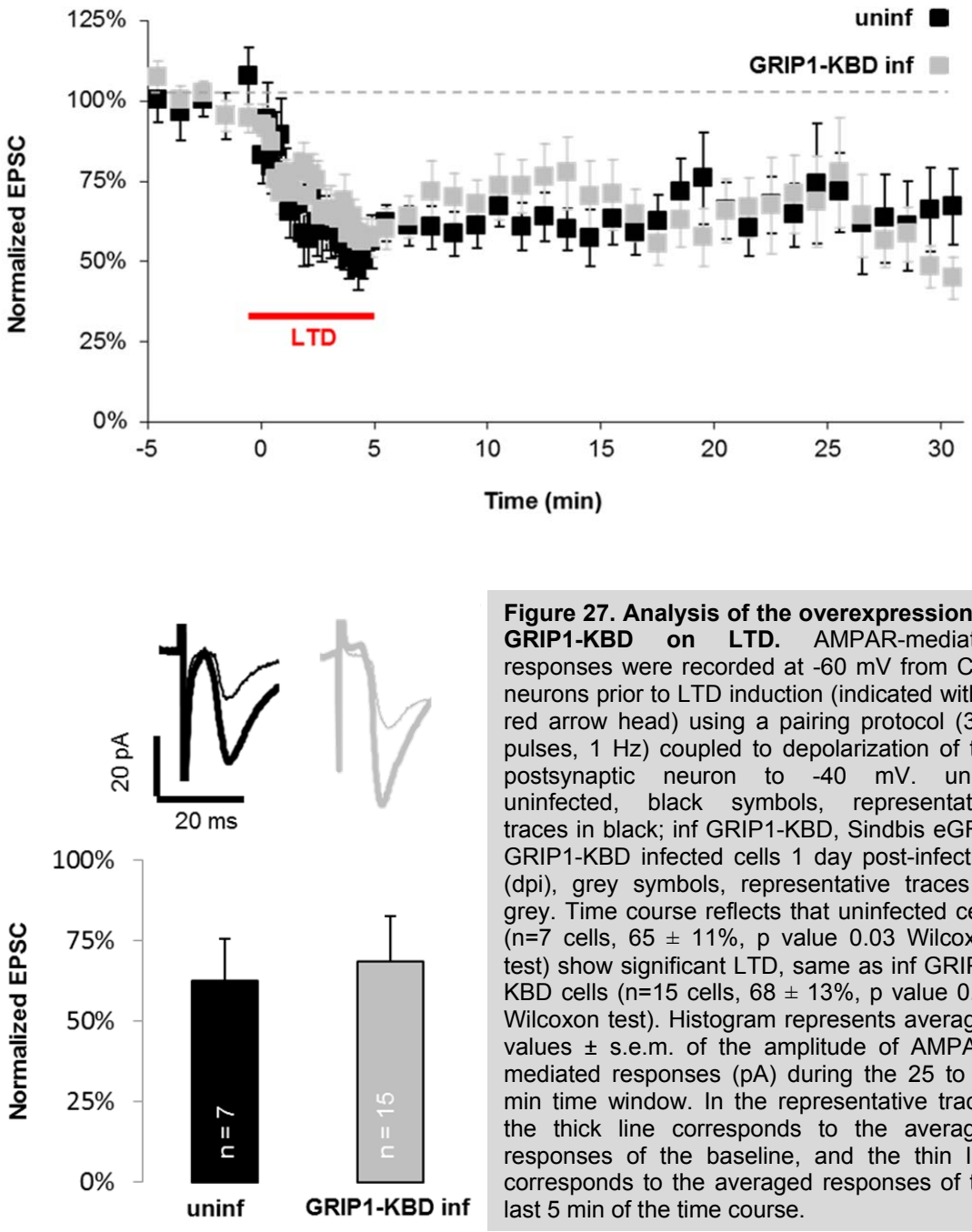

Figure 27. Analysis of the overexpression of GRIP1-KBD on LTD. AMPAR-mediated responses were recorded at -60 mV from CA1 neurons prior to LTD induction (indicated with a red arrow head) using a pairing protocol (300 pulses, 1 Hz) coupled to depolarization of the postsynaptic neuron to -40 mV. uninf, uninfected, black symbols, representative traces in black; inf GRIP1-KBD, Sindbis eGFP-GRIP1-KBD infected cells 1 day post-infection (dpi), grey symbols, representative traces in grey. Time course reflects that uninfected cells (n=7 cells, 65 ± 11%, p value 0.03 Wilcoxon test) show significant LTD, same as inf GRIP1-KBD cells (n=15 cells, 68 ± 13%, p value 0.02 Wilcoxon test). Histogram represents averaged values ± s.e.m. of the amplitude of AMPAR-mediated responses (pA) during the 25 to 30 min time window. In the representative traces the thick line corresponds to the averaged responses of the baseline, and the thin line corresponds to the averaged responses of the last 5 min of the time course.

5. FUNCTIONAL CHARACTERIZATION OF KINESINS KIF5A AND KIF5C: KNOCK-DOWN OF THE PROTEIN EXPRESSION

To further validate our previous results (see above) regarding the –LT and –ST mutants, and evaluate the role of KIF5 and KIF17 in synaptic function, we thought that analyses in the absence of endogenous proteins expression were highly valuable. We took advantage of the shRNA technology, previously set up in our laboratory (Benoist et al., 2013). The critical step to use shRNAs is to find a sequence that knocks-down completely or at least downregulates substantially the expression of the protein of interest in our system, hippocampal neurons.

To test the efficiency of individual shRNAs, primary hippocampal cultures were infected on DIV7 with the lentiviruses containing the sequence of the shRNA targeting the protein of interest (see Materials and Methods). After 7 days of infection, it was visually confirmed that the vast majority of the cells were infected (data not shown), as the lentiviral vector contained also the coding sequence of mCherry fluorescent protein. Moreover, representative Western blot analysis showed a strong and specific knock-down of KIF5a (Figure 28A) and KIF5c (Figure 28B). Similar results were obtained with shRNAs targeting KIF3A (preliminary data not shown).

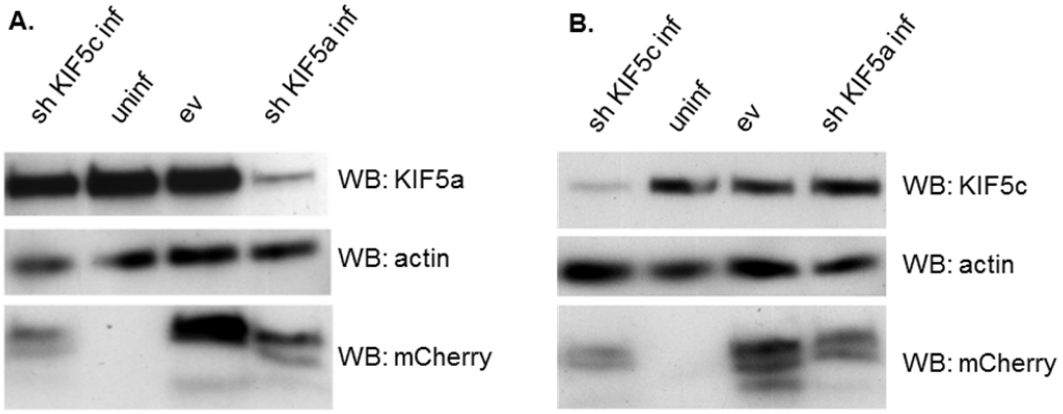

Figure 28. Specific downregulation of KIF5a and KIF5c expression. WB showing the specific downregulation of KIF5a and KIF5c achieved by delivering shRNAs to primary hippocampal cultures using lentivirues (see Materials & Methods). uninf, unifected sample from primary hippocampal cultures collected on day in vitro (DIV) 14; sh KIF5a inf, sample from primary hippocampal cultures collected on DIV 14 expressing a shRNA designed against KIF5a for 7 days; sh KIF5c inf, sample from primary hippocampal cultures collected on DIV 14 expressing a shRNA designed against KIF5c for 7 days; ev, sample from primary hippocampal cultures collected on DIV 14 expressing a lentiviral empty vector for 7 days. Actin was used as loading control, mCherry was used as a reporter of the level of infection.

Assuming that the efficiency of the knock-down will be the same in organotypic hippocampal slices, these were infected at DIV0/1 and electrophysiological recordings were done 6 to 9 days post infection. Synaptically induced LTD was evaluated in cells where either KIF5a or KIF5c were knocked-down, and compared to cells that were not infected with any lentiviral vector. When the expression of one of the kinesins, KIF5a or KIF5c, was abolished, NMDAR-dependent LTD occurred. However, in cells where there was not knocked-down, depression was slightly stronger (Figure 29). These data suggested that neither KIF5a nor KIF5c were required for LTD to occur normally. However, a promising and subtle trend was observed that may be further analyzed if both isoforms were knocked-down simultaneously.

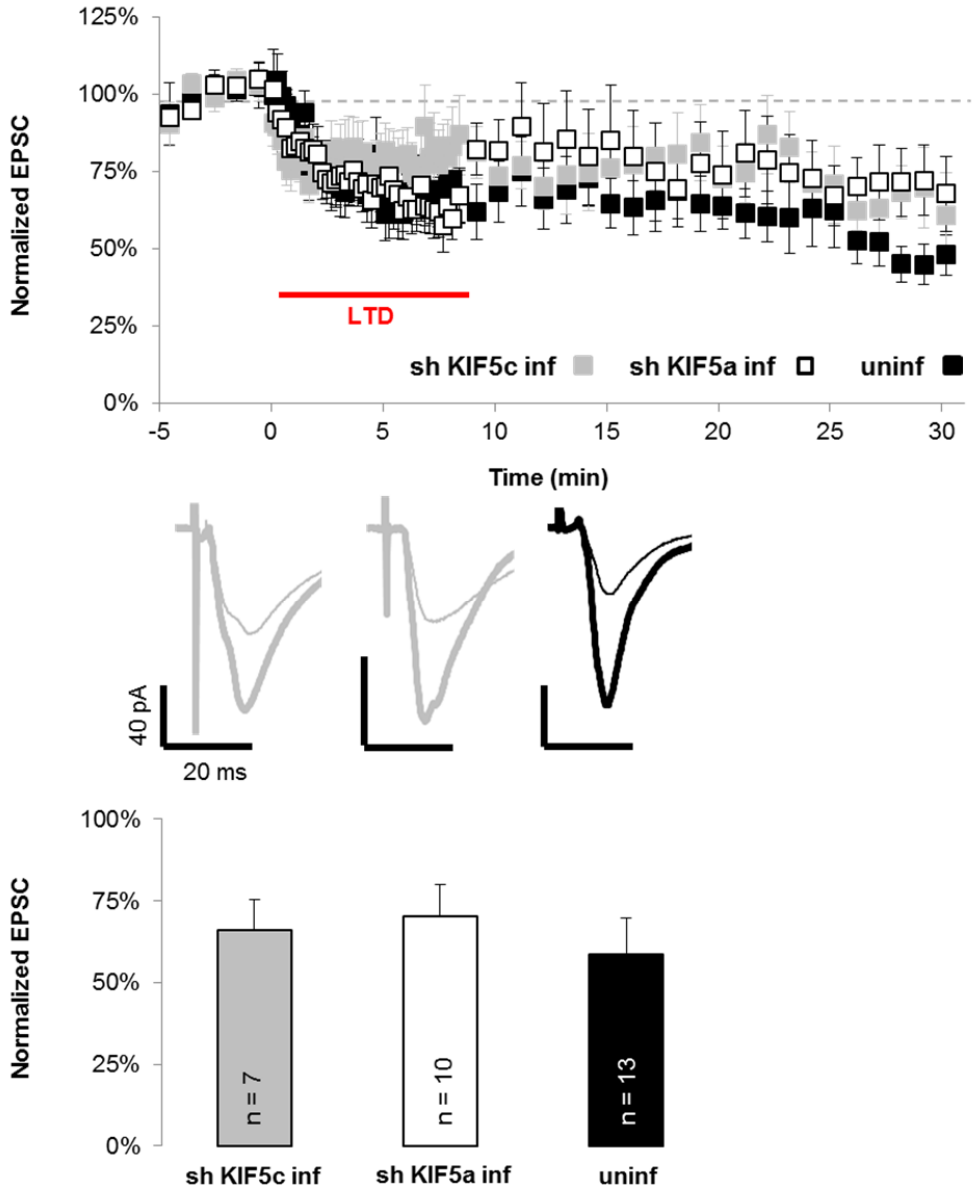

Figure 29. Analysis of the effect of the downregulation of either KIF5a or KIF5c on LTD. AMPAR-mediated responses were recorded at -60 mV from CA1 neurons prior to LTD induction (indicated with a red arrow head) using a pairing protocol (500 pulses, 1 Hz) coupled to depolarization of the postsynaptic neuron to -40 mV. uninf, uninfected, black symbols, representative traces in black; inf sh KIF5c, cells expressing a shRNA designed against KIF5c for 6 to 9 days, grey symbols, representative traces in grey; inf sh KIF5a, cells expressing a shRNA designed against KIF5a for 6 to 9 days, white symbols, representative traces in grey. Time course reflects that uninfected cells (n=13 cells, 59 ± 11%, p value 0.01 Wilcoxon test) show significant LTD, similar to inf sh KIF5c (n=7 cells, 66 ± 10% p value 0.03 Wilcoxon test) and inf sh KIF5a (n=10 cells, 74 ± 9%, p value 0.03 Wilcoxon test). Histogram represents averaged values ± s.e.m. of the amplitude of AMPAR-mediated responses (pA) during the 25 to 30 min time window. In the representative traces the thick line corresponds to the averaged responses of the baseline, and the thin line corresponds to the averaged responses of the last 5 min of the time course.

B. ASSESMENT OF THE ROLE OF THE MINUS-END DIRECTED MICROTUBULE-DEPENDENT TRANSPORT IN MODULATION OF SYNAPTIC FUNCTION

So far, all the experiments done were dealing with molecular motors that move towards the plus-end of the MTs. There is a general consensus on the idea that the MTs are all equally oriented in the axon (minus-end towards the soma). In contrast, in dendrites, at least on the proximal regions, they show mixed polarities (Baas and Lin, 2011; Conde and Cáceres, 2009). Therefore, minus-end directed trafficking could also, potentially, play a role in the modulation of synaptic plasticity.

We wanted to address whether dynein, the principal minus-end directed motor protein, plays a role in synaptic plasticity modulation in our system. For that, two different experimental approaches were designed, similarly as those used to address the possible role of kinesins KIF5 and KIF17 in synaptic plasticity modulation: a *dominant* negative approach (disrupting the formation of the dynein-dinactin complex), and knockdown the expression level of the dynein heavy chain (DHC).

1. POSSIBLE DYNACTIN DEPENDENT FUNCTIONS OF DYNEIN IN THE MODULATION OF SYNAPTIC RESPONSE

It is well-known that overexpression of dynamitin, a subunit of the dynein-dynactin complex, prevents its formation (Burkhardt et al., 1997), inhibiting dynein function in a dynactin-dependent manner. Although from the molecular point of view this approach is clearly different, the concept is similar to the *dominant negative* approach used to study KIF5 and KIF17 function in synaptic plasticity.

1.1. Validation of dynamitin as a tool to disrupt dynactin dependent functions of dynein

By the use of confocal imaging techniques, the distribution of dynamitin when overexpressed in organotypic hippocampal slices was analyzed. This recombinant protein was excluded from the nucleus, and presented a diffuse but not completely smooth or homogeneous pattern (some clusters might be seen) of expression (Figure 30).

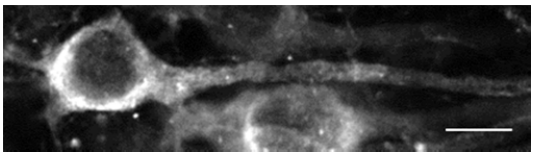

Figure 30. Detection of dynamitin.. Representative confocal image (right panel) of a CA1 neuron overexpressing eGFP-dynamitin 1 day post-infection (dpi). Scale bar: 10 µm.

1.2. Functional characterization of dynamitin as a tool to disrupt dynactin dependent functions of dynein

The effects of the overexpression of dynamitin in organotypic hippocampal slices in basal transmission and in synaptically induced LTD were evaluated using the same electrophysiological approach previously utilized (see above).

Those cells in which dynamitin was overexpressed presented normal AMPAR and NMDAR-mediated basal transmission (Figure 31).

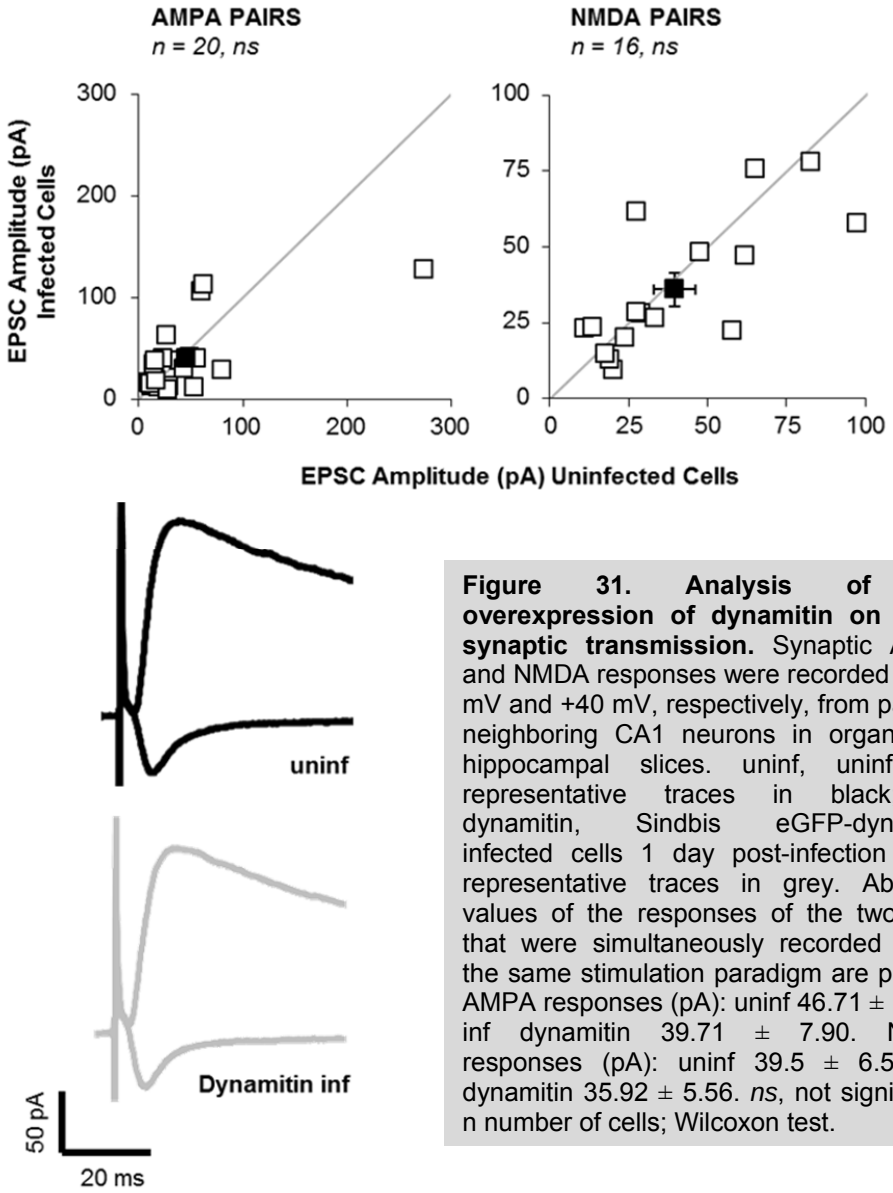

Figure 31. Analysis of the overexpression of dynamitin on basal synaptic transmission. Synaptic AMPA and NMDA responses were recorded at -60 mV and +40 mV, respectively, from pairs of neighboring CA1 neurons in organotypic hippocampal slices. uninf, uninfected, representative traces in black; inf dynamitin, Sindbis eGFP-dynamitin infected cells 1 day post-infection (dpi), representative traces in grey. Absolute values of the responses of the two cells that were simultaneously recorded under the same stimulation paradigm are plotted. AMPA responses (pA): uninf 46.71 ± 12.79, inf dynamitin 39.71 ± 7.90. NMDA responses (pA): uninf 39.5 ± 6.54, inf dynamitin 35.92 ± 5.56. *ns*, not significant; n number of cells; Wilcoxon test.

In addition, they presented virtually the same degree of NMDAR-dependent LTD compared with the not infected cells that were recorded as controls (Figure 32).

These results suggested that, if minus-end MT-dependent traffic plays a role in synaptic plasticity modulation, it will be independent of dynein fuctions dependent on dynactin.

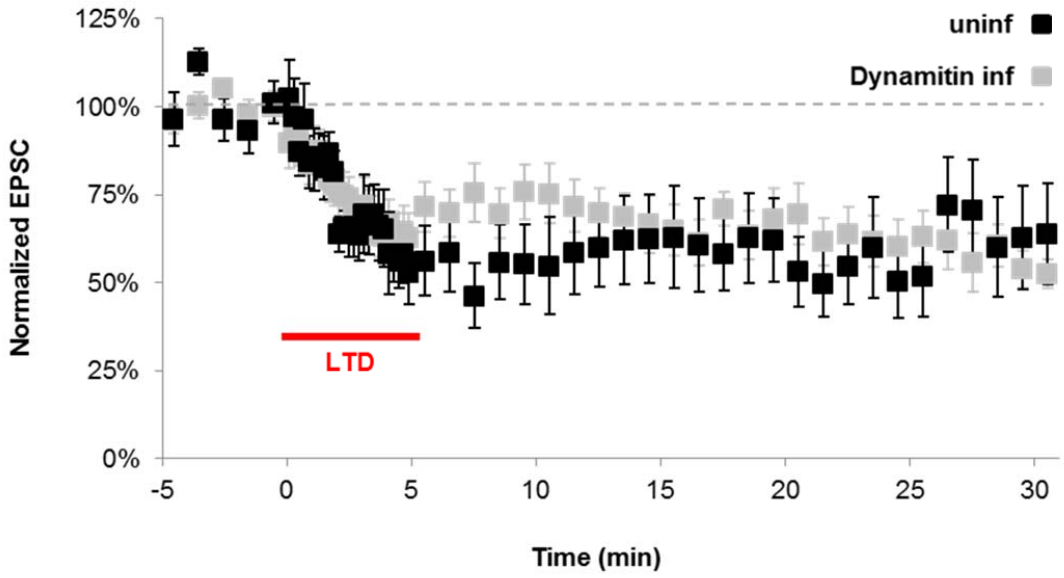

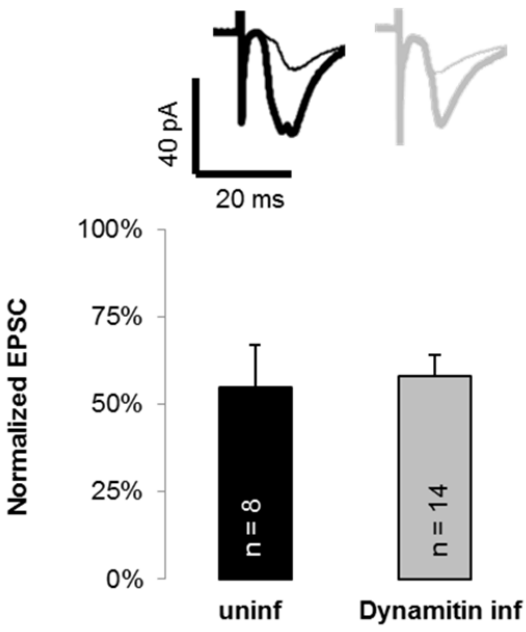

Figure 32. Analysis of the overexpression of dynamitin on LTD. AMPAR-mediated responses were recorded at -60 mV from CA1 neurons prior to LTD induction (indicated with a red line) using a pairing protocol (300 pulses, 1 Hz) coupled to depolarization of the postsynaptic neuron to -40 mV. uninf, uninfected, black symbols, representative traces in black; inf dynamitin, Sindbis eGFP-dynamitin infected cells 1 day post-infection (dpi), grey symbols, representative traces in grey. Time course reflects that uninfected cells (n=8 cells, 55 ± 12, p value 0.01 Wilcoxon test) show significant LTD, same as inf dynamitin cells (n=14 cells, 58 ± 6%, p value 0.001 Wilcoxon test). Histogram represents averaged values ± s.e.m. of the amplitude of AMPAR-mediated responses (pA) during the 25 to 30 min time window. In the representative traces the thick line corresponds to the averaged responses of the baseline, and the thin line corresponds to the averaged responses of the last 5 min of the time course.

2. FUNCTIONAL CHARACTERIZATION OF DYNEIN HEAVY CHAIN (DHC): KNOCK-DOWN OF THE PROTEIN EXPRESION

Once we had established that dynein functions dependent on dynactin were not relevant for the maintenance of basal transmission or for the expression of NMDAR-dependent LTD (see results above), we wanted to evaluate whether dynein itself would be needed. In order to do so we knocked-down DHC expression by using shRNA technology.

To test the efficiency of individual shRNAs, primary hippocampal cultures were infected on DIV7 with the lentiviruses containing the sequence of the shRNA targeting the protein of interest (see Materials and Methods). After 7 days of infection, it was visually confirmed that the vast majority of the cells were infected (data not shown), as the lentiviral vector contained also the coding sequence of mCherry fluorescent protein. Moreover, representative Western blot analysis showed a strong and specific knock-down of DHC (Figure 33).

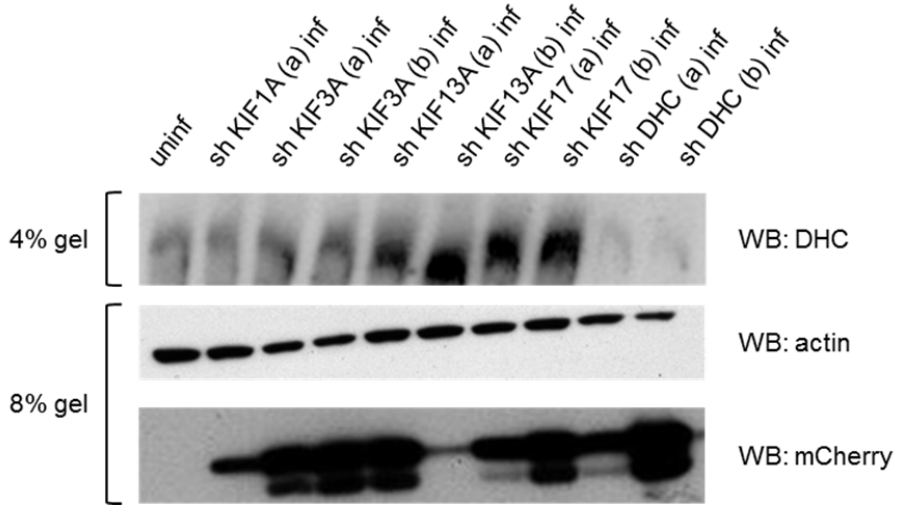

Figure 33. Specific downregulation of DHC expression. WB showing the specific downregulation of DHC achieved by delivering shRNAs to primary hippocampal cultures using lentivirues (see Materials & Methods). uninf, unifected sample from primary hippocampal cultures collected on day in vitro (DIV) 14; sh XXX(x) inf, sample from primary hippocampal cultures collected on DIV 14 expressing a shRNA designed against the protein of interest (KIF1A, KIF3, KIF13A, KIF17 or DHC) for 7 days. Small letters in between parenthesis corresponds to different shRNA sequences. As DHC has a very high molecular weight (approximately 500 kDa), the same sample was analyzed in two different gels (4% or 8%). Actin was used as loading control, mCherry was used as a reporter of the level of infection.

Assuming that the efficiency of the knock-down will be the same in organotypic hippocampal slices, these were infected at DIV0/1 and electrophysiological recordings were done 6 to 9 days post infection. Synaptically induced LTD was evaluated in cells where DHC was knocked-down (Figure 34). In this particular case, the data is very preliminary and the cells used as controls, i.e. cells not infected with any lentiviral vector, belong to the experiment shown in Figure 29.

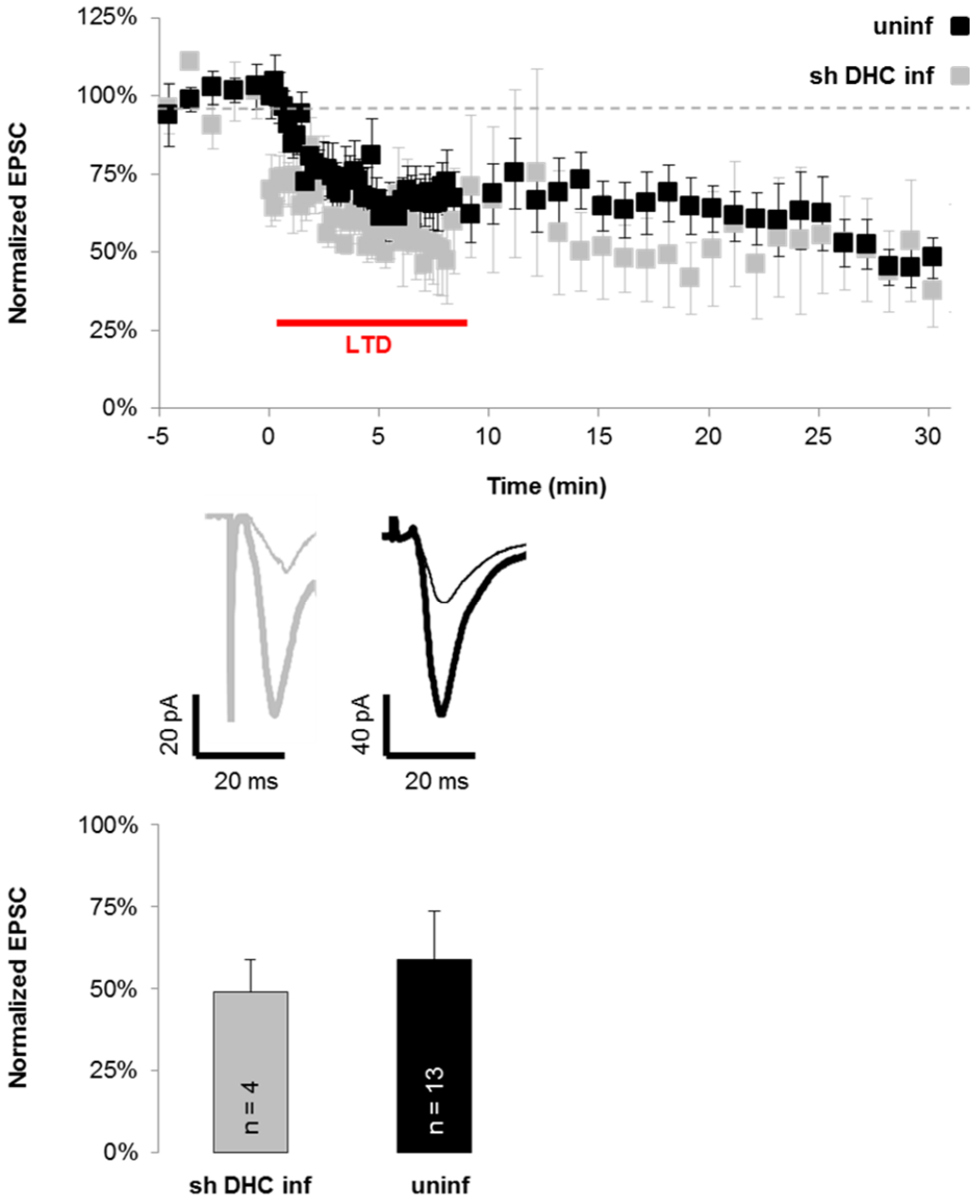

Figure 34. Analysis of the effect of the downregulation of DHC on LTD.

Figure 34. Analysis of the effect of the downregulation of DHC on LTD. AMPAR-mediated responses were recorded at -60 mV from CA1 neurons prior to LTD induction (indicated with a red arrow head) using a pairing protocol (500 pulses, 1 Hz) coupled to depolarization of the postsynaptic neuron to -40 mV. uninf, uninfected, black symbols, representative traces in black; inf sh DHC, cells expressing a shRNA designed against DHC for 6 to 9 days, grey symbols, representative traces in grey. Time course reflects that uninfected cells (n=13 cells, 59 ± 11%, p value 0.01 Wilcoxon test, experiment from Figure 29) show significant LTD. Cells in which DHC was downregulated show similar LTD to uninfected ones, although the degree of LTD is not significat (n=4 cells, 49 ± 15%, p value 0.08 Wilcoxon test), probably because of the small n. Histogram represents averaged values ± s.e.m. of the amplitude of AMPAR-mediated responses (pA) during the 25 to 30 min time window. In the representative traces the thick line corresponds to the averaged responses of the baseline, and the thin line corresponds to the averaged responses of the last 5 min of the time course.

Despite the fact that the result shown in Figure 34 is still very preliminary, it seems that NMDAR-dependent LTD does not require dynein activity.

Discussion

Molecular motors are key components of the cellular machinery, especially in cells as highly polarized as neurons. Classically, actin-associated motors, myosins, were the ones associated with synaptic transmission (Correia et al., 2008; Wang et al., 2008). This was due to the fact that actin was thought to be the only cytoskeletal component inside dendritic spines, where most of the AMPAR trafficking related with the modulation of the synaptic response occurs. Also, Myosin motors have been always associated with transport processes that take place in the vicinity of the plasma membrane, based on the presence of an "actin cortex" underneath the plasma membrane. This, again, placed them as the ideal candidates for the regulation of the transport of AMPAR in synaptic function (Kneussel and Wagner, 2013). However, in the late 2000s, several groups showed that MTs and MT-associated proteins could enter the spines during spine development, and in an activity dependent manner (Dent et al., 2011; Gu et al., 2008; Hoogenraad and Bradke, 2009; Hu et al., 2008; Jaworski et al., 2009; Merriam et al., 2011; Penzes et al., 2009). Thus, we wondered that if synaptic plasticity could affect MT-behavior, this influence might be bidirectional and MTs and MT-associated transport might modulate synaptic function (Figure 35).

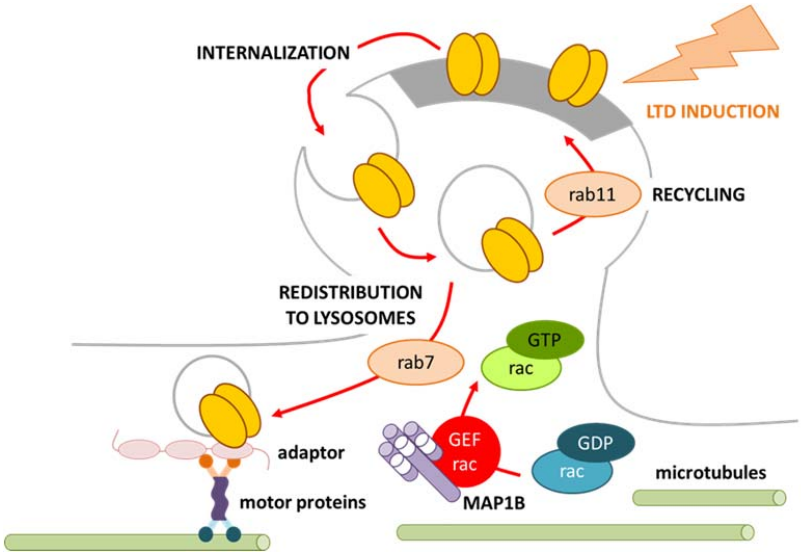

Figure 35. Possible role of MT-dependent transport on the removal of receptors from the spine after LTD induction. Our group has provided evidence for the MT-associated protein MAP1B to be required for LTD induction, relating MT dynamics and regulation with synaptic plasticity. Once LTD is induced, AMPARs (yellow ovals) need to abandon the spine surface, and then they can either recycle back to the plasma membrane or be transported elsewhere, for instance to lysosomes. In our working hypothesis, motor proteins such as kinesins or dyenin could be implicated in the removal and transport of receptors away from the spine. In this situation, an impairment of the transport would lead to a decrease in LTD expression, as recycling within the spine would be promoted.

In line with this hypothesis, our group has shown that MAP1B, a classical MT associated protein normally studied for its role as a modulator of axogenesis, is required to provide the Rac activity required for LTD to occur (Benoist et al., 2013). In addition, our group has shown that the light chain of MAP1B (MAP1B-LC) can regulate the surface expression of GluA2 containing AMPARs by interacting with GRIP1 (Palenzuela et al, unpublished results). So, we have indeed provided evidence of MT-interacting proteins playing a role in the modulation of synaptic transmission in the hippocampus.

1. ROLE OF PLUS END TRAFFICKING IN SYNAPTIC PLASTICITY

In addition to the proposed role of MT-interacting proteins in synaptic transmission, the interaction of KIF5 with AMPARs and GABARs, and of KIF17 with NDMARs has already been described (Hoogenraad et al., 2005; Mandal et al., 2011; Setou et al., 2000; Twelvetrees et al., 2010). Therefore, two main biological questions were proposed in this thesis: can KIF5 or KIF17 indeed modulate synaptic function? If so, what are the molecular mechanism and the interactions that are allowing them to?

1.1. The presence of the motor domain of KIF5c or of KIF17 is not necessary for basal transmission maintenance, but seems to be needed for LTD expression

Our FRAP experiments in which we overexpressed KIF5c-LT or KIF17-LT mutant proteins in organotypic hippocampal slices demonstrated that their motor domains were required for them to move in a directed manner (Figure 15). However, it seems from their pattern of distribution, which is not confined to the vicinity of the soma, that they are being transported somehow. Probably, they do so as cargoes in other vesicles. The idea that several motors can be attached at the same time to the same vesicle is not new at all. On one hand, KIF5 transports cytoplasmic dynein in the axon towards the plus-end of MTs (Hirokawa et al., 2009), which constitutes an example of a motor being transported as cargo. On the other hand, the fact that two motors can be bound at the same time to the same vesicle is the basis for the “tug-of-war” theory on how vesicles can move bidirectionally on the same MT (Hancock, 2014).

From a functional point of view, KIF5 was found to be required for the proper targeting of GluA2 to the neuronal surface via GRIP1 interaction (Hoogenraad et al., 2005). Strikingly, in our system we found that overexpression of KIF5c-LT had no impact whatsoever on the GluA2 levels that were transported along the dendrite (Figure 18). This apparent

contradiction could be explained because, in our experiments, no difference was made between intracellular and extracellular GluA2. Therefore, if KIF5c motor activity is required for the last targeting step, i.e., to contribute to the insertion of the receptors in the spine surface, and not to transport the receptor from the synthesis region to the vicinity of the spine, we could have missed the effect.

In any case, considering that the motor activity of KIF5c was not needed for GluA2 normal targeting to the surface, AMPA currents in the presence of KIF5c-LT would be expected to remain normal. This is indeed what we found. AMPA and NMDA currents were in the presence of KIF5c-LT, compared to uninfected cells. Similar results were obtained for KIF17-LT overexpression. These results were contradicting expectations from published data (Hoogenraad et al., 2005; Yin et al., 2011). Even more, if KIF5c-LT and KIF17-LT acted as *dominant negatives*, they were expected to be in a constitutively active conformation, as they lacked their motor domain which is critical for them to achieve an autoinhibited conformation (Verhey and Hammond, 2009). So, in principle, they should be able to bind to every possible cargo and inhibit its transport.

We found that NMDAR-dependent LTP was not affected by the presence of a KIF5c-LT (Figure 19), suggesting that the insertion of AMPARs into the surface of the spine is kinesin-motor-independent.

We also found that, independently of the induction protocol, NMDAR-dependent LTD was impaired when KIF5c-LT was overexpressed (Figures 20 and 21). These data indicated that, indeed, the motor activity of KIF5 was needed for the removal of receptors away from the spine area. This is a plausible scenario, as our own group has shown that when LTD is induced and AMPARs are internalized, they have to abandon the spine, not only the surface, probably to undergo lysosomal degradation (Fernández-Monreal et al., 2012).

Altogether, these results led us to hypothesize that kinesin motor activity would not be needed for the delivery of receptors to the vicinity of the spine, but for the removal of receptors.

When receptors cannot abandon the spine after LTD is induced and they have been already internalized, they might go back to the membrane, a process controlled by Rab11 (Fernández-Monreal et al., 2012). Rab11 is negatively regulated by protrudin, a protein that binds KIF5a through a region in the stalk domain (Matsuzaki et al., 2011). This region

is highly conserved at the amino acid sequence level between KIF5a, KIF5b and KIF5c (Kanai et al., 2000). Then, although further interaction studies are required, it is tempting to speculate that KIF5c-LT could sequester protrudin, leading to an over-activation of Rab11, and promoting the recycling of AMPARs within the spine. This phenomenon, along with the avoidance of transportation to remove receptors from the spine vicinity, could explain the observed impairment in LTD.

Overexpression of KIF17-LT also provoked an impairment of LTD expression and maintenance (Figure 21). Our working hypothesis is that KIF17-LT would negatively regulate Rab8, preventing the forward trafficking of NMDARs towards the spine, which could explain the impairment in LTD. In line with this hypothesis, the *Caenorhabditis elegans* KIF17 homolog, OSM-3, plays very important roles in ciliogenesis by membrane addition and intraflagellar transport in a Rab8 related manner (Hao and Scholey, 2009; Sung and Leroux, 2013). Moreover, Rab8 has been proposed to control processes that involve membrane outgrowth, also in neurons (Huber et al., 1995), and to control membrane-directed trafficking of AMPARs during basal transmission and LTP paradigms (Brown et al., 2007; Gerges et al., 2004).

1.2. The absence of both the motor domain and the neck-stalk regions of KIF5c or KIF17 have specific effects depressing basal transmission, but have no impact on LTD expression

In general, kinesins have most of the regulatory and binding sequences in the cargo and in the motor domain, whereas the neck-stalk domain is generally used for dimerization of the protein (Verhey and Hammond, 2009). In addition, the neck-stalk domain has been involved in the autoihibition of kinesins. By using this domain as a hinge, kinesins can bend over themselves and approximate to different degrees the cargo and the motor domains (Verhey and Hammond, 2009).

By generating new *dominant negatives* just containing the cargo binding domain, not only motor function, but also dimerization and autoinhibition abilities of the kinesins would be avoided. Therefore, we expected these “minimal” *dominant negatives* to compete more directly with the adaptor proteins, binding to the cargo domain, and therefore disrupt the interaction endogenous kinesin-cargo in a more specific manner.

In the case of KIF5c-ST, theoretically this mutant could still interact with endogenous KIF5 through a small region that contains the motor inhibiting site (MIS) (Seeger and Rice, 2010). Therefore this *dominant negative* could act as such by either competing with the cargo or by binding to the motor domain of endogenous KIF5 and preventing its movement.

In the case of KIF17-ST, Dr. Kristen J. Verhey (University of Michigan, USA), who kindly provided us with some plasmids, found that in the shortest versions of KIF17 the presence of the nuclear localization signal (NLS) was targeting the recombinant protein to the nucleus in such a high concentration that the health of the cells was compromised (unpublished observations). By removing the NLS, the Ser1029 was also removed, which is the target residue for CaMKII to phosphorylate KIF17 and promote the dissociation of the KIF17-mLin10/mLin2/mLin7-GluN2B complex (Ally et al., 2008). Moreover, the KIF17 PDZ binding motif was also removed in this mutant (Guillaud et al., 2008). Therefore, without further evidences, we cannot affirm that KIF17-ST mutant still binds GluN2B through the mLin10/mLin2/mLin7 complex or, alternatively, could still dissociate from this complex.

When KIF5c-ST was overexpressed, a depression in both AMPAR- and NMDAR-mediated currents was observed (Figure 22A), whereas in the case of KIF17-ST only NMDAR-mediated responses were decreased (Figure 22B). The impairment in NMDAR-mediated currents in the presence of KIF17-ST suggests that the cargo binding domain of KIF17 is regulating basal transport of NMDARs to the spine surface. Further experiments are required to determine at which step the regulation occurs. The impairment of AMPAR-mediated transmission by overexpression of KIF5c-ST can be also explained if the cargo binding domain regulates transport of AMPARs to the spine surface. To really confirm these results, imaging experiments coexpressing GluA2 and KIF5c-ST should be done, including the surface vs. intracellular control. Still, we do not fully understand how KIF5c-ST is impairing NMDAR-dependent transmission.

LTD was completely normal in the presence of either KIF5c-ST or KIF17-ST (Figure 23). Even if there was a KIF5c-LT mediated depression of AMPA basal transmission, NMDA-dependent LTD could be normal (even if NMDAR-dependent transmission was also depressed). We propose two possible explanations for this phenomenon: (a) KIF5c-ST lacks the region used to bind to protrudin (Matsuzaki et al., 2011), so the Rab11-recycling pathway (Fernández-Monreal et al., 2012) cannot be overactivated by this mutant,

therefore, once AMPARs are endocytosed as a consequence of LTD induction, their re-insertion to the plasma membrane is simply not promoted. (b) Alternatively, the fact that LTD is normal when basal transmission is reduced, suggests that the absolute number of receptors removed during LTD is in fact reduced. This can be explained as follows. AMPAR mediated transmission was depressed under basal circumstances, suggesting there were less receptors in the surface, for instance, n/2 AMPARs compared with the n AMPARs present in a KIF5c-ST not infected cell. When LTD was induced, receptors will be equally internalized, for instance, at a 50% internalization rate: uninfected cells will go from having n to having n/2 AMPARs on the surface, and KIF5c-ST infected cells will go from n/2 AMPARs to n/4 AMPARs. The absolute number of AMPARs in the surface would be affected, but not the relative one, suggesting that the quantity of LTD was still the same independently of the impairment of the normal function of the KIF5c cargo binding domain.

How can we reconcile these results with the effects observed with the Long Tails? The main difference between the –LT and –ST mutants is the presence or absence of the neck-stalk domain. This region, apart from kinesin dimerization, has been involved in some protein-protein interactions, such as the mentioned interaction of KIF5 and protrudin (Matsuzaki et al., 2011), or binding to non-motor proteins Vik-1 and Cik-1 by yeast Kinesin-14 family members (Barrett et al., 2000; Manning et al., 1999). Moreover, this domain contains functionally relevant regions, i.e., motor directionality is controlled by the neck-linker or Ncd neck domain in the case of Kinesin-1 (Endow, 1999). Therefore, differential regulation of the motor activity by regions in the neck-stalk domain is a plausible explanation for the effects observed in –LT and –ST mutants. Further biochemical experiments, or even proteomics analysis, would definitely clarify the molecular basis of these effects.

1.3. Disruption of the KIF5–GRIP1 interaction has no effect on synaptic transmission

GRIP1 is a multi-PDZ domain protein that binds to GluA2 and GluA3 subunits but not GluA1 or GluA4 (Dong et al., 1999). GRIP1 facilitates the formation of the KIF5-GRIP1-GluR2-containing vesicles complex (Setou et al., 2002) and is required for proper surface targeting of GluA2 to the neuronal surface (Hoogenraad et al., 2005). The assembly and dendritic-targeting of this complex can be regulated by different proteins, even axonal ones as semaphorine-3 (Yamashita et al., 2014).

The precise role of GRIP1 is still under debate. The binding of GRIP1 to AMPAR subunits has been proposed to be fundamental for maintaining receptors at the synapses by limiting their endocytosis (Osten et al., 2000). It also could prevent the recycling of AMPAR after LTD by retaining them in an intracellular pool (Daw et al., 2000). Although, recently it has been suggested to do exactly the opposite and facilitate the recycling of receptors to the plasma membrane (Mao et al., 2010; Mejias et al., 2011).

Overexpressing a previously described GRIP1-KBD mutant (Figure 24) that interferes with the formation of the complex (Setou et al., 2002), AMPAR- and NMDAR-dependent transmission was completely normal, in basal conditions (Figure 26) and in an LTD paradigm (Figure 27). These results suggested that the formation of the complex was not needed for the maintenance of basal transmission or NMDAR-dependent LTD. This hypothesis is in agreement with recent results of LTD expressed in GluA1 and GluA2 lacking mice models (Granger and Nicoll, 2014). Therefore, GRIP1-KBD could be sequestering efficiently GluA2 subunits, and still LTD could happen independently of the availability of GluA2. Alternatively, we cannot formally exclude that GRIP1-KBD mutant was not acting as *dominant negative* in our system. Further biochemical experiments are required to determine whether there was a disruption of the KIF5-GRIP1-GluR2-containing vesicles complex after overexpression of this mutant in our experimental system.

1.4. When KIF5a or KIF5c expression is independently abolished, LTD is still present

Analyses in the absence of the endogenous protein would be a very valuable approach to unequivocally assign a role to KIF5 in synaptic plasticity. In our preliminary experiments, the two isoforms with a tissue-restricted expression, KIF5a and KIF5c, were independently knocked-down (Figure 28), and their possible functions in LTD were analyzed. In both cases, LTD expression and maintenance was still present, although there was a trend for a slight reduction (Figure 29).

Regarding KIF5a depleted expression or impaired function, a missense mutation in the motor domain of KIF5a in humans was identified and correlated with hereditary spastic paraplegia. This mutation prevents the stimulation of the motor ATPase by MT-binding. Therefore, a loss-of-function is experienced, leading to dramatic perturbations in

axoplasmic flow, both anterograde and retrograde, and axonal degeneration (Reid et al., 2002).

In vivo models lacking KIF5 expression have also been addressed. The generation of the KIF5a knock-out (KO) mice has been attempted, but KIF5a null mice were neonatal lethal. To overcome this problem, a conditional KO for KIF5a inactivation post-natally in neurons has been designed. The synapsin I promoter was used to control the inactivation of KIF5a, as it is neuron-specific and has a regulated postnatal expression (Xia et al., 2003). In this conditional KO model, KIF5a is vital for proper axon development, according to its role in the transport of cytoskeletal components such as neurofilaments and tubulin itself, and KIF5a expression is critical for survival. That is also the case for KIF5b, as null KIF5b mice are embryonic lethal (Tanaka et al., 1998), although the phenotype of KIF5b-lacking cells is rescued when other KIF5s where introduced in the system (Kanai et al., 2000).

It is worth noting that KIF5c is the predominant variant in the hippocampus (Kanai et al., 2000). In contrast to the other KIF5 proteins KOs, KIF5c null mice are viable and fertile, present normal body size and no gross morphological alterations, except a smaller brain compared to that of wild type littermates. The smaller brain size was attributed to a reduction in the number of neurons, as it was observed that KIF5c null mice present a relative loss of motor to sensory neurons (Kanai et al., 2000). In addition, abolishment of expression of either isofrom does not upregulate the expression levels of the other two isoforms (Kanai et al., 2000).

The fact that KIF5a can be knocked-down after birth and was related with axonal transport could suggest that, in agreement with our results, this isoform is not needed for NMDAR-dependent plasticity. A similar explanation could be applied to the absence of effect on synaptic plasticity when KIF5c expression is abolished, in contrast with our previous results using KIF5c-LT mutant. However, considering the high structural similarity and functional redundancy of the three KIF5 variants, and considering our electrophysiological results, we can speculate that some compensatory mechanisms are occurring. Specially, because it has been shown that KIF5s can work as homo or heterodimers (Kanai et al., 2000). Further experiments, knocking-down two variants simultaneously, should be performed to confirm whether there is indeed a compensatory effect, making that other KIF5s take over the functions of the absent KIF5 isoform.

2. ROLE OF MINUS END TRAFFICKING IN SYNAPTIC PLASTICITY

In our working model, molecular motors might be needed for the removal of receptors from the vicinity of the spine. As it was mentioned before, MTs can be present in inverted polarities in, at least, some areas of the dendrites, but it is also thought that in the more distal parts they can all be in the same orientation (Baas and Lin, 2011).

2.1. Dynein functions dependent on dynactin are not required for synaptic plasticity

The main knowledge on dynein and dynein function comes from studying mitotic processes, because of the critical role that MTs play in it. Dynein binding to dynactin is disrupted by overexpressing dynamitin (also called p50), a subunit of the dynactin complex. In that case, mitosis is delayed (Wadsworth and Lee, 2013). Other mitotic functions such as the force generation in the mitotic spindle are also dynactin independent (Raaijmakers et al., 2013).

In neurons, dynein has been long known to be responsible for retrograde axonal transport (Schnapp and Reese, 1989). In our experimental system, disruption of the dynein-dynactin complex by dynamitin overexpression had no effect on either basal transmission (Figure 31) or LTD expression (Figure 32). Suggesting that, if any, the role of dynein in modulation of synaptic transmission would be dynactin independent, and dynactin would not be required for the maintenance of AMPAR or NMDAR transmission. The endosomal pathway is critical for LTD expression, and it is tightly regulated by Rab-GTPases, such as Rab5 (Brown et al., 2005). This protein has been co-isolated with dynein suggesting an interaction between them (Jordens et al., 2005). Nevertheless, despite this putative interaction, dynein can be independently recruited to lysosomes by RILP-Rab7 (Tan et al., 2011), in agreement with our data showing that dynactin was not needed for a process tightly related with the endosomal pathway .

2.2. When dynein heavy chain (DHC) expression is abolished, LTD is still present

Dynein, as explained before, is a multisubunit complex, so it is not trivial to decide how to disrupt its function. It has been shown that when depletion of DHC leads to a loss in all dynein functions, at least in mitosis (Raaijmakers et al., 2013). For the same structural complexity, it is virtually impossible to create a “dynein knockout” model. Instead, different

knockout organisms of the different subunits of dynein have been created to try and determine their functions (Pfister et al., 2006).

For these reasons, we decided to abolish expression of the DHC gene responsible for the minus-end directed transport in axons and dendrites (DYNC1H1) (Hirokawa et al., 2010) and study the consequences in synaptic plasticity.

Surprisingly, we found that NMDAR-dependent LTD is not affected (Figure 34) when DHC expression is abolished. This very preliminary result, along with our results pointing to the fact that dynein functions dependent on dynactin were not needed either for basal transmission (Figure 31) or for synaptic plasticity (Figure 32), might indicate that minus-end directed transport based on dynein is not needed at all for NMDAR-dependent LTD to occur.

However, dynein is not the only molecular motor that can move towards the minus-end of MTs: Kinesin-14 family member KIFC2 (Verhey and Hammond, 2009). Interestingly enough, KIFC2 is abundantly expressed in brain and has been intimately related with the transport of multivesicular bodies in dendrites (Yang et al., 2001), although there is still controversy regarding its localization and it is not clear if it is exclusively present in dendrites or it can also be found in axons (Saito et al., 1997; Yang et al., 2001).

Taking into account these results, even if they are very preliminary, we could propose that dynein-dependent transport is not needed for synaptic plasticity; but we could hypothesize that other minus-end directed molecular motors might be involved in the regulation of synaptic plasticity. Hypothesis that might be strengthen if we accept that MTs have the same orientation on the distal parts of the dendrites – in this configuration, minus-end directed transport would have to exist, same as in the axon, and might play a role in regulating synaptic function.

3. AN INTEGRATIVE MODEL FOR MICROTUBULE-DEPENDENT TRANSPORT IN THE MODULATION OF SYNAPTIC TRANSMISSION IN THE HIPPOCAMPUS

As discussed in this thesis, endosomal trafficking has been shown by many groups, including ours, to be a key player in the regulation of synaptic plasticity (Esteban, 2008). In the same line, MT-dependent transport has been largely shown to participate in the regulation of endosomal trafficking (Parton et al., 1992). Therefore, our working model

proposed that molecular motors moving along MTs play a role in the modulation of synaptic function, by maybe interacting with AMPARs and NMDARs, as well as with some Rab proteins that are key to this process.

In that context, KIF5 would play a dual role in the removal and the delivery of receptors during synaptic plasticity and basal synaptic function. Our results suggest that both KIF5 motor and neck-stalk domains are needed to modulate LTD expression. Once receptors are internalized after LTD, they must be transported away, a step requiring KIF5 motor activity, in agreement with our studies performed using KIF5c-LT mutant. Moreover, integrating the reinsertion of AMPARs to the plasma membrane during LTD required the neck-stalk domain of KIF5, most likely in a Rab11 dependent manner, as suggested by our results using KIF5c-ST mutant. Regarding KIF5 role on the regulation of basal transmission, its neck-stalk domain seems to be needed, as our data using KIF5c-LT mutant indicated that inhibition of the motor activity *per se* does not seem to be sufficient to impact on basal transmission. In that scenario, the KIF5c–ST mutant would act by sequestering the cargo or by inhibiting motor activity of endogenous KIF5. Alternatively, this cargo binding domain could be inhibiting the motor activity of KIF5 and other KIFs, an effect that when using the KIF5c–LT mutant was taken over due to the structural and functional redundancy. Additional and exhaustive molecular characterization would be required to determine the precise role of KIF5 domains in basal transmission.

Concerning KIF17 function, its motor domain was required for normal LTD expression, as suggested by our results using KIF17-LT mutant. This situation would be similar to that described for Rab11-KIF5, but in a Rab8-KIF17 manner. KIF17 PDZ-binding domain (PBD) is involved in its binding to NMDARs through the mLin complex. Surprisingly, we found that KIF17-ST mutant, lacking PBD, specifically depressed NMDA transmission, suggesting that still was trapping those receptors. It is tempting to speculate that KIF17 could contain unknown regulatory sequences also binding NMDARs, being *underused* when the PBD is present but that become active in its absence. A similar regulation has been described for the NLS present in the cargo binding domain of KIF17. The NLS becomes hyperactivated in the absence of certain domains of the protein, suggesting that there are intramolecular mechanisms regulating its function, even if those are still unknown, according to unpublished observations from our own group and from Dr. Verhey's laboratory (who kindly provided us with some of the constructs).

In summary, the work presented in this thesis provides evidence to support that MT-dependent transport is necessary for the regulation of synaptic function. And, as it usually happens in science, sets the starting point and provides new tools to answer the many questions that it has opened.

Conclusions

1. KIF5c-LT and KIF17-LT kinesin mutant proteins, lacking their motor domain, were immobile when overexpressed in hippocampal organotypic slices. However, their expression pattern suggests they can be transported as cargoes along the dendrites.

2. Overexpression of KIF5c-LT has no effect on either dendritic transport of GFP-GluA2, basal synaptic transmission, and LTP expression. In contrast, KIF5c-LT overexpression specifically impaired NMDAR-dependent LTD, independently of the induction protocol used.

3. Overexpression of KIF17-LT has no effect on basal synaptic transmission, but impairs NMDAR-dependent LTD.

4. Overall, our data indicated that the motor activity of KIF5 and KIF17 was needed for synaptic plasticity but not for the maintenance of basal transmission.

5. Overexpression of KIF5c-ST, a mutant form of KIF5 that consists of just the cargo binding domain, globally depresses basal transmission but has no effect on NMDAR-dependent LTD.

6. Overexpression of KIF17-ST, a mutant form of KIF17 that consists of just the cargo binding domain without the NLS, specifically depresses NMDAR basal transmission but has no effect on AMPAR basal transmission or on NMDAR-dependent LTD.

7. Taking together conclusions 5 and 6, KIF5c and KIF17 might contain regulatory domains in the neck-stalk region required for the maintenance of basal transmission.

8. Overexpression of GRIP1-KBD has no effect on either basal synaptic transmission or NMDAR-dependent LTD, indicating that the KIF5-GRIP1-GluA2 association might not be crucial for synaptic plasticity to occur.

9. Knock-down of KIF5a or KIF5c in organotypic hippocampal slices has little effect on NMDAR-dependent LTD, suggesting neither of them, individually, are indispensable for it to occur

10. Overexpression of dynamitin, a component of the dynactin complex whose overexpression prevents assembly of the dynein-dynactin complex, has no effect on either basal synaptic transmission or NMDAR-dependent LTD. Knock-down of DHC has no effect on NMDAR-dependent LTD. These results suggests that dynein functions in modulation of synaptic response are not needed at all.

Conclusiones

1. Las formas mutantes de las kinesinas KIF5c-LT y KIF17-LT, a las que les falta el dominio motor, son inmóviles cuando se sobreexpresan en rodajas organotípicas de hipocampo. Sin embargo, su patrón de expresión sugiere que pueden ser transportadas como cargo a lo largo de las dendritas.

2. La sobreexpresión KIF5c-LT no tiene efecto alguno en el transporte dendrítico de GFP-GluA2, en transmisión basal o en la expresión de LTP. En cambio, la sobreexpresión de KIF5c-LT impide específicamente la LTD dependiente de NMDAR, independientemente del protocolo de inducción utilizado.

3. La sobreexpresión de KIF17-LT no tiene efecto en transmisión basal, pero impide la LTD dependiente de NMDAR.

4. En general, nuestros datos indican que la actividad motora de KIF5 y KIF17 es necesaria para la expresión de plasticidad sináptica pero no para el mantenimiento de la transmisión basal.

5. La sobreexpresión de KIF5c-ST, forma mutante de KIF5 que consta solamente del dominio de unión a cargo, deprime la transmisión basal pero no tiene efecto sobre la expresión de la LTD dependiente de NMDAR.

6. La sobreexpresión de KIF17-ST, forma mutante de KIF17 que consta solamente del dominio de unión a cargo pero sin la NLS, deprime específicamente la transmisión basal de NMDAR, pero no tiene efecto en la transmisión basal de AMPAR o el la LTD dependiente de NMDAR.

7. Las conclusiones 5 y 6 indican que tanto KIF5c como KIF17 pueden contener dominios reguladores en la región del cuello-tallo necesarias para el mantenimiento de la transmisión basal.

8. La sobreexpresión de GRIP1-KBD no tiene efectos sobre la transmisión basal ni sobre la LTD dependiente de NMDAR, sugiriendo que la asociación KIF5-GRIP1-GluA2 puede ser prescindible para la expresión de plasticidad sináptica.

9. La prevención de la expresión de KIF5a o KIF5c mediante técnicas de shRNA en rodajas organotípicas de hipocampo no tiene efectos significativos sobre la LTD dependiente de NMDAR, indicando que ninguna de estas dos variantes individualmente es indispensable en dicho proceso.

10. La sobreexpresión de la dinamitina, una subunidad del complejo de la dinactina cuya sobreexpresión previene la formación del complejo dineina-dinactina, no tiene efectos sobre la transmisión basal ni sobre la LTD dependiente de NMDAR. La prevención de la expresión de DHC tampoco tiene efectos en la LTD dependiente de NMDA. Estos resultados sugieren que la dineina no cumple función alguna en la regulación de la función sináptica.

References

Ally, S., Jolly, A.L., Gelfand, V.I., 2008. Motor-cargo release: CaMKII as a traffic cop. Nat. Cell Biol. 10, 3–5. doi:10.1038/ncb0108-3

Baas, P.W., Lin, S., 2011. Hooks and comets: The story of microtubule polarity orientation in the neuron. Dev. Neurobiol. 71, 403–18. doi:10.1002/dneu.20818

Barr, F., Lambright, D.G., 2010. Rab GEFs and GAPs. Curr. Opin. Cell Biol. 22, 461–70. doi:10.1016/j.ceb.2010.04.007

Barrett, J.G., Manning, B.D., Snyder, M., 2000. The Kar3p kinesin-related protein forms a novel heterodimeric structure with its associated protein Cik1p. Mol. Biol. Cell 11, 2373–85.

Baskys, A., Bayazitov, I., Zhu, E., Fang, L., Wang, R., 2007. Rab-mediated endocytosis: linking neurodegeneration, neuroprotection, and synaptic plasticity? Ann. N. Y. Acad. Sci. 1122, 313–29. doi:10.1196/annals.1403.023

Benoist, M., Palenzuela, R., Rozas, C., Rojas, P., Tortosa, E., Morales, B., González-Billault, C., Ávila, J., Esteban, J.A., 2013. MAP1B-dependent Rac activation is required for AMPA receptor endocytosis during long-term depression. EMBO J. 32, 2287–99. doi:10.1038/emboj.2013.166

Bliss, T. V, Lomo, T., 1973. Long-lasting potentiation of synaptic transmission in the dentate area of the anaesthetized rabbit following stimulation of the perforant path. J. Physiol. 232, 331–56.

Brown, T.C., Correia, S.S., Petrok, C.N., Esteban, J.A., 2007. Functional compartmentalization of endosomal trafficking for the synaptic delivery of AMPA receptors during long-term potentiation. J. Neurosci. 27, 13311–5. doi:10.1523/JNEUROSCI.4258-07.2007

Brown, T.C., Tran, I.C., Backos, D.S., Esteban, J.A., 2005. NMDA receptor-dependent activation of the small GTPase Rab5 drives the removal of synaptic AMPA receptors during hippocampal LTD. Neuron 45, 81–94. doi:10.1016/j.neuron.2004.12.023

Burkhardt, J.K., Echeverri, C.J., Nilsson, T., Vallee, R.B., 1997. Overexpression of the dynamitin (p50) subunit of the dynactin complex disrupts dynein-dependent maintenance of membrane organelle distribution. J. Cell Biol. 139, 469–84.

Cai, D., McEwen, D.P., Martens, J.R., Meyhofer, E., Verhey, K.J., 2009. Single molecule imaging reveals differences in microtubule track selection between Kinesin motors. PLoS Biol. 7, e1000216. doi:10.1371/journal.pbio.1000216

Castellucci, V., Pinsker, H., Kupfermann, I., Kandel, E.R., 1970. Neuronal mechanisms of habituation and dishabituation of the gill-withdrawal reflex in Aplysia. Science 167, 1745–8.

Coleman, S.K., Möykkynen, T., Cai, C., von Ossowski, L., Kuismanen, E., Korpi, E.R., Keinänen, K., 2006. Isoform-specific early trafficking of AMPA receptor flip and flop variants. J. Neurosci. 26, 11220–9. doi:10.1523/JNEUROSCI.2301-06.2006

Collingridge, G.L., Olsen, R.W., Peters, J., Spedding, M., 2009. A nomenclature for ligand-gated ion channels. Neuropharmacology 56, 2–5. doi:10.1016/j.neuropharm.2008.06.063

Conde, C., Cáceres, A., 2009. Microtubule assembly, organization and dynamics in axons and dendrites. Nat. Rev. Neurosci. 10, 319–32. doi:10.1038/nrn2631

Correia, S.S., Bassani, S., Brown, T.C., Lisé, M.-F., Backos, D.S., El-Husseini, A., Passafaro, M., Esteban, J. a, 2008. Motor protein-dependent transport of AMPA receptors into spines during long-term potentiation. Nat. Neurosci. 11, 457–66. doi:10.1038/nn2063

Coultrap, S.J., Freund, R.K., O'Leary, H., Sanderson, J.L., Roche, K.W., Dell'Acqua, M.L., Bayer, K.U., 2014. Autonomous CaMKII mediates both LTP and LTD using a mechanism for differential substrate site selection. Cell Rep. 6, 431–7. doi:10.1016/j.celrep.2014.01.005

Daw, M.I., Chittajallu, R., Bortolotto, Z.A., Dev, K.K., Duprat, F., Henley, J.M., Collingridge, G.L., Isaac, J.T., 2000. PDZ proteins interacting with C-terminal GluR2/3 are involved in a PKC-dependent regulation of AMPA receptors at hippocampal synapses. Neuron 28, 873–86.

Dent, E.W., Merriam, E.B., Hu, X., 2011. The dynamic cytoskeleton: backbone of dendritic spine plasticity. Curr. Opin. Neurobiol. 21, 175–81. doi:10.1016/j.conb.2010.08.013

Dingledine, R., Borges, K., Bowie, D., Traynelis, S.F., 1999. The glutamate receptor ion channels. Pharmacol. Rev. 51, 7–61.

Dishinger, J.F., Kee, H.L., Jenkins, P.M., Fan, S., Hurd, T.W., Hammond, J.W., Truong, Y.N.-T., Margolis, B., Martens, J.R., Verhey, K.J., 2010. Ciliary entry of the kinesin-2 motor KIF17 is regulated by importin-beta2 and RanGTP. Nat. Cell Biol. 12, 703–10. doi:10.1038/ncb2073

Dong, H., Zhang, P., Song, I., Petralia, R.S., Liao, D., Huganir, R.L., 1999. Characterization of the glutamate receptor-interacting proteins GRIP1 and GRIP2. J. Neurosci. 19, 6930–41.

Dull, T., Zufferey, R., Kelly, M., Mandel, R.J., Nguyen, M., Trono, D., Naldini, L., 1998. A third-generation lentivirus vector with a conditional packaging system. J. Virol. 72, 8463–71.

Dunwiddie, T., Lynch, G., 1978. Long-term potentiation and depression of synaptic responses in the rat hippocampus: localization and frequency dependency. J. Physiol. 276, 353–67.

Endow, S.A., 1999. Determinants of molecular motor directionality. Nat. Cell Biol. 1, E163–7. doi:10.1038/14113

Esteban, J.A., 2003. AMPA receptor trafficking: a road map for synaptic plasticity. Mol. Interv. 3, 375–85. doi:10.1124/mi.3.7.375

Esteban, J.A., 2008. Intracellular machinery for the transport of AMPA receptors. Br. J. Pharmacol. 153 Suppl , S35–43. doi:10.1038/sj.bjp.0707525

Fernández-Monreal, M., Brown, T.C., Royo, M., Esteban, J.A., 2012. The balance between receptor recycling and trafficking toward lysosomes determines synaptic strength during long-term depression. J. Neurosci. 32, 13200–5. doi:10.1523/JNEUROSCI.0061-12.2012

Fernández-Monreal, M., Kang, S., Phillips, G.R., 2009. Gamma-protocadherin homophilic interaction and intracellular trafficking is controlled by the cytoplasmic domain in neurons. Mol. Cell. Neurosci. 40, 344–53. doi:10.1016/j.mcn.2008.12.002

Fletcher, D.A., Mullins, R.D., 2010. Cell mechanics and the cytoskeleton. Nature 463, 485–92. doi:10.1038/nature08908

Froger, A., Hall, J.E., 2007. Transformation of plasmid DNA into E. coli using the heat shock method. J. Vis. Exp. 253. doi:10.3791/253

Frolov, I., Agapov, E., Hoffman, T.A., Prágai, B.M., Lippa, M., Schlesinger, S., Rice, C.M., 1999. Selection of RNA replicons capable of persistent noncytopathic replication in mammalian cells. J. Virol. 73, 3854–65.

Fuller, L., Dailey, M.E., 2010. Preparation of Rodent Hippocampal Slice Cultures. Cold Spring Harb. Protoc. 2007, pdb.prot4848–pdb.prot4848. doi:10.1101/pdb.prot4848

Gähwiler, B., 1997. Organotypic slice cultures: a technique has come of age. Trends Neurosci. 20, 471–477. doi:10.1016/S0166-2236(97)01122-3

Gerges, N.Z., Backos, D.S., Esteban, J.A., 2004. Local control of AMPA receptor trafficking at the postsynaptic terminal by a small GTPase of the Rab family. J. Biol. Chem. 279, 43870–8. doi:10.1074/jbc.M404982200

Goldstein, L.S., Yang, Z., 2000. Microtubule-based transport systems in neurons: the roles of kinesins and dyneins. Annu. Rev. Neurosci. 23, 39–71. doi:10.1146/annurev.neuro.23.1.39

González-González, I.M., Konopacki, F.A., Rocca, D.L., Doherty, A.J., Jaafari, N., Wilkinson, K.A., Henley, J.M., 2012. Kainate receptor trafficking. Wiley Interdiscip. Rev. Membr. Transp. Signal. 1, 31–44. doi:10.1002/wmts.23

Granger, A.J., Nicoll, R.A., 2014. LTD expression is independent of glutamate receptor subtype. Front. Synaptic Neurosci. 6, 15. doi:10.3389/fnsyn.2014.00015

Granger, A.J., Shi, Y., Lu, W., Cerpas, M., Nicoll, R.A., 2013. LTP requires a reserve pool of glutamate receptors independent of subunit type. Nature 493, 495–500. doi:10.1038/nature11775

Granger, E., McNee, G., Allan, V., Woodman, P., 2014. The role of the cytoskeleton and molecular motors in endosomal dynamics. Semin. Cell Dev. Biol. 31, 20–9. doi:10.1016/j.semcdb.2014.04.011

Grosshans, B.L., Andreeva, A., Gangar, A., Niessen, S., Yates, J.R., Brennwald, P., Novick, P., 2006. The yeast lgl family member Sro7p is an effector of the secretory Rab GTPase Sec4p. J. Cell Biol. 172, 55–66. doi:10.1083/jcb.200510016

Gu, J., Firestein, B.L., Zheng, J.Q., 2008. Microtubules in dendritic spine development. J. Neurosci. 28, 12120–4. doi:10.1523/JNEUROSCI.2509-08.2008

Guillaud, L., Setou, M., Hirokawa, N., 2003. KIF17 dynamics and regulation of NR2B trafficking in hippocampal neurons. J. Neurosci. 23, 131–40.

Guillaud, L., Wong, R., Hirokawa, N., 2008. Disruption of KIF17-Mint1 interaction by CaMKII-dependent phosphorylation: a molecular model of kinesin-cargo release. Nat. Cell Biol. 10, 19–29. doi:10.1038/ncb1665

Hammond, J.W., Blasius, T.L., Soppina, V., Cai, D., Verhey, K.J., 2010. Autoinhibition of the kinesin-2 motor KIF17 via dual intramolecular mechanisms. J. Cell Biol. 189, 1013–25. doi:10.1083/jcb.201001057

Hancock, W.O., 2014. Bidirectional cargo transport: moving beyond tug of war. Nat. Rev. Mol. Cell Biol. 15, 615–628. doi:10.1038/nrm3853

Hao, L., Scholey, J.M., 2009. Intraflagellar transport at a glance. J. Cell Sci. 122, 889–92. doi:10.1242/jcs.023861

Hayashi, Y., 2000. Driving AMPA Receptors into Synapses by LTP and CaMKII: Requirement for GluR1 and PDZ Domain Interaction. Science (80-.). 287, 2262–2267. doi:10.1126/science.287.5461.2262

Hirokawa, N., Niwa, S., Tanaka, Y., 2010. Molecular motors in neurons: transport mechanisms and roles in brain function, development, and disease. Neuron 68, 610–38. doi:10.1016/j.neuron.2010.09.039

Hirokawa, N., Noda, Y., 2008. Intracellular transport and kinesin superfamily proteins, KIFs: structure, function, and dynamics. Physiol. Rev. 88, 1089–118. doi:10.1152/physrev.00023.2007

Hirokawa, N., Noda, Y., Tanaka, Y., Niwa, S., 2009. Kinesin superfamily motor proteins and intracellular transport. Nat. Rev. Mol. Cell Biol. 10, 682–96. doi:10.1038/nrm2774

Hoogenraad, C.C., Bradke, F., 2009. Control of neuronal polarity and plasticity--a renaissance for microtubules? Trends Cell Biol. 19, 669–76. doi:10.1016/j.tcb.2009.08.006

Hoogenraad, C.C., Milstein, A.D., Ethell, I.M., Henkemeyer, M., Sheng, M., 2005. GRIP1 controls dendrite morphogenesis by regulating EphB receptor trafficking. Nat. Neurosci. 8, 906–15. doi:10.1038/nn1487

Horgan, C.P., McCaffrey, M.W., 2011. Rab GTPases and microtubule motors. Biochem. Soc. Trans. 39, 1202–6. doi:10.1042/BST0391202

Hotulainen, P., Hoogenraad, C.C., 2010. Actin in dendritic spines: connecting dynamics to function. J. Cell Biol. 189, 619–29. doi:10.1083/jcb.201003008

Hu, X., Viesselmann, C., Nam, S., Merriam, E., Dent, E.W., 2008. Activity-dependent dynamic microtubule invasion of dendritic spines. J. Neurosci. 28, 13094–105. doi:10.1523/JNEUROSCI.3074-08.2008

Huber, L., Dupree, P., Dotti, C., 1995. A deficiency of the small GTPase rab8 inhibits membrane traffic in developing neurons. Mol. Cell. Biol. 15, 918–924.

Jaworski, J., Kapitein, L.C., Gouveia, S.M., Dortland, B.R., Wulf, P.S., Grigoriev, I., Camera, P., Spangler, S.A., Di Stefano, P., Demmers, J., Krugers, H., Defilippi, P., Akhmanova, A., Hoogenraad, C.C., 2009. Dynamic microtubules regulate dendritic spine morphology and synaptic plasticity. Neuron 61, 85–100. doi:10.1016/j.neuron.2008.11.013

Johansson, M., Rocha, N., Zwart, W., Jordens, I., Janssen, L., Kuijl, C., Olkkonen, V.M., Neefjes, J., 2007. Activation of endosomal dynein motors by stepwise assembly of Rab7-RILP-p150Glued, ORP1L, and the receptor betalll spectrin. J. Cell Biol. 176, 459–71. doi:10.1083/jcb.200606077

Jordens, I., Fernandez-Borja, M., Marsman, M., Dusseljee, S., Janssen, L., Calafat, J., Janssen, H., Wubbolts, R., Neefjes, J., 2001. The Rab7 effector protein RILP controls lysosomal transport by inducing the recruitment of dynein-dynactin motors. Curr. Biol. 11, 1680–5.

Jordens, I., Marsman, M., Kuijl, C., Neefjes, J., 2005. Rab proteins, connecting transport and vesicle fusion. Traffic 6, 1070–7. doi:10.1111/j.1600-0854.2005.00336.x

Kaech, S., Banker, G., 2006. Culturing hippocampal neurons. Nat. Protoc. 1, 2406–15. doi:10.1038/nprot.2006.356

Kanai, Y., Okada, Y., Tanaka, Y., Harada, A., Terada, S., Hirokawa, N., 2000. KIF5C, a novel neuronal kinesin enriched in motor neurons. J. Neurosci. 20, 6374–84.

Kapitein, L.C., Hoogenraad, C.C., 2011. Which way to go? Cytoskeletal organization and polarized transport in neurons. Mol. Cell. Neurosci. 46, 9–20. doi:10.1016/j.mcn.2010.08.015

Karki, S., Holzbaur, E.L., 1999. Cytoplasmic dynein and dynactin in cell division and intracellular transport. Curr. Opin. Cell Biol. 11, 45–53.

Kauer, J.A., Malenka, R.C., 2007. Synaptic plasticity and addiction. Nat. Rev. Neurosci. 8, 844–58. doi:10.1038/nrn2234

Kennedy, M.J., Ehlers, M.D., 2006. Organelles and trafficking machinery for postsynaptic plasticity. Annu. Rev. Neurosci. 29, 325–62. doi:10.1146/annurev.neuro.29.051605.112808

Kingston, R.E., Chen, C.A., Okayama, H., 2001. Calcium phosphate transfection. Curr. Protoc. Immunol. Chapter 10, Unit 10.13. doi:10.1002/0471142735.im1013s31

Kneussel, M., Wagner, W., 2013. Myosin motors at neuronal synapses: drivers of membrane transport and actin dynamics. Nat. Rev. Neurosci. 14, 233–47. doi:10.1038/nrn3445

Konishi, Y., Setou, M., 2009. Tubulin tyrosination navigates the kinesin-1 motor domain to axons. Nat. Neurosci. 12, 559–67. doi:10.1038/nn.2314

Korobova, F., Svitkina, T., 2010. Molecular architecture of synaptic actin cytoskeleton in hippocampal neurons reveals a mechanism of dendritic spine morphogenesis. Mol. Biol. Cell 21, 165–76. doi:10.1091/mbc.E09-07-0596

Lee, H.-K., Kameyama, K., Huganir, R.L., Bear, M.F., 1998. NMDA Induces Long-Term Synaptic Depression and Dephosphorylation of the GluR1 Subunit of AMPA Receptors in Hippocampus. Neuron 21, 1151–1162. doi:10.1016/S0896-6273(00)80632-7

Lerma, J., 2003. Roles and rules of kainate receptors in synaptic transmission. Nat. Rev. Neurosci. 4, 481–95. doi:10.1038/nrn1118

Lisman, J., Lichtman, J.W., Sanes, J.R., 2003. LTP: perils and progress. Nat. Rev. Neurosci. 4, 926–9. doi:10.1038/nrn1259

Lisman, J.E., 2009. The pre/post LTP debate. Neuron 63, 281–4. doi:10.1016/j.neuron.2009.07.020

Lodge, D., 2009. The history of the pharmacology and cloning of ionotropic glutamate receptors and the development of idiosyncratic nomenclature. Neuropharmacology 56, 6–21. doi:10.1016/j.neuropharm.2008.08.006

Lois, C., Hong, E.J., Pease, S., Brown, E.J., Baltimore, D., 2002. Germline transmission and tissue-specific expression of transgenes delivered by lentiviral vectors. Science 295, 868–72. doi:10.1126/science.1067081

Lu, W.-Y., Man, H.-Y., Ju, W., Trimble, W.S., MacDonald, J.F., Wang, Y.T., 2001. Activation of Synaptic NMDA Receptors Induces Membrane Insertion of New AMPA Receptors and LTP in Cultured Hippocampal Neurons. Neuron 29, 243–254. doi:10.1016/S0896-6273(01)00194-5

Madden, D.R., 2002. The structure and function of glutamate receptor ion channels. Nat. Rev. Neurosci. 3, 91–101. doi:10.1038/nrn725

Malenka, R.C., Bear, M.F., 2004. LTP and LTD: an embarrassment of riches. Neuron 44, 5–21. doi:10.1016/j.neuron.2004.09.012

Mandal, M., Wei, J., Zhong, P., Cheng, J., Duffney, L.J., Liu, W., Yuen, E.Y., Twelvetrees, A.E., Li, S., Li, X.-J., Kittler, J.T., Yan, Z., 2011. Impaired alpha-amino-3-hydroxy-5-

methyl-4-isoxazolepropionic acid (AMPA) receptor trafficking and function by mutant huntingtin. J. Biol. Chem. 286, 33719–28. doi:10.1074/jbc.M111.236521

Manning, B.D., Barrett, J.G., Wallace, J.A., Granok, H., Snyder, M., 1999. Differential regulation of the Kar3p kinesin-related protein by two associated proteins, Cik1p and Vik1p. J. Cell Biol. 144, 1219–33.

Mao, L., Takamiya, K., Thomas, G., Lin, D.-T., Huganir, R.L., 2010. GRIP1 and 2 regulate activity-dependent AMPA receptor recycling via exocyst complex interactions. Proc. Natl. Acad. Sci. U. S. A. 107, 19038–43. doi:10.1073/pnas.1013494107

Matsuzaki, F., Shirane, M., Matsumoto, M., Nakayama, K.I., 2011. Protrudin serves as an adaptor molecule that connects KIF5 and its cargoes in vesicular transport during process formation. Mol. Biol. Cell 22, 4602–20. doi:10.1091/mbc.E11-01-0068

Matus, A., 2000. Actin-based plasticity in dendritic spines. Science 290, 754–8.

Mayer, M.L., Westbrook, G.L., Guthrie, P.B., 1984. Voltage-dependent block by Mg2+ of NMDA responses in spinal cord neurones. Nature 309, 261–263. doi:10.1038/309261a0

Mejias, R., Adamczyk, A., Anggono, V., Niranjan, T., Thomas, G.M., Sharma, K., Skinner, C., Schwartz, C.E., Stevenson, R.E., Fallin, M.D., Kaufmann, W., Pletnikov, M., Valle, D., Huganir, R.L., Wang, T., 2011. Gain-of-function glutamate receptor interacting protein 1 variants alter GluA2 recycling and surface distribution in patients with autism. Proc. Natl. Acad. Sci. U. S. A. 108, 4920–5. doi:10.1073/pnas.1102233108

Merriam, E.B., Lumbard, D.C., Viesselmann, C., Ballweg, J., Stevenson, M., Pietila, L., Hu, X., Dent, E.W., 2011. Dynamic microtubules promote synaptic NMDA receptor-dependent spine enlargement. PLoS One 6, e27688. doi:10.1371/journal.pone.0027688

Mulkey, R.M., Endo, S., Shenolikar, S., Malenka, R.C., 1994. Involvement of a calcineurin/inhibitor-1 phosphatase cascade in hippocampal long-term depression. Nature 369, 486–8. doi:10.1038/369486a0

Navone, F., Niclas, J., Hom-Booher, N., Sparks, L., Bernstein, H.D., McCaffrey, G., Vale, R.D., 1992. Cloning and expression of a human kinesin heavy chain gene: interaction of the COOH-terminal domain with cytoplasmic microtubules in transfected CV-1 cells. J. Cell Biol. 117, 1263–75.

Nimchinsky, E.A., Sabatini, B.L., Svoboda, K., 2002. Structure and function of dendritic spines. Annu. Rev. Physiol. 64, 313–53. doi:10.1146/annurev.physiol.64.081501.160008

Niswender, C.M., Conn, P.J., 2010. Metabotropic glutamate receptors: physiology, pharmacology, and disease. Annu. Rev. Pharmacol. Toxicol. 50, 295–322. doi:10.1146/annurev.pharmtox.011008.145533

Niwa, S., Tanaka, Y., Hirokawa, N., 2008. KIF1Bbeta- and KIF1A-mediated axonal transport of presynaptic regulator Rab3 occurs in a GTP-dependent manner through DENN/MADD. Nat. Cell Biol. 10, 1269–79. doi:10.1038/ncb1785

Nowak, L., Bregestovski, P., Ascher, P., Herbet, A., Prochiantz, A., 1984. Magnesium gates glutamate-activated channels in mouse central neurones. Nature 307, 462–5.

Osten, P., Khatri, L., Perez, J.L., Köhr, G., Giese, G., Daly, C., Schulz, T.W., Wensky, A., Lee, L.M., Ziff, E.B., 2000. Mutagenesis reveals a role for ABP/GRIP binding to GluR2 in synaptic surface accumulation of the AMPA receptor. Neuron 27, 313–25.

Paoletti, P., Bellone, C., Zhou, Q., 2013. NMDA receptor subunit diversity: impact on receptor properties, synaptic plasticity and disease. Nat. Rev. Neurosci. 14, 383–400. doi:10.1038/nrn3504

Parton, R.G., Simons, K., Dotti, C.G., 1992. Axonal and dendritic endocytic pathways in cultured neurons. J. Cell Biol. 119, 123–37.

Passafaro, M., Piëch, V., Sheng, M., 2001. Subunit-specific temporal and spatial patterns of AMPA receptor exocytosis in hippocampal neurons. Nat. Neurosci. 4, 917–26. doi:10.1038/nn0901-917

Pei, W., Huang, Z., Wang, C., Han, Y., Park, J.S., Niu, L., 2009. Flip and flop: a molecular determinant for AMPA receptor channel opening. Biochemistry 48, 3767–77. doi:10.1021/bi8015907

Peineau, S., Nicolas, C.S., Bortolotto, Z.A., Bhat, R. V, Ryves, W.J., Harwood, A.J., Dournaud, P., Fitzjohn, S.M., Collingridge, G.L., 2009. A systematic investigation of the protein kinases involved in NMDA receptor-dependent LTD: evidence for a role of GSK-3 but not other serine/threonine kinases. Mol. Brain 2, 22. doi:10.1186/1756-6606-2-22

Penfield, W., Milner, B., 1958. Memory deficit produced by bilateral lesions in the hippocampal zone. AMA. Arch. Neurol. Psychiatry 79, 475–97.

Penzes, P., Srivastava, D.P., Woolfrey, K.M., 2009. Not just actin? A role for dynamic microtubules in dendritic spines. Neuron 61, 3–5. doi:10.1016/j.neuron.2008.12.018

Pfister, K.K., Shah, P.R., Hummerich, H., Russ, A., Cotton, J., Annuar, A.A., King, S.M., Fisher, E.M.C., 2006. Genetic analysis of the cytoplasmic dynein subunit families. PLoS Genet. 2, e1. doi:10.1371/journal.pgen.0020001

Prota, A.E., Magiera, M.M., Kuijpers, M., Bargsten, K., Frey, D., Wieser, M., Jaussi, R., Hoogenraad, C.C., Kammerer, R.A., Janke, C., Steinmetz, M.O., 2013. Structural basis of tubulin tyrosination by tubulin tyrosine ligase. J. Cell Biol. 200, 259–70. doi:10.1083/jcb.201211017

Purves, D., Augustine, G.J., Fitzpatrick, D., Katz, L.C., LaMantia, A.-S., McNamara, J.O., Williams, S.M., 2001. Neuroscience.

Raaijmakers, J.A., Tanenbaum, M.E., Medema, R.H., 2013. Systematic dissection of dynein regulators in mitosis. J. Cell Biol. 201, 201–15. doi:10.1083/jcb.201208098

Ramírez, O.A., Couve, A., 2011. The endoplasmic reticulum and protein trafficking in dendrites and axons. Trends Cell Biol. 21, 219–27. doi:10.1016/j.tcb.2010.12.003

Reid, E., Kloos, M., Ashley-Koch, A., Hughes, L., Bevan, S., Svenson, I.K., Graham, F.L., Gaskell, P.C., Dearlove, A., Pericak-Vance, M.A., Rubinsztein, D.C., Marchuk, D.A., 2002. A kinesin heavy chain (KIF5A) mutation in hereditary spastic paraplegia (SPG10). Am. J. Hum. Genet. 71, 1189–94. doi:10.1086/344210

Saito, N., Okada, Y., Noda, Y., Kinoshita, Y., Kondo, S., Hirokawa, N., 1997. KIFC2 is a novel neuron-specific C-terminal type kinesin superfamily motor for dendritic transport of multivesicular body-like organelles. Neuron 18, 425–38.

Schlesinger, S., 1999. Alphavirus vectors for gene expression and vaccines. Curr. Opin. Biotechnol. 10, 434–439. doi:10.1016/S0958-1669(99)00006-3

Schnapp, B.J., Reese, T.S., 1989. Dynein is the motor for retrograde axonal transport of organelles. Proc. Natl. Acad. Sci. U. S. A. 86, 1548–52.

Schneider, C.A., Rasband, W.S., Eliceiri, K.W., 2012. NIH Image to ImageJ: 25 years of image analysis. Nat. Methods 9, 671–675. doi:10.1038/nmeth.2089

Schroer, T.A., 2004. Dynactin. Annu. Rev. Cell Dev. Biol. 20, 759–79. doi:10.1146/annurev.cellbio.20.012103.094623

Schubert, V., Dotti, C.G., 2007. Transmitting on actin: synaptic control of dendritic architecture. J. Cell Sci. 120, 205–12. doi:10.1242/jcs.03337

Scoville, W.B., Milner, B., 1957. Loss of recent memory after bilateral hippocampal lesions. J. Neurol. Neurosurg. Psychiatry 20, 11–21.

Seeger, M.A., Rice, S.E., 2010. Microtubule-associated protein-like binding of the kinesin-1 tail to microtubules. J. Biol. Chem. 285, 8155–62. doi:10.1074/jbc.M109.068247

Setou, M., 2000. Kinesin Superfamily Motor Protein KIF17 and mLin-10 in NMDA Receptor-Containing Vesicle Transport. Science (80-.). 288, 1796–1802. doi:10.1126/science.288.5472.1796

Setou, M., Nakagawa, T., Seog, D.H., Hirokawa, N., 2000. Kinesin superfamily motor protein KIF17 and mLin-10 in NMDA receptor-containing vesicle transport. Science 288, 1796–802.

Setou, M., Seog, D.-H., Tanaka, Y., Kanai, Y., Takei, Y., Kawagishi, M., Hirokawa, N., 2002. Glutamate-receptor-interacting protein GRIP1 directly steers kinesin to dendrites. Nature 417, 83–7. doi:10.1038/nature743

Shepherd, J.D., Huganir, R.L., 2007. The cell biology of synaptic plasticity: AMPA receptor trafficking. Annu. Rev. Cell Dev. Biol. 23, 613–43. doi:10.1146/annurev.cellbio.23.090506.123516

Shi, S., Hayashi, Y., Esteban, J.A., Malinow, R., 2001. Subunit-specific rules governing AMPA receptor trafficking to synapses in hippocampal pyramidal neurons. Cell 105, 331–43.

Shi, S.-H., Hayashi, Y., Esteban, J.A., Malinow, R., 2001. Subunit-Specific Rules Governing AMPA Receptor Trafficking to Synapses in Hippocampal Pyramidal Neurons. Cell 105, 331–343. doi:10.1016/S0092-8674(01)00321-X

Soldati, T., Schliwa, M., 2006. Powering membrane traffic in endocytosis and recycling. Nat. Rev. Mol. Cell Biol. 7, 897–908. doi:10.1038/nrm2060

Sommer, B., Köhler, M., Sprengel, R., Seeburg, P.H., 1991. RNA editing in brain controls a determinant of ion flow in glutamate-gated channels. Cell 67, 11–9.

Staff, N.P., Benarroch, E.E., Klein, C.J., 2011. Neuronal intracellular transport and neurodegenerative disease. Neurology 76, 1015–20. doi:10.1212/WNL.0b013e31821103f7

Sung, C.-H., Leroux, M.R., 2013. The roles of evolutionarily conserved functional modules in cilia-related trafficking. Nat. Cell Biol. 15, 1387–97. doi:10.1038/ncb2888

Tan, S.C., Scherer, J., Vallee, R.B., 2011. Recruitment of dynein to late endosomes and lysosomes through light intermediate chains. Mol. Biol. Cell 22, 467–77. doi:10.1091/mbc.E10-02-0129

Tanaka, Y., Kanai, Y., Okada, Y., Nonaka, S., Takeda, S., Harada, A., Hirokawa, N., 1998. Targeted disruption of mouse conventional kinesin heavy chain, kif5B, results in abnormal perinuclear clustering of mitochondria. Cell 93, 1147–58.

Tardin, C., Cognet, L., Bats, C., Lounis, B., Choquet, D., 2003. Direct imaging of lateral movements of AMPA receptors inside synapses. EMBO J. 22, 4656–65. doi:10.1093/emboj/cdg463

Twelvetrees, A.E., Yuen, E.Y., Arancibia-Carcamo, I.L., MacAskill, A.F., Rostaing, P., Lumb, M.J., Humbert, S., Triller, A., Saudou, F., Yan, Z., Kittler, J.T., 2010. Delivery of GABAARs to synapses is mediated by HAP1-KIF5 and disrupted by mutant huntingtin. Neuron 65, 53–65. doi:10.1016/j.neuron.2009.12.007

Verhey, K.J., Hammond, J.W., 2009. Traffic control: regulation of kinesin motors. Nat. Rev. Mol. Cell Biol. 10, 765–77. doi:10.1038/nrm2782

Wadsworth, P., Lee, W.-L., 2013. Microtubule motors: doin' it without dynactin. Curr. Biol. 23, R563–5. doi:10.1016/j.cub.2013.05.026

Wang, Z., Edwards, J.G., Riley, N., Provance, D.W., Karcher, R., Li, X.-D., Davison, I.G., Ikebe, M., Mercer, J.A., Kauer, J.A., Ehlers, M.D., 2008. Myosin Vb mobilizes

recycling endosomes and AMPA receptors for postsynaptic plasticity. Cell 135, 535–48. doi:10.1016/j.cell.2008.09.057

Wenthold, R.J., Petralia, R.S., Blahos J, I.I., Niedzielski, A.S., 1996. Evidence for multiple AMPA receptor complexes in hippocampal CA1/CA2 neurons. J. Neurosci. 16, 1982–9.

Wong, R.W.-C., Setou, M., Teng, J., Takei, Y., Hirokawa, N., 2002. Overexpression of motor protein KIF17 enhances spatial and working memory in transgenic mice. Proc. Natl. Acad. Sci. U. S. A. 99, 14500–5. doi:10.1073/pnas.222371099

Wong-Riley, M.T.T., Besharse, J.C., 2012. The kinesin superfamily protein KIF17: one protein with many functions. Biomol. Concepts 3, 267–282. doi:10.1515/bmc-2011-0064

Woods, G., Zito, K., 2008. Preparation of gene gun bullets and biolistic transfection of neurons in slice culture. J. Vis. Exp. e675. doi:10.3791/675

Xia, C.-H., Roberts, E.A., Her, L.-S., Liu, X., Williams, D.S., Cleveland, D.W., Goldstein, L.S.B., 2003. Abnormal neurofilament transport caused by targeted disruption of neuronal kinesin heavy chain KIF5A. J. Cell Biol. 161, 55–66. doi:10.1083/jcb.200301026

Yamashita, N., Usui, H., Nakamura, F., Chen, S., Sasaki, Y., Hida, T., Suto, F., Taniguchi, M., Takei, K., Goshima, Y., 2014. Plexin-A4-dependent retrograde semaphorin 3A signalling regulates the dendritic localization of GluA2-containing AMPA receptors. Nat. Commun. 5, 3424. doi:10.1038/ncomms4424

Yang, Z., Roberts, E.A., Goldstein, L.S., 2001. Functional analysis of mouse C-terminal kinesin motor KifC2. Mol. Cell. Biol. 21, 2463–6. doi:10.1128/MCB.21.7.2463-2466.2001

Yap, C.C., Winckler, B., 2012. Harnessing the power of the endosome to regulate neural development. Neuron 74, 440–51. doi:10.1016/j.neuron.2012.04.015

Yin, X., Takei, Y., Kido, M.A., Hirokawa, N., 2011. Molecular motor KIF17 is fundamental for memory and learning via differential support of synaptic NR2A/2B levels. Neuron 70, 310–25. doi:10.1016/j.neuron.2011.02.049

Annex: publications

Published articles:

- Jurado S, Benoist M, Lario A, Knafo S, Petrok CN, Esteban JA. PTEN is recruited to the postsynaptic terminal for NMDA receptor-dependent long-term depression. EMBO J. 2010 Aug 18;29 (16):2827-40.
- Arendt KL, Benoist M, Lario A, Draffin JE, Muñoz M, Esteban JA. PTEN dampens PIP_3 upregulation in spines during NMDA receptor-dependent long-term depression. J Cell Sci, doi: 10.1242/jcs.156554, 2014 (*Advanced Online Publication)*.

Manuscripts in preparation:

- Lario A, Brachet A, Muñoz M, Esteban JA. Kinesin-dependent transport of AMPA receptors is required for long-term depression.
- Palenzuela R, Benoist M, Lario A, Muñoz M, Esteban JA. MAP1B-LC regulates AMPA receptor trafficking and synaptic transmission through GRIP1.